

**Toxicity and Transcriptome Sequencing (RNA-seq) Analyses of Adult Zebrafish in
Response to Exposure to Stabilized FeS and Fe₃O₄ Nanoparticles**

by

Min Zheng

A dissertation submitted to the Graduate Faculty of
Auburn University
in partial fulfillment of the
requirements for the Degree of
Doctor of Philosophy

Auburn, Alabama
Dec 16, 2017

Keywords: FeS Nanoparticles, Fe₃O₄ Nanoparticles, Coating,
Toxicity, RNA-seq, Zebrafish

Copyright 2017 by Min Zheng

Approved by

Dongye Zhao, Chair, Huff Professor of Environmental Engineering
Mark Barnett, Malcolm Pirnie Professor of Environmental Engineering
Clifford R. Lange, Associate Professor of Environmental Engineering
Mark R. Liles, Professor of Biological Sciences
Yucheng Feng, Professor of Agronomy & Soils

Abstract

Iron-based nanoparticles (NPs) have been widely studied for potential applications in many fields, particularly in environmental remediation and biomedical areas. For example, iron sulfide (FeS) nanoparticles, have been frequently tested for removal and immobilization of pollutants in soil and groundwater because of their reducing and adsorbing properties. Magnetite (Fe₃O₄) nanoparticles have been applied to various biomedical areas such as cell tracking and drug delivery, as well as various environmental remediation settings. This is not only because of their small particle size and high surface-area-to-volume ratio, but also their magnetism.

However, bare NPs have a strong tendency to form large aggregates, impeding their delivery and performance. To prevent particle aggregation, various stabilizers are often employed. For instance, polysaccharide stabilizers, carboxymethyl cellulose (CMC) and starch have been used to successfully stabilize FeS and Fe₃O₄ NPs. While such surface modifications can greatly facilitate their applications, there is limited information available regarding the toxicity and potential environmental impacts of stabilized NPs.

As the applications of stabilized NPs continue to expand, it is imperative to understand and assess the associated toxicity to key ecosystem organisms. The zebrafish (*Danio rerio*) has been widely used as a model organism in eco-toxicological testing, particularly for assessing the risk of chemicals and nanoparticles. Two representative iron based nanoparticles, CMC-stabilized FeS and starch-stabilized Fe₃O₄ NPs, will be evaluated. The overall goal of this research is to investigate the stress response of adult zebrafish to stabilized FeS and Fe₃O₄ NPs through the

state of the art of transcriptome sequencing (RNA-seq) technique together with tissue burdens and histological alternations assessment.

Adult zebrafish were exposed to 10 mg/L bare and CMC stabilized FeS NPs for 96 hours, demonstrating striking differences in gene expression profiles in the liver. This exposure caused significant alterations in gene expression related to immune and inflammatory responses, detoxification, oxidative stress and DNA damage/repair. The Kyoto encyclopedia of genes and genomes (KEGG) pathways related to immune system response and complement and coagulation cascades were found to be significantly up-regulated. A quantitative real-time polymerase chain reaction (RT-qPCR) of candidate genes commonly regulated in the liver confirmed the RNA-seq results. Hepatic inflammation was further confirmed by histological observation of pyknotic nuclei, as well as vacuole formation upon exposure. Additionally, tissue accumulation tests showed a 2.2-times higher iron concentration in the fish tissue upon exposure. Further, when CMC-FeS NPs toxicity was compared with bare FeS NPs, we discovered that CMC coating can alleviate the toxicity caused by FeS NPs. This study provides preliminary mechanistic insights into potential toxic effects of organic matter stabilized FeS NPs, which will improve our understanding of the genotoxicity caused by stabilized NPs.

In an effort to understand the impact of coating on NPs induced toxicity, we used RNA-seq to characterize gill and liver transcriptomes from adult zebrafish exposed to Fe₃O₄ NPs and starch-Fe₃O₄ NPs for 7 days. Striking differences in gene expression profiles were observed in both tissues. Surface coating dependent toxicity was revealed on both the gill and liver. Fe₃O₄ NPs exerted greater toxicity than starch-Fe₃O₄ NPs in the gill. In contrast, starch-Fe₃O₄ NPs

triggered more severe damage on the liver, but likely shared a similar regulatory mechanism with Fe₃O₄ NPs. The RNA-seq results were verified through RT-qPCR using six genes each for two tissues. Surface coating plays an important role in determining the nanoparticle toxicity, which in turn modulates cell uptake and biological responses. Consequently, surface coating impacts the potential safety and efficacy of nanomaterials.

Our findings will aid with the evaluation of risks associated with fate, transport and toxicity of NPs. Additionally, these findings guide the application of NPs and their coatings for optimal utility and decrease the potential for deleterious environmental impacts.

Acknowledgments

I would like to express my sincere appreciation to my advisor Dr. Dongye Zhao. He inspired my interest in research and gave me direction by suggesting interesting problems. It has been my pleasure to have him as my advisor. His technical and editorial advice was essential to the completion of this dissertation. I express my sincere thanks for his support, advice, patience, and encouragement throughout my graduate studies. His persistence in tackling problems, confidence, and great teaching will always be an inspiration.

My thank goes to the members of my Ph.D. committee, Prof. Mark Barnett, Prof. Clifford R. Lange, Prof. Mark R. Liles and Prof. Yucheng Feng, and my university reader Prof. Vishnu Suppiramaniam who provided valuable feedback and suggestions to my dissertation proposal defense and dissertation drafts. All these helped to improve the presentation and content of this dissertation.

I would like to thank Jinling Zhuang for the analytical and mechanical assistance. It is also a pleasure to work with my fellow students here at AU for their research advice and for creating a supportive environment.

I would also like to express my love and gratitude to my husband for his infinite support and loving care. I wish to thank my two sons for bringing the happiness and the joy of my life. Finally, I wish to thank my parents and other family members for their support. It is their constant encouragement that made this dissertation possible.

Table of Contents

| | |
|--|----|
| Abstract..... | ii |
| Acknowledgments..... | v |
| Chapter 1. General Introduction | 1 |
| 1.1 Engineered Nanoparticles..... | 1 |
| 1.2 Mechanisms of Nanoparticles Toxicity..... | 2 |
| 1.3 Effect of Coatings on NPs-induced Toxicity | 7 |
| 1.4 Approaches for Evaluating Toxicity of Nanomaterials..... | 9 |
| 1.5 Iron Based Engineered Nanoparticles | 21 |
| 1.6 RNA-seq Technology and Zebrafish..... | 23 |
| 1.7 Objectives of This Research..... | 24 |
| 1.8 Organization of This Dissertation | 25 |
| Chapter 2 Toxicity and Transcriptome Sequencing (RNA-seq) Analyses of Adult Zebrafish in Response to Exposure Carboxymethyl Cellulose Stabilized Iron Sulfide Nanoparticles..... | 26 |
| 2.1 Introduction | 26 |
| 2.2 Materials and Methods | 28 |
| 2.2.1 Synthesis and characterization of bare and CMC-FeS NPs nanoparticles | 28 |
| 2.2.2 Zebrafish experimental study | 29 |

| | |
|--|-----------|
| 2.2.3 Tissue accumulations..... | 31 |
| 2.2.4 Histopathology of liver tissue..... | 31 |
| 2.2.5 High-throughput transcriptomic sequencing | 32 |
| 2.3 Results and Discussion..... | 35 |
| 2.3.1 Characterization of bare FeS NPs and CMC-FeS NPs..... | 35 |
| 2.3.2 Acute toxicity evaluation..... | 36 |
| 2.3.3 Histological analysis of liver tissue | 38 |
| 2.3.4 Transcriptomic analysis for bare and CMC-FeS NPs | 39 |
| 2.4 Conclusions | 56 |
| | |
| Chapter 3 Effects of Surface Coating of Magnetite Nanoparticles on Cellular Uptake, Toxicity and Gene Expression Profiles in Adult Zebrafish..... | 58 |
| 3.1 Introduction | 58 |
| 3.2 Materials and Methods | 62 |
| 3.2.1 Chemicals | 62 |
| 3.2.2 Synthesis and characterization of Fe ₃ O ₄ NPs and starch-Fe ₃ O ₄ NPs | 62 |
| 3.2.3 Zebrafish exposure to magnetite nanoparticles | 63 |
| 3.2.4 Accumulations of NPs in fish tissue..... | 64 |
| 3.2.5 High-throughput transcriptomic sequencing | 65 |
| 3.3 Results and Discussion..... | 67 |

| | |
|---|-----|
| 3.3.1 Particle characterization | 67 |
| 3.3.2 Tissue burden..... | 70 |
| 3.3.3 Transcriptomic analysis..... | 71 |
| 3.4 Conclusions | 97 |
| Chapter 4 Conclusions and Suggestions for Future Research | 99 |
| 4.1 Summary and Conclusions..... | 99 |
| 4.2 Suggestions for Future Work | 100 |
| References..... | 101 |

List of Tables

| | |
|--|----|
| Table 1. 1 Microscopic methods to assess NPs and their advantages and disadvantages | 9 |
| Table 1. 2 Cytotoxicity assays of nanoparticles and their advantages and disadvantages | 13 |
| Table 1. 3 The summary of methods applied for in vitro and in vivo genotoxicity testing for NPs and their advantages and disadvantages | 16 |
| Table 1. 4 Common methods of detection of ROS generation and their advantages and disadvantages | 18 |
| Table 1. 5 Genomics, transcriptomics, and proteomics methods and their advantages and disadvantages | 20 |
| Table 2. 1 Tap water parameters for raising adult zebrafish..... | 30 |
| Table 2. 2 Sequences of primers for selected genes. | 35 |
| Table 2. 3 Mean hydrodynamic diameters and zeta potential of freshly prepared and 24-h aged bare and CMC-FeS NPs..... | 36 |
| Table 2. 4 Summary of sequence data generated for zebrafish transcriptome and quality filtering. | 40 |
| Table 2. 5 GO enrichment statistics for bare and CMC coated FeS NPs | 50 |
| Table 2. 6 Up or down-regulated and common KEGG pathways statistics for bare and CMC coated FeS NPs treated groups | 51 |
| Table 2. 7 Top 10 differentially up or down regulated KEGG pathways in CMC-FeS treated zebrafish compared with the control..... | 53 |
| Table 2. 8 Top 10 differentially up or down regulated KEGG pathways in bare FeS NPs treated zebrafish compared with the control..... | 54 |
| Table 3. 1 Sequences of primers for selected genes in qPCR validation..... | 67 |
| Table 3. 2 Mean hydrodynamic diameters and zeta potential of freshly prepared and 24-h aged Fe ₃ O ₄ | 69 |

| | |
|---|----|
| Table 3. 3 Summary of sequence data generated for zebrafish gill and liver transcriptome and qualify filtering. | 72 |
| Table 3. 4 Statistical analysis of GO enrichment numbers and percentage in each category, biological process, molecular function and cellular component in gill and liver of zebrafish exposed to bare or starch-coated Fe ₃ O ₄ nanoparticles..... | 84 |
| Table 3. 5 Impact of bare and starch-coated Fe ₃ O ₄ nanoparticles on the KEGG pathways in zebrafish gill and liver (P<0.05). | 87 |
| Table 3. 6 KEGG pathways impacted by bare and starch-coated Fe ₃ O ₄ NPs in zebrafish gill (P<0.05). | 89 |
| Table 3. 7 KEGG pathways impacted by bare or starch-coated Fe ₃ O ₄ NPs in zebrafish liver (P<0.05). | 92 |

List of Figures

- Figure 2. 1 Transmission electron microscopy (TEM) image (a) and the histogram of size distribution (b) of CMC-stabilized FeS nanoparticles (FeS = 10 mg/L, CMC = 0.001 wt.%). The mean particle size is 32.18 ± 5.25 nm. (Scale bar represents 200 nm)..... 36
- Figure 2. 2 Histological analysis of the liver of Zebrafish in control (a) and upon CMC-FeS exposure (b).The liver of control zebrafish had normal hepatocytes, while the nanoparticle treated groups showed pyknotic nuclei (pn), and vacuole formation (vf). The scale bar represents 20 μ m. 39
- Figure 2. 3 Volcano plots for gene libraries of zebrafish liver showing variance in gene expression with respect to fold change and significance (P-value). (a) Expressed genes for untreated (control) and bare FeS NPs treated zebrafish, (b) Expressed genes for untreated and CMC-coated FeS NPs treated zebrafish. Each dot represents an individual gene: Red dots refer to the up-regulated DEGs, Blue dots to the down-regulated DEGs, and black dots to not differentially expressed genes (NDE)..... 41
- Figure 2. 4 Venn diagram showing number of genes identified with up- or down-regulated expression ($P < 0.05$) in zebrafish livers upon exposure to bare and CMC-coated FeS nanoparticles. (a) Overlap of up-regulated DEGs, (b) Overlap of down-regulated DEGs..... 42
- Figure 2. 5 Fold changes of representative genes in zebrafish livers in relation to: (a) immune and inflammation response, (b) oxidative stress and antioxidant response, (c) ER stress and unfolded protein response, (d) heat shock response, (e) mitochondria energy metabolism pathways, (f) mitochondria dysfunction pathway, (g) DNA damage and repair, and (h) apoptosis pathway upon treatments with bare or CMC-coated FeS NPs for 96h (Data shown having fold change < -2 and > 2 at $P < 0.05$). 48
- Figure 2. 6 Gene ontology (GO) category patterns of the differentially expressed genes in livers of zebrafish upon exposure to treatments with bare or CMC-coated FeS NPs for 96h. The GO was assigned into three categories: biological process, cellular component and molecular function. 50
- Figure 2. 7 Validation of liver tissue transcriptome results by qRT-PCR using twelve selected differentially expressed genes in CMC-FeS treated zebrafish. The qRT-PCR fold changes are relative to the control samples and normalized by changes in beta-actin values. The averages of three relative quantities of biological replications were used in a two-tailed Student's t test with a 95% confidence level ($P < 0.05$) to determine the gene expression significance..... 56

Figure 3. 1 Transmission electron microscopy images and histograms showing size distributions of bare and starch-stabilized Fe₃O₄ NPs (total Fe = 100 mg/L, starch = 0.04 wt.%): (a) TEM image of bare Fe₃O₄ NPs, (b) Histogram of bare Fe₃O₄ NPs size (mean size = 20.92 ± 7.48 nm), (c) TEM image of starch-coated Fe₃O₄ NPs, and (d) Histogram of starch-coated Fe₃O₄ NPs size (mean size = 4.26 ± 0.84 nm). 69

Figure 3. 2 Venn diagram showing number of genes identified with up- or down-regulated expression (P<0.05) in zebrafish gills and livers upon exposure to bare and starch-coated Fe₃O₄ nanoparticles. (a) Up-regulated DEGs in gills, (b) Down-regulated DEGs in gills, (c) Up-regulated DEGs in livers, and (d) Down-regulated DEGs in livers..... 76

Figure 3. 3 Volcano plots for gene libraries of zebrafish showing variance in gene expression with respect to fold change and significance (P-value). (a) Expressed genes in gill for untreated (control) and bare Fe₃O₄ NPs treated zebrafish, (b) Expressed genes in gill for untreated and starch-coated Fe₃O₄ NPs treated zebrafish, (c) Expressed genes in liver for untreated and bare Fe₃O₄ NPs treated zebrafish, and (d) Expressed genes in liver for untreated and starch-coated Fe₃O₄ NPs treated zebrafish. Each dot represents an individual gene: Red dots refer to the up-regulated DEGs, Blue dots to the down-regulated DEGs, and black dots to not differentially expressed genes (NDE)..... 77

Figure 3. 4 Representative genes in zebrafish gills involved in immune and inflammation response, oxidative stress and antioxidant response, ER stress and unfolded protein response, mitochondria energy metabolism pathways, DNA damage and repair and apoptosis upon exposure to bare and starch-coated Fe₃O₄ NPs for 7 days (Data shown having fold change < -2 and > 2 at P<0.05). 79

Figure 3. 5 Fold changes of representative genes in zebrafish livers in relation to: (a) immune and inflammation response, (b) oxidative stress and antioxidant response, (c) ER stress and unfolded protein response, (d) heat shock response, (e) mitochondria energy metabolism pathways, (f) mitochondria dysfunction pathway, (g) DNA damage and repair, and (h) apoptosis pathway upon treatments with bare or starch-coated Fe₃O₄ NPs for 7 days (Data shown having fold change < -2 and > 2 at P<0.05). 82

Figure 3. 6 Gene ontology (GO) category patterns of the differentially expressed genes in gills and livers of zebrafish upon exposure to bare or starch-coated Fe₃O₄ NPs for 7 days. (a) GO categories in gills, and (b) GO categories in livers. The GO was assigned into three categories: biological process, cellular component and molecular function..... 85

Figure 3.7 Validation of gill and liver tissue transcriptome results by qRT-PCR using twelve selected differentially expressed genes upon exposure to bare or starch-stabilized Fe₃O₄ NPs for 7 days. The qRT-PCR fold changes are relative to control samples and are normalized by changes in beta-actin values. The mean of three relative quantities of biological replicates were

used in a two-tailed Student's t test with a 95% confidence level ($P < 0.05$) to determine the gene expression significance. 97

Chapter 1. General Introduction

1.1 Engineered Nanoparticles

Engineered nanoparticles (ENPs) are materials with at least one dimension of 100 nanometers or less. They have attracted numerous attention and been successfully applied in various areas including electronic, chemical, biological, medical, environmental remediation fields and many more due to their unique properties (Adlakha-Hutcheon et al., 2009). Investment in nanotechnology research and the market for nanotech products has been steadily growing all over the world. There were 1814 nano-enabled consumer products from 622 companies in 32 countries listed in the Nanotechnology Consumer Products Inventory (CPI) in 2015 (Vance et al., 2015). Due to the active production and utilization of nanotechnology, nanoparticles have emerged as a new class of environmental pollutants that may eventually release into atmospheric, terrestrial, and aquatic environments and significantly impact the environment and human health (Gottschalk et al., 2011).

The aquatic environment is particularly at risk of exposure to ENPs, as it acts as a sink for most environmental contaminants. Fish, as aquatic organisms, can accumulate pollutants directly from contaminated water and indirectly via the food chain (Sasaki et al., 1997). Since fish occupy the top of the aquatic food chain, they are widely used as a bio-indicator to evaluate the health of aquatic ecosystems (Camargo and Martinez, 2007).

Bioaccumulation of potentially harmful substances in fish presents a major threat to human health. Understanding nanoparticle and fish interactions is important for determining the potential risks of nanoparticles, because they have demonstrated toxicity to fish and may adversely affect the human being by substantial bioaccumulation.

NPs used in commercial products are typically coated with polymers to enhance their stability and mobility (He and Zhao, 2007; Saleh et al., 2007). Bare NPs may also become coated with natural organic matter (NOM) when they are released into the environment (Chen and Elimelech, 2007; Domingos et al., 2009; Johnson et al., 2009). These coatings may modify the physicochemical properties of nanoparticles and affect the cell-particle interactions. Numerous studies have reported NP-fish interactions. However, the connections between physicochemical properties of NPs and coating and their subsequent interaction with fish are still needed for further investigation.

1.2 Mechanisms of Nanoparticles Toxicity

The main focus of current nanomaterial toxicity research is engineered nanoparticles, such as metals, metal oxides, single-walled and multiwalled carbon nanotubes, C-60, polymeric nanoparticles used as drug carriers, and quantum dots (Dhawan and Sharma, 2010).

Some of the paradigms for NP-mediated toxicity is proposed to be oxidative stress, inflammation, immunotoxicity and genotoxicity (Dusinska et al. 2012b). Studying the toxic effects of ENPs is complex and challenging due to their multiplicity of their physicochemical parameters such as size, shape, structure, and coatings (Poljak-Blaži et al., 2010). The proposed nanoparticle toxicity mechanisms in the literatures are reviewed in the following paragraphs.

1.2.1 Reactive oxygen species (ROS) and oxidative stress

Most studies have addressed that reactive oxygen species (ROS) generation and consequent oxidative stress are associated with NP toxicity (Li et al., 2008). ROS are the key signaling molecules during cell signaling and homeostasis. Many NP intrinsic properties can catalyze the ROS production, therefore, the physicochemical characterization of NPs including particle size,

surface charge, and chemical composition can be considered as key indicators for the resulting ROS response and NP-induced damage (Shvedova et al., 2012).

ROS can be induced by endogenous sources including mitochondrial respiration, inflammatory response, microsomes, and peroxisomes, while engineered NPs may act as exogenous ROS generators. Various physiological stimuli can induce trace amount of ROS. Free radicals will also be produced as essential byproducts of mitochondrial respiration and transition metal ion-catalyzed Fenton-type reactions (Vallyathan and Shi, 1997). Inflammatory phagocytes such as neutrophils and macrophages induce oxidative outburst as a defense mechanism towards environmental pollutants, tumor cells, and microbes. One of the principal mechanisms for a variety of NP cytotoxicity is considered as the a consequences of ROS generation. A variety of NPs including metal oxide particles can induce ROS (Risom et al., 2005). The key factors involved in NP-induced ROS include (i) prooxidant functional groups on the reactive surface of NPs; (ii) active redox cycling on the surface of NPs due to transition metal-based NPs; and (iii) particle-cell interactions (Knaapen et al., 2004; Risom et al., 2005). (iv) Dissolution of NPs and subsequent release of metal ions (Knaapen et al., 2004). NPs also have been reported to influence intracellular calcium concentrations, activate transcription factors, and modulate cytokine production via generation of free radicals (Huang et al., 2010a; Li et al., 2010a).

When plenty of ROSs are induced, oxidative stress can be provoked as a damaging biological response. Enzymatic and nonenzymatic antioxidant systems in the cell can be activated to overcome the excess ROS response. It is well known that uncontrolled generation of ROS triggers a cascade of proinflammatory cytokines and mediators via activation of redox sensitive mitogen-activated protein kinase (MAPK) and nuclear factor kappa-light-chain enhancer of activated B cells (NF- κ B) signaling pathways that control transcription of inflammatory genes

such as IL-1 β , IL-8, and TNF- α (Thannickal and Fanburg, 2000). The mechanism of NP-mediated oxidative stress is further described by a hierarchical model (Huang et al., 2010b; Li et al., 2008). According to this model, cells and tissues respond to increasing levels of oxidative stress via antioxidant enzyme systems upon NPs exposure. When oxidative stress is mild, transcriptional activation of phase II antioxidant enzymes are initiated via nuclear factor (erythroid-derived 2)-like 2 (Nrf2) induction. Under intermediate oxidative stress, redox-sensitive MAPK and NF- κ B cascades increased proinflammatory response. At extremely toxic levels, mitochondrial membrane damage and electron chain dysfunction can be induced by oxidative stress, and eventually eliciting cell death.

Glutathione, (GSH) a potent free-radical scavenger, is responsible for maintaining the cellular redox state and protecting cells from oxidative damage (Habib et al., 2007; Rahman et al., 2005). NPs-triggered free radicals reduce GSH into its oxidized form glutathione disulfide (GSSG), thereby contributing to oxidative stress, apoptosis, and sensitization to oxidizing stimuli (Fenoglio et al., 2008; Rahman, 2007). Besides GSH, NPs-induced ROS regulate the antioxidant activities of ROS-metabolizing enzymes including NADPH-dependent flavoenzyme, catalase, glutathione peroxidase, and superoxide dismutase (Stambe et al., 2004).

Interference with the normal redox state can induce peroxidation and free radical production leading to detrimental effects on cell components including proteins, lipids, and DNA (Huang et al., 2010a). Given NPs' chemical reactivity, oxidative stress can cause DNA damage, lipid peroxidation, and activation of signaling networks correlated to loss of cell growth, fibrosis, and carcinogenesis (Buzea et al., 2007; Knaapen et al., 2004; Valko et al., 2006). Besides cellular damage, interactions of NPs with several biological targets will induce ROS as an effect of cell respiration, metabolism, ischemia/reperfusion, inflammation, and metabolism of various

nanomaterials (NM) (Risom et al., 2005). Nanomaterials with different chemical composition such as fullerenes, carbon nanotubes (CNT), and metal oxides have been shown to induce oxidative stress (Bonner, 2007; Vallyathan and Shi, 1997). Apoptosis has been indicated as a major mechanism of cell death caused by NP-induced oxidative stress (Eom and Choi, 2010; Hsin et al., 2008). Among the different apoptotic pathways, the intrinsic mitochondrial apoptotic pathway plays a major role in metal oxide NP-induced cell death as mitochondria serves as one of the major target organelles for NPs-induced oxidative stress (Xia et al., 2006). Various metal oxide NPs including Zn, Cu, Ti, and Si elicit ROS-mediated cell death via mitochondrial dysfunction (Manna et al., 2012; Shi et al., 2010; Wang et al., 2005; ZHANG et al., 2011).

1.2.2 Mechanism of NP-induced immunotoxicity

Besides ROS production, another major toxicological effect of nanoparticles is inflammation of cells. Many recent studies have demonstrated that various nanoparticles cause inflammation by activating the NF- κ B pathway (Deng et al., 2011; Heng et al., 2011; Lonkar and Dedon, 2011; Masamune et al., 2009; Pasparakis, 2009; Pazin et al., 1996; Sitrin et al., 1998). NF- κ B is vital to the growth and development of the immune system and interfere with it can cause severe consequences (Pazin et al. 1996). Nonetheless, NF- κ B is mainly involved in the innate immune response and serve as an essential regulator of inflammation (Silverman and Maniatis, 2001).

In general, cationic particles are more likely to induce inflammatory reactions than anionic and neutral species (Dobrovolskaia and McNeil, 2007). Anionic generation-4.5 polyamidoamine (PAMAM) dendrimers did not cause human leukocytes to secrete cytokines, but cationic liposomes provoked secretion of cytokines such as TNF, IL-12, and IFN γ (Tan et al., 1999).

1.2.3 Mechanism of NP-induced genotoxicity

Genotoxicity may be induced by direct interaction of NPs with the genetic material, or by indirect damage from NP-induced ROS, or by toxic ions released from soluble NPs (Kisin et al. 2007; Barnes et al. 2008).

NPs that are present in the nucleus (entering either by penetration via nuclear pores or during mitosis) might directly interact with chromatin or chromosomes DNA depending on cell cycle phase. During interphase NPs could interact or bind with DNA molecules to interrupt DNA replication and transcription. Carbon NPs were bound to single-stranded DNA and incorporated into DNA duplex structures, probably during DNA replication (An et al. 2010). During mitosis, NPs might break into chromosomes or interrupt mitosis mechanically or by chemical binding, leading to clastogenic or aneugenic effects. NPs can also induce primary genotoxicity by indirectly contacting with DNA, in the following ways i) Interaction with nuclear protein involved in replication, transcription and repair; ii) Interaction of NPs with the mitotic spindle or its components resulting in aneugenic effects; iii) Disturbance of cell cycle checkpoint functions; iv) ROS arising from the NPs surface; v) Transition metals from the NPs surface; vi) ROS produced by cell components (mitochondria); vii) Inhibition of antioxidant defense.

Secondary genotoxicity can be a result of oxidative DNA attack by ROS via activated phagocytes (neutrophils, macrophages), which can interact directly with DNA when NPs cross cellular membranes and may be able to reach the nucleus through diffusion across the nuclear membrane or transportation through the nuclear pore complexes. ROS could cause oxidative DNA damage in the form of DNA strand breaks, DNA protein cross-links, and alkali-labile sites (Kawanishi et al., 2002; Shi et al., 2004). Transition metal NPs can induce chromosomal aberrations, DNA strand breaks, oxidative DNA damage, and mutations (Xie et al., 2011b). A

recent study comparing metal oxide NP including Cu, Fe, Ti, and Ag reported ROS-mediated genotoxicity characterized by micronuclei and DNA damage in vivo (Song et al., 2012).

1.3 Effect of Coatings on NPs-induced Toxicity

Nanoparticles used in commercial products are typically coated with polymer to enhance their stability and mobility. Furthermore, nanoparticles may become coated with natural organic matter (NOM) after exposed to the environment. Polymer or NOM coating may affect the fate and transport and toxicity of nanoparticles, due to the change of their physical and chemical properties. Surface coatings can modify the surface composition, which can influence intracellular distribution and the production of ROSs that cause further toxicity. The adverse effects of NPs maybe alleviated or eliminated by incorporation of surface coatings. Proper surface coatings can stabilize particles and avoid agglomeration (An et al., 2011; Liang and Zhao, 2014; Liang et al., 2012). Coating is also an effective means of preventing the dissolution and release of toxic ions (Kirchner et al., 2005). However, the steric hindrance of coatings can retard the cellular uptake and accumulation of NPs, or coatings can facilitate NP endocytosis (Kato et al., 2003; Moon et al., 2007; Otsuka et al., 2003).

Most studies have indicated that surface coatings can alter the pharmacokinetics, distribution, accumulation, and toxicity of NPs. The magnitude of the effect depends on physical properties of the coatings (e.g. type, molecular weight, concentration and configuration). Coating may alleviate or enhance, or even exert the similar toxicity as the bare NPs. Here we discuss a few.

Coatings and functionalization can reduce the in vivo toxicity of carbon nanotubes. Lacerda et al. (2008) intravenously injected multiwall carbon nanotubes (MWCN) functionalized with diethylenetriamine penta-acetic di-anhydride (DTPA), which resulted in stable dispersions with high excretion rates in rat renal.

Polyethylene glycol (PEG) has been used extensively for coating quantum dots (QDs) as a FDA approved biocompatible polymer, it is generally considered as non-toxic. Ballou et al. (2004) applied PEG coatings of different molecular weights (MW), and the NPs were observed for differential tissue and organ deposition in mice in a time- and size-(MW) dependent manner. The particles coated with lower MW PEG were eliminated from circulation 1 h after injection, but QDs coated with PEG with high MW remained in the blood circulation for 3 h. Xie et al. (2007) showed that coating PEG on monodisperse Fe₃O₄ NPs produced negligible aggregation in cell culture conditions and reduced nonspecific uptake by macrophage cells. In contrast, Cho et al. (2009) found that 13 nm sized Au NPs coated with PEG 5000 induced acute inflammation and apoptosis in the mouse liver, and these NPs were found to accumulate in the liver and spleen for up to 7 days after injection and to have a long blood circulation time of about 30 h. A relatively high concentration of PEG on the NPs surface alone does not lead to a lower NP uptake, but rather the spatial configurational freedom of PEG chains on the particle surface plays a determinant role (Cho et al., 2009).

Poly (acrylic acid)-coated gold nanoparticles (PAA-GNP) serve to increase inflammation by prompting activation of NF- κ B through a conformational change in fibrinogen which leads to binding with the MAC-1 receptor. The downstream results of binding of the MAC-1 receptor included increased production of IL-8 and TNF- α of which the latter is directly implicated in increasing NF- κ B activity (Zhu et al., 2009). It has been shown that dextran-magnetite (Fe₃O₄) NPs cause cell death and reduced proliferation similar to uncoated iron oxide particles, which was attributed to the breakdown of the dextran shell exposing the cellular components to chains or aggregates of iron oxide NPs (Ballou et al., 2004; Oostendorp et al., 2010).

The exact nature of how coatings in ENPs may affect their interaction with organism is complex and remains unclear. A systematic study probing the fundamental physicochemical reasons for the beneficial or adverse effects of nanoparticle coatings on their toxicity are lacking so it is not yet possible to make predications of about how specific coatings may affect their toxicity with organisms for specific particles. Understanding this impact is necessary to design NPs with coatings that prevent adverse effects of NPs to organisms in the environment.

1.4 Approaches for Evaluating Toxicity of Nanomaterials

In spite of the presence of voluminous studies, knowledge about the interactions of nanoparticles with biological systems is still not clear. The current approaches to evaluate the NPs toxicity are summarized here including NPs internalization assessment, cytotoxicity assay, genotoxicity assay, tests for inflammatory and oxidative stress responses as well as genomics, transcriptomics and proteomics approaches. The pros and cons are also listed for each method.

1.4.1 Nanoparticle internalization Assessment methods

Tracking nanoparticle internalization in cellular systems is of the utmost importance for understanding and correlating the biological effects elicited by these nanoparticles. However, the challenge lies in detecting the uptake of nanoparticles, the mode of uptake, and the fate of nanoparticles inside the cells due to their small size and quantity. Microscopic tools are often

Table 1. 1 Microscopic methods to assess NPs and their advantages and disadvantages

| Tests | Advantages | Disadvantages | References |
|------------|--|--|------------------------|
| Microscopy | Tissue organ histological observation, observe the damage directly | The staining and sliding procedures can introduce artifacts; Confined to imaging a few cells | (Marquis et al., 2009) |

| | | | |
|---|--|---|---|
| | | due to the complicated sample preparation and image analysis involved. | |
| TEM (Transmission electron microscopy) | Detecting the intracellular localization, it provides a detailed view of the interaction of nanoparticles with cell structures; Due to its high resolution, transmission electron microscopy enables the imaging of membrane invaginations, vesicle formation, and organelles; Helps to understand the NPs effects associated with their characteristic. | Only a qualitative tool for assessing nanoparticle uptake; Confined to imaging a few cells due to the complicated sample preparation and image analysis involved. | (Motskin et al., 2009; Song et al., 2010; Xie et al., 2010) |
| SEM (Scanning electron microscope) | Observe nanoparticles inside cells; Backscattered electron detection is used instead of the normal secondary electron mode of detection; Bright nanoparticles to be seen against the cellular dark background. | The staining procedures can introduce electron-dense artifacts that may be mistaken for nanoparticles. | (Baroli et al., 2007; Marquis et al., 2009; Pelka et al., 2009) |
| EFTEM (Energy-filtered transmission electron microscopy) | Electrons undergoing inelastic scattering lose some energy, which can be measured by an electron spectrometer; a well-defined energy loss (ionization edge), elemental distribution maps can be generated. | Only electrons with particular kinetic energies are used to form the image. | (Thomas and Midgley, 2002) |
| FTIR spectroscopy | Characterize the damage of the bacterial cells after the exposure to nanoparticles; enable detection of the changes in phospholipids and proteins. | Sample making may alter the NP characteristics | (Lu et al., 2012) |

utilized to perform a qualitative assessment of nanoparticles in the environment or in living systems (Table 1.1).

However, microscopy methods cannot detect very small amounts of nanoparticles in the environment or in living systems, and become ineffective when it comes to the analytical

quantification of nanoparticles. In this case, inductively coupled plasma mass spectroscopy (ICP-MS) can be used as a sensitive and quantitative tool for the determination of even trace amounts of nanoparticles (Tang et al., 2009b). Even trace amounts of nanoparticles that enter through a different route can be detected in various body organs by these methods. However, the digestion step involved in the sample preparation method for ICP-MS may lead to contamination and dilution, and it makes it difficult to differentiate between ions formed as a result of nanoparticle dissolution and nanoparticles per se (Allabashi et al., 2009; Marquis et al., 2009).

Flow cytometry is yet another technique that can be used to study nanoparticle uptake in mammalian cells (Xu et al., 2009). It is not only simple, easy and sensitive, but it is also a cost-effective and noninvasive approach. Thus, flow cytometry can be used for the detection of fluorescent as well as nonfluorescent nanoparticles inside cells.

1.4.2 Cytotoxicity assays of nanoparticles

Cytotoxicity assays are classified as *in vivo* and *in vitro* tests. *In vivo* toxicity assays (cell-based assay) are time-consuming and expensive and involve ethical issues, however, *in vitro* toxicity tests (cell cultured-based assay) are faster, convenient, less expensive and devoid of any ethical issues. Due to these advantages, *in vitro* assays comes first when toxicity assessment of most nanomaterials is concerned (Mahmoudi et al., 2011).

In vitro methods include approaches for assessment of integrity of the cell membrane and the metabolic activity of viable cells. Evaluation of cell membrane integrity is one of the most common approaches to measure cell viability. It is based on the leakage of substances such as lactate dehydrogenase (LDH) that normally reside inside cells to the external environment and the measurement of LDH activity in the extracellular media. Alternatively, membrane integrity

can be determined by penetration of dyes such as trypan blue and neutral red into the damaged cells and staining intracellular components. These dyes cannot enter living cells. Metabolic activity of viable cells could be determined through colorimetric assays, such as the MTT (3-(4,5-Dimethylthiazol-2-yl)-2,5-Diphenyltetrazolium Bromide) and MTS (3-(4,5-dimethylthiazol-2-yl)-5-(3-carboxymethoxyphenyl)-2-(4-sulfophenyl)-2H-tetrazolium) assays (Fischer et al., 2010; Fotakis and Timbrell, 2006; Kumbıçak et al., 2014; Rabolli et al., 2010). Cytotoxicity assays of nanoparticles and their advantages and disadvantages are shown in Table 1.2.

Table 1. 2 Cytotoxicity assays of nanoparticles and their advantages and disadvantages

| Tests | Principle of the test methods | Advantages | Disadvantages | References |
|-----------|---|---|---|---|
| LDH test | DH test is a colorimetric assay that quantitatively measures LDH, a marker of cell membrane integrity, released from damaged cells into the culture media | Fast, simple and reliable method for determining cellular toxicity | Poor correlation between turbidity and triglycerides Concentration; Highly lipemic samples may cause ABS flags. | (Korzeniewski and Callewaert, 1983) |
| MTT assay | MTT assay is another candidate assay for measurement of cytotoxicity of NPs. MTT is a yellow substance which reduces to purple insoluble formazan crystals by mitochondrial succinate dehydrogenases in viable cells. | This method is directly related to the number of viable cells | Less accurate in detecting changes in cell number; Glycolysis inhibitors interference with the MTT assay | (van Meerloo et al., 2011; Van Tonder et al., 2015) |
| MTS assay | In the MTS assay, viable cells will convert tetrazolium salt into a colored soluble formazan product by mitochondrial dehydrogenase enzymes. | A colorimetric product is formed, the formazan produced is directly proportional to the number of living cells in the culture | Accuracy depends on chemical nature and cell reads. | (Malich et al., 1997; Wang et al., 2010) |

1.4.3 Genotoxicity assays of nanoparticles

The research on mechanisms of NP genotoxicity is still in its infancy, it is still unknown if an effect on DNA is nano-specific. NPs can cause primary and secondary genotoxicity according to their ways of their exposure to the target organism. Direct interaction of NPs with genetic material may cause genotoxicity, indirect damage may be aroused by NP-induced reactive

oxygen species (ROS), or by toxic ions released from soluble NPs (Barnes et al., 2008; Kisin et al., 2007). Secondary genotoxicity can be a consequence of oxidative DNA attack by ROS via activated phagocytes (neutrophils, macrophages) during NP-elicited inflammation (Stone et al., 2009).

Genotoxicity testing of NPs can be conducted *in vitro* or *in vivo*. The primary genotoxicity for testing is usually carrying out *in vitro*, while *in vivo* models will deliver information on secondary effects such as inflammation (Arora et al., 2012; Kisin et al., 2007; Vega-Villa et al., 2008). Initial approach for genotoxicity is examined by the bacterial reverse mutation assay (Ames test) (Warheit et al., 2007). Subsequent tests in cultured mammalian cells (either permanent cell lines or primary cultures) exhibit various endpoints. The comet assay is used for detecting DNA damage (Shukla et al., 2013; Shukla et al., 2011). The HPRT (hypoxanthine phosphoribosyltransferase) gene mutation tests are used for assessing a specific mutation locus (Wang et al., 2007). Chromosomal damage is scored either in mitotic cells as chromosome aberrations or in interphase cells as micronucleus (MN). *In vivo*, DNA damage (Bourdon et al., 2012; Schulz et al., 2012), chromosome aberrations (Dandekar et al., 2010) and MN (Estevanato et al., 2011; Li et al., 2012) can be examined in different tissues, and transgenic rodents are often used for these type of tests. The summary of methods applied for *in vitro* and *in vivo* genotoxicity testing for NPs and their advantages and disadvantages are showed in Table 1.3.

1.4.4 Oxidative stress and inflammatory responses detection methods

The toxicity of NPs is frequently attributed to reactive oxygen species (ROS) generation. However, it should be noted that oxidative stress could be a result of particle interactions with the cells even in the case when particles do not spontaneously produce ROS by themselves.

Oxidative stress can be determined in different ways. This commonly includes the detection of the ROS production as the first step, followed by the investigation of biological effects of ROS. Common methods of detection of ROS generation are summarized in Table 1.4.

Oxidative stress and inflammatory responses caused by NPs can be detected by other cytotoxicity and genotoxicity assays, for instance, human lung cells are often used to indicate the oxidative stress and inflammatory responses of NPs (Bayram et al., 2006; Elder et al., 2007; Xiao et al., 2003) induced inflammatory responses (Becker et al., 2005). In addition, NPs can also induce an increase in the cell number of human lung epithelium (Bayram et al., 2006). Another method of detecting oxidative stress is the measurement of superoxide dismutase (SOD) activity, which can be performed with commercial assay kits (Kim and An, 2012). Other methods of detecting oxidative stress include the detection of protein oxidation and/or the detection of lipid peroxidation. Protein oxidation can be investigated using an enzyme-linked immunosorbent assay (ELISA) to examine the formation of protein carbonyl derivatives (products of the oxidation reaction) (Sun et al., 2013).

Table 1. 3 The summary of methods applied for in vitro and in vivo genotoxicity testing for NPs and their advantages and disadvantages

| Tests | Principle of the test methods | Advantages | Disadvantages | OECD guideline | References |
|---|--|---|--|---|--|
| Ames test (bacterial reverse mutation) | Induction of back-mutations in a defective histidine gene; reversal of this mutation will enable the bacterium to synthesize histidine and form a visible colony when plated in minimal histidine medium. | Quick and convenient; Estimate the mutagenic potential of chemical compounds | Larger NPs are unable to cross the cell wall. If they do enter the cell, NPs could possibly interfere with histidine synthesis and induce false-negative (down-regulation) or positive (up-regulation) results; so far given largely negative results. | OECD 471 for the bacterial reverse mutation test | (Kumar et al., 2011a; Kumar et al., 2011b; Landsiedel et al., 2009; Mori et al., 2006; Shinohara et al., 2009; Wirnitzer et al., 2009) |
| Comet assay (single-cell gel electrophoresis) | DNA breaks relax supercoiling, and relaxed loops of DNA are able to extend during electrophoresis (normally at high pH), to form a 'comet tail', visualized by fluorescence microscopy. Relative tail intensity indicates break frequency. | One of the most common tests for genotoxicity; Uncomplicated and sensitive technique; Photogenotoxic effects of NPs can be measured by the comet assay in combination with ultraviolet radiation. | The incubation of NPs and ions with FPG leads to the total loss of the ability of the enzyme to detect oxidatively damaged DNA. | OECD guidelines are under preparation for the in vivo comet assay test (http://www.jacvam.jp/en_effort/en_oecd.html). | (Collins et al., 1996; Hudecová et al., 2012; Jha, 2008; Kain et al., 2012; Karlsson, 2010; Magdolenova et al., 2012; Shukla et al., 2011; Stone et al., 2009) |
| CHA (Chromosomal aberration) test | At predetermined intervals after the start of exposure of cell cultures to the test substance, they are treated | Identifies agents that cause structural chromosome or chromatid | Time consuming; Not suitable for automation | OECD 473 for the in vitro CHA test, OECD 474 | (Aoshima et al., 2010; Bonassi et al., 2008; Galloway et al., |

| | | | | | |
|----------------------------|--|---|---|--|---|
| | with a metaphase-arresting substance (e.g. Colcemid® or colchicine), harvested, stained and metaphase cells are analyzed microscopically for the presence of chromosome aberrations. | breaks, dicentrics and other abnormal chromosomes, notably translocations which are implicated in the aetiology of various human genetic diseases and cancers. | | and 475 for the mammalian erythrocyte and bone marrow CHA tests. | 1987; Galloway et al., 1994) |
| MN (Micronucleus) assay | MN are formed during anaphase from chromosomal fragments or whole chromosomes that are left behind when the nucleus divides. Excluded from the nuclei of daughter cells, they form single or multiple MN in the cytoplasm, detected by visual (or automated) examination after staining. | Less time-consuming and more suitable for automation; Histological staining with labelled DNA probes reduces the risk of falsely identifying NP aggregates as MN fragments; Visual (or automated) examination after staining. | The interpretation of data is influenced by statistical power. | OECD 487 draft for the in vitro MN test | (Doak et al., 2009; Fenech et al., 2011; Hayashi, 2016; Schmid, 1975) |
| HPRT gene mutation test | Cells are cultured for several generations to dilute out pre-existing enzyme, a toxic purine analogue that is taken up by wild-type cells, which die, HPRT cells survive to form colonies, which are scored. | The assay can detect a wide range of chemicals capable of causing DNA damage that leads to gene mutation. | Original phenotype may get lost after mutation; It is difficult to treat a sufficiently large number of cells (>10 ⁵ cells per petri dish) to produce statistically robust assays. | None | (Johnson, 2012; Wang et al., 2007; Wang et al., 2011) |

Table 1. 4 Common methods of detection of ROS generation and their advantages and disadvantages

| Tests | Advantages | Disadvantages | References |
|--|---|---|----------------------------|
| Luminescent probes | Determine intracellular ROS generation as well as the direct examination of the ability of nanomaterial to generate ROS. | The artifacts due to issues with the stability of the probes, undesired probe reactions, the lack of specificity of the probe, and the perturbation of the studied system by the probe. | (Long et al., 2006) |
| UV-visible spectroscopy | Detect superoxide ion radicals | | (Brunet et al., 2009) |
| Pressure liquid chromatography | Hydroxyl radical detection | | (Brunet et al., 2009) |
| HPLC (High pressure liquid chromatography) | Monitor degradation of probe molecules, such as p-chlorobenzoic acid | Require more time-consuming sample preparation | (Cho et al., 2004) |
| ESR (Electron spin resonance) spectroscopy | One of most powerful tools for studying free radicals; it is promising for both in vitro and in vivo studies; more direct and more specific detection method. | High cost of Instrumentation; Low sensitivity | (Pierzchała et al., 2012) |
| TBA (Thiobarbituric acid) assay | Lipid peroxidation detection | Direct interaction of nanomaterial with TBA leading to artifacts; strongly dependent on the pH. | (Premanathan et al., 2011) |

1.4.5 Genomics, transcriptomics, and proteomics approaches

Besides different physical and/or chemical methods to determine genotoxicity, understanding the biological response at the molecular level of cells is also important and will provide another line of information to evaluate the interactions between nanomaterials and cells. Incubating cells with nanomaterials should induce either strong, weak or no expression of genes and these responses can be measured by analyzing messenger RNAs (mRNAs) and/or proteins (Djurišić et al., 2015). The methods to query gene expression have improved substantially in recent years,

enabling a far more comprehensive evaluation of the mechanism of nanotoxicity than in the past. Various methods have been adopted to measure the molecular responses to evaluate the toxicity of nanomaterials, including genomics, transcriptomics, and proteomics investigations (Table 1.5). Complementing molecular analysis with other physical and/or chemical assays would be ideal as molecular responses should be manifested into metabolites or some other traits measurable with various assays.

Commonly used approaches to assess the toxicity of nanomaterials and their pros and cons were reviewed in this section (Table 1.5). Most of the methods used for toxicity assessment have been designed and standardized with the chemical toxicity in mind. However, nanoparticles with several unique physicochemical properties that can interfere with or pose challenges to the use of classical toxicity assays. More extensive particle characterization (of factors such as size, shape, solubility, agglomeration, elemental purity, surface area, etc.) is required compared with regular chemical compounds. Incomplete characterization may cause failure attempts for finding a correlation between various biological effects and particle properties. Also, an absence of standardized methodologies and guidelines hinders the comparison of the safety/toxicity assessments from different research groups. This impedes nanotoxicology and results in much apprehension regarding the possible adverse health and environmental implications of nanomaterials. Furthermore, the scarcity of genomics, transcriptomics and proteomics studies of nanomaterial toxicity further hamper the process of improving our understanding of the nanomaterial toxicity.

Table 1. 5 Genomics, transcriptomics, and proteomics methods and their advantages and disadvantages

| Tests | Advantages | Disadvantages | References |
|--|--|---|---|
| Fluorescence spectrophotometry | Quantify DNA or RNA content per cell | Highly purified DNA and RNA are required for this method, unpureed samples may lead to failure | (Kemp et al., 1993) |
| Northern blot and gene mutagenesis and transduction test | Detect the target gene mutation | Only small number of target genes can be detected. | (Bradley et al., 1997) |
| Reverse transcription (RT)-quantitative polymerase chain reaction (qPCR) | Study the changes in expression of mRNA after exposure to nanomaterials; accurate quantification of the change in transcripts abundances and a relatively large number of genes can be analyzed in parallel. Present the least biased results. Often used to validate the results of microarray and RNA-seq. | Relative lowest quantification limits compared with microarray, RNA-seq. | (Chae et al., 2009; Roh et al., 2009) |
| Microarray approach | Genome-wide high-throughput analysis of mRNA expression within a short period of time. | Low dynamic range and the need of having the sequences for probe design; Out of fashion since the arrival of next generation sequencing (NGS). | (Bouwmeester et al., 2011; Fielding et al., 2012) |
| RNA-sequencing approach | Relative to microarrays, RNA-seq has been reported to offer higher precision estimates of transcript abundance, a greater dynamic range, and detection of novel transcripts with a broader dynamic range. | Gene expression data are supported statistically and interpreted correctly; more expensive than arrays; Large amount of data needs intensive bioinformatics and statistical analysis. | (Tang et al., 2009a; Wang et al., 2009) |
| Proteomic analysis | Understand gene expression at the translation level; can provide further insights into the effects of nanomaterials on cells. | Gene expression data are supported statistically and interpreted correctly. | (Ge et al., 2011) |

1.5 Iron Based Engineered Nanoparticles

Iron-based nanoparticles (NPs) have been used in many fields, particularly in environmental cleanup and biomedical. Because of their high surface area, NPs have more prominent number of active sites for interaction with diverse chemical species (Zeng et al., 1998), which in turn expanding their applications in tackling the environmental contamination problems.

Among the most widely used iron based NPs, iron sulfides (FeS) NPs, have attracted much more attention from the scientific community due to their high removal capacity. It has been used for removing of pollutant materials covering a broad spectrum from groundwater and soil reviewed by Gong et al. (2016). Moreover, magnetite (Fe₃O₄) NPs have sparked an immense interest in research for engineering application (Li et al., 2006; Shen et al., 2009; Yantasee et al., 2007). It has been intensively used in various biomedical applications such as cell tracking, and drug delivery as it behaves superparamagnetically as their particle size is reduced to a few nanometers. Additionally, it has been applied to wide range of environmental remediation settings as reviewed by Su (2017).

However, bare NPs have a strong tendency to form large aggregates, impeding their delivery and performances. To prevent the particle aggregation, various stabilizers are often employed. For instances, polysaccharide stabilizers, carboxymethyl cellulose (CMC) and starch have been used to successfully stabilize FeS (Gong et al., 2012; Gong et al., 2014) and magnetite NPs (An et al., 2011; Liang and Zhao, 2014; Liang et al., 2012). More and more studies have demonstrated that the stabilized NPs can enhance reactivity and exhibit good mixing and mobility to pollutants to produce rapid and effective cleanup for various contaminants. As a result, the application of coated NPs is showing a great increase. The increasing application of

these iron base NPs will inevitably release to the aquatic system, which could potential impact human health and the environmental safety.

Literature about the toxicity of FeS and its NPs is very limited. To date, there is no research concerning the toxicity of coated FeS NPs. There is also very limited information about coated Fe₃O₄ NPs toxicity when it is applied in environmental remediation fields. Elucidating the fate and eco-toxicologic risk of them in the aquatic environment is urgently needed before they are widely used as remediation materials.

To fill these data gaps, we investigated the effects of selected polymeric coatings for two popular ENPs including FeS NPs and Fe₃O₄ NPs. These particles were selected because they are widely used NPs for environmental remediation. Coatings were selected to test effects when the interaction between nanoparticles and fish are concerned. CMC was used to coat FeS NPs, because it is a commonly used modified biopolymer; while starch, a long-chain polymer of d-glucose, was used as a coating agent for Fe₃O₄ NPs as it is one of the most abundant naturally occurring polysaccharides,.

The ζ potential is an important parameter that governs the interparticle electrostatic interactions and stability of nanoparticles in water. In addition, ζ potential also plays a big role on sorption/desorption behavior of the nanoparticles for contaminants (Liang et al., 2012) . CMC and starch were reported to alter NPs characterization. CMC-stabilized Fe₃O₄ nanoparticles displayed a much more negative surface with a ζ value ranging from -120 to -150 mV at pH above the pK_a value of CMC. Whereas starch coating, a nearly neutral surface was detected over a pH range of 2-9 for starch-stabilized Fe₃O₄ NPs (Liang et al., 2012). CMC and starch were used in our work aiming to evaluate the toxicity of popular iron based NPs coating with these commonly used “green” and cost-effective agents with different characterization, and predict

NPs' environmental impact and potential risk. An understanding of the toxicological effects of each NP type is critical for any prediction of their immediate and long-term risks for humans and ecosystems.

1.6 RNA-seq Technology and Zebrafish

It is claimed that toxicological effects are related to the size, shape, or the stability of the NPs, if so, similar toxicity effects would occur even if the NP composition is different (Pujalté et al., 2011), whereas different toxicological effects would be predicted if particle composition controls the interaction with the biological surface (Griffitt et al., 2007; Nair and Choi, 2011). It raised the key question of whether toxicological effects are due to general properties shared by diverse NP types or whether they are specific to each NPs.

A powerful approach to determine how an organism responds to a particular abiotic condition is to determine how it alternates the expression of its genome. Modern transcriptome methodologies can quantify the expression of most genes in an organism with their RNA transcripts levels when exposed to an abiotic condition and under normal physiological conditions (Chen et al., 2012). Comparisons of the effects of other specific biotic or abiotic conditions can tell degrees of similarity or difference. For example, if NP exposure triggers a particular stress condition, then this can be recognized by differential expression in the transcript levels of specific sets of genes. Effects on specific physiological or biochemical processes can be evaluated by alteration of transcript levels of genes that are known or predicted to function in them. The transcriptome sequencing (RNA-seq) approach generates a vast inventory of gene transcripts using massive parallel DNA sequencing technologies, bioinformatics, and sequence databases (Wang et al., 2009). Therefore, transcriptome profiling offers substantial and detailed

information about toxicological responses, suitable to identifying potential new biomarker of acute and chronic stress, which can complement the results of other approaches.

Zebrafish (*Danio rerio*) have become a popular biology model for nanotoxicology due to its exceptional set of characteristics (Bar-Ilan et al., 2009; Hill et al., 2005). Moreover, it's easy to handle, smaller size, genetics amenability and breeding potential. Importantly similarity at the molecular and physiological levels with humans (Westerfield, 2000b) renders these organisms as the most suited model organism for toxicological studies.

1.7 Objectives of This Research

This work aims to gain insight into the molecular mechanisms underlying the adaptive response of zebrafish to coated NPs, identify nanoparticle-specific genes and signaling pathways in the fish, and determine coating effects on NP toxicity.

The two-representative iron based NPs, CMC-stabilized FeS and starch-stabilized magnetite NPs, will be evaluated. The overall goal of this research is to investigate the stress response of adult zebrafish to stabilized FeS and Fe₃O₄ NPs through state of the art of RNA-sequencing techniques together with tissue burdens and a histological alternations assessment. Differentially expressed gene (DEG) profiles, gene ontology (GO) and the Kyoto encyclopedia of genes and genomes (KEGG) pathways will be acquired and analyzed to ascertain genomic responses to the specific stress under the stabilized NPs. The reliability of the transcriptomic results will be validated by qPCR analysis of selected genes.

The specific objectives of this study are to:

- (1) Determine the physiological effects of stabilized FeS and Fe₃O₄ NPs on adult zebrafish;

- (2) Examine of the bioaccumulation levels of the NPs in adult zebrafish tissue;
- (3) Analyze the gill and liver histological alteration;
- (4) Perform gill and liver transcriptomics analysis to evaluate the gene regulation response and signaling pathway under the nanoparticle-induced stress.

1.8 Organization of This Dissertation

This dissertation includes four chapters. Chapter 1 (General Introduction) outlined the background information and objectives of this dissertation. Chapter 2 and 3 of this dissertation are formatted in a standard journal paper. Chapters 2 present the analysis on toxicity of CMC stabilized FeS NPs on zebrafish. This chapter prepared in the format of “*Scientific Reports*” is under review. Chapter 3 introduces coating effects of magnetite NPs on cellular uptake, toxicity and gene profiles of zebrafish. This chapter prepared in the format of “*Science of the Total Environment*” is also under review. Chapter 4 (Conclusions and Suggestions for Future Research) gives a summary of major conclusions of this research and suggestions for future work.

Chapter 2 Toxicity and Transcriptome Sequencing (RNA-seq) Analyses of Adult Zebrafish in Response to Exposure Carboxymethyl Cellulose Stabilized Iron Sulfide Nanoparticles

2.1 Introduction

Iron sulfide (FeS) nanoparticles (NPs) have attracted increasing attention in the environmental remediation field due to their high adsorption capacity and reduction power for a variety of important pollutants (Gong et al., 2016). It has been used for removal or immobilization of a broad spectrum of pollutants (e.g., heavy metals, metalloids, oxyanions, radionuclides, chlorinated organic compounds, nitroaromatic compounds, and polychlorinated biphenyls) in soil and water (Butler and Hayes, 1998; Han et al., 2011a; Han et al., 2011b; Hyun et al., 2012; Jeong and Hayes, 2007; Livens et al., 2004; Mullet et al., 2004; Oh et al., 2011; Skyllberg and Drott, 2010; Watson et al., 2001).

To facilitate in situ remediation of contaminated soil and groundwater, stabilized FeS nanoparticles are often employed. Typically, stabilized nanoparticles are prepared by coating certain organic molecules on nanoparticles to prevent the nanoparticles from aggregation. Of the various stabilizers reported so far, carboxymethyl cellulose (CMC) represents one of the best stabilizers, which is not only effective, but also green and inexpensive. For instance, Gong et al. (Gong et al., 2012; Gong et al., 2014) prepared and tested CMC-stabilized FeS for highly effective removal/immobilization of mercury in soil and groundwater. In addition to purposely stabilized nanoparticles, particles in the environment may become “passively” stabilized by

dissolved organic matter (DOM) in the natural environmental systems. Compared to the non-stabilized counterparts, stabilized nanoparticles are often much smaller in size, more mobile in the environment, and more reactive. They are more transportable in soil or water, and may pose broader and more severe toxic effects on the environment and biota. Yet, little information is available on the toxicity of stabilized nanoparticles.

To assure environmentally safe application of stabilized FeS nanoparticles, it is important to understand the potential environmental risks to the ecosystem and human health. The aquatic environment is particularly vulnerable to manufactured nanoparticles, as it acts as a sink for virtually all environmental contaminants (Scown et al., 2010). Consequently, understanding the fate and eco-toxicological risks of nanoparticles in the aquatic systems is urgently needed.

However, our knowledge about the toxicity of FeS, especially stabilized FeS, is very limited. Bare FeS particles were reported to bind with DNA, limiting the ability of DNA to interact with other nucleic acids and amino acids (Hatton and Rickard, 2008). Furthermore, it was shown that FeS at concentrations below its solubility limit particles may pose genotoxicity by reacting with polynucleic acids, whereas FeS at concentrations above the solubility limit may nick DNA molecules, resulting in relaxation to more stable configurations and a consequent modification of function (Rickard et al., 2011). It was also reported that FeS particles can suppress the growth of microorganisms and plants. For instance, in the presence of 2×10^{-5} M to 5×10^{-3} M of non-stabilized FeS particles, *E. coli* growth rate was reduced under anaerobic conditions (Higgins, 2011). FeS particles may impede nutrient uptake and were found partially responsible for the reduced seed production and viability when precipitated on the roots of wild rice plants (Pastor et al., 2017). However, the underlying molecular mechanisms governing the genotoxicity of FeS remain largely unknown.

The recently developed transcriptome sequencing (RNA-seq) technique provides a powerful tool for investigating the genotoxic effects and the molecular mechanisms in organisms after a chemical exposure. It is particularly useful for studying emerging environmental pollutants, such as nanoparticles, with limited toxicological information since it allows for a global examination of biological response through gene expression. Zebrafish (*Danio rerio*), whose genome has been completely sequenced, is a common model organism for investigating genotoxic effects of chemicals, and it has been used in studying the eco-toxicological effects of manufactured nanoparticles (Bar-Ilan et al., 2009; Hill et al., 2005).

As the environmental applications of stabilized NPs continue to rise, it becomes critical to understand their potential environmental implications. To this end, this study aimed to investigate the stress response of adult zebrafish to bare and CMC-stabilized FeS nanoparticles (CMC-FeS) through the state of the art of RNA-seq technique together with the tissue burdens. And histological alternations of CMC-FeS NPs was assessed. Differentially expressed genes profiles, gene ontology (GO) and Kyoto encyclopedia of genes and genomes (KEGG) pathways were acquired and analyzed to ascertain genomic responses to the specific stress under bare and CMC-FeS NPs exposure. The reliability of the transcriptomic results was validated by qPCR analysis of selected genes.

2.2 Materials and Methods

2.2.1 Synthesis and characterization of bare and CMC-FeS NPs nanoparticles

Stabilized CMC-FeS NPs were prepared in 1000 mL flask with nitrogen purging/mixing. First, a CMC solution (0.1%, w/w) was prepared by dissolving CMC with deionized (DI) water and the solution was purged with purified N₂ (>99%) for half an hour to remove dissolved oxygen (DO). Likewise, a solution of 0.0114 M FeSO₄ and 0.0152 M Na₂S were also prepared

with N₂ purged DI water. Then, the FeSO₄ solution was mixed with the CMC solution to yield a desired concentration of iron and the stabilizer. In this work, 0.001% (w/w) of the CMC was used to stabilize 10 mg/L FeS nanoparticles (i.e. a CMC-to-FeS molar ratio of 0.0005). The mixture was then purged with purified N₂ for half an hour to complete the formation of Fe²⁺-CMC complexes. Then, the Na₂S solution was introduced into Fe²⁺-CMC solution at an Fe-to-S molar ratio of 1:1 to yield the FeS nanoparticles. For comparison, bare FeS NPs were prepared without CMC in otherwise identical conditions. The nanoparticles were characterized within 1h of preparation.

The morphology of CMC-FeS was determined by Transmission Electron Microscopy (TEM) at 200KV accelerating voltage (JEM-2100, JEOL, Tokyo, Japan). The hydrodynamic diameter and zeta potential (ζ) of bare and CMC- FeS NPs were determined by dynamic light scattering (DLS) using a Malvern Zetasizer Nano ZS (Malvern Instruments, Worcestershire, U.K.), bare FeS NPs were subjected to sonication for 10 mins before testing. In this paper, all data on particle sizes are given as mean \pm standard deviation.

2.2.2 Zebrafish experimental study

All procedures involving the handling and treatment of fish used during this study were approved by the Animal Care and Use Committee at the Heilongjiang River Fisheries Research Institute (ACUC-HRFRI). All experiments were conducted in accordance with the relevant guidelines and regulations.

The zebrafish (*Danio rerio*) were obtained from the Heilongjiang River Fisheries Research Institute Zebrafish Facilities. Adult zebrafish of both sexes with an average age of 6 months, average weight of 0.61 ± 0.10 g and average length of 44.27 ± 2.77 mm was selected for the study. The fish were fed daily with commercially purchased fish food and maintained in aquaria with

dechlorinated tap water at a temperature of $25\pm 1^\circ\text{C}$ with a 14h:10h light and dark cycle with continuous aeration with an aeration pump for four weeks before use. As suggested in “The Zebrafish Book”, adult zebrafish can be raised in tap water (Westerfield, 2000a), the detailed tap water parameters are listed in **Table 2.1**. The fish were removed from aquaria and placed in static tanks with dechlorinated tap water and fasted for 24 h prior to each experiment, and no fish died before the intended exposure.

Table 2. 1 Tap water parameters for raising adult zebrafish

| Parameters | pH | Conductivity ($\mu\text{S}/\text{cm}$) | Ca (mg/L) | Mg (mg/L) | Al (mg/L) | Fe (mg/L) | Cl ⁻ (mg/L) | SO ₄ ²⁻ (mg/L) | Cu ($\mu\text{g}/\text{L}$) | Hardness (mg/L) |
|------------|------|---|--------------------------------|--------------------------------|--------------------------------|--------------------------------|---|---|----------------------------------|--------------------------------------|
| Values | 7.12 | 388 | 11.970 | 5.892 | 0.015 | 0.027 | 5.95 | 5.35 | 7.29 | 54.153 |

The sub lethal concentrations (LC_{50}) were determined following the Organization for Economic Cooperation and Development (OECD) guidelines for testing chemicals (OECD). Five different concentrations of CMC-FeS suspensions (100, 50, 25, 10 and 5 mg/L as total Fe) were prepared prior to use. The zebrafish were randomly assigned to 5 groups (10 fish each) and in turn exposed to each concentration for 96 h in 1 L beaker containing 1 L of a test solution. The sixth group of 10 fish was used as no-dose control. Each treatment was run in triplicates under the same conditions with the natural light/dark cycle. For maintaining the quality of water, the fish were not fed for 24 h prior to the experiments and during the experiments for minimizing the absorption of nanoparticles by the food. The water temperature was maintained at $25\pm 1^\circ\text{C}$ and pH in the range of 6.8-7.3. The number of dead fish was recorded every 12 h and they were removed from the treatment beaker immediately to avoid contamination.

After the LC_{50} was determined to be 21.0 mg/L as total Fe, approximately half of the LC_{50} dose, i.e., the LC_{25} ($\text{LC}_{25}=10.5 \text{ mg}/\text{L}$ as total Fe) was applied once in every day to 10 fresh

zebrafish in 1 L test solution beaker for 96 h. For comparison, 96h acute toxicity test was also performed with 10 mg/L bare FeS NPs in triplicate in otherwise identical conditions. After exposure for 96 h, zebrafish in each treatment were rinsed with DI water for three times to remove the nanoparticles on fish surface for further testing. To measure the amount of Fe²⁺ released from CMC-FeS into the solution, control testing suspensions were filtered at time zero and 24 h of preparation using a 25 nm Millipore membrane filter (Millipore Corp., Billerica, MA, USA) and dissolved Fe concentrations were analyzed using an Agilent 7500 cx ICP-MS (Agilent Technologies, USA) equipped with an Octopole Reaction System (ORS).

2.2.3 Tissue accumulations

After 96 h of exposure, three zebrafish were removed from each of the triplicate testing beakers including the control, and then euthanized with tricaine methanesulfonate (MS222). The tissue samples were weighed 0.41 ± 0.10 g, and then digested for analyzing the Fe content. The digestion was performed in a MarXpress microwave system (CEM, USA). A homogenized tissue sample was transferred into a PTFE (polytetrafluoroethylene) vessel. Then, 5 mL HNO₃, 2 mL H₂O₂ and 3 mL ultra-pure water were added, and then the temperature was ramped to 185 °C in 10.5 min, and kept at this temperature for 14.5 min. After cooling to room temperature, the samples were filtered using 0.45µm filter. Finally, 0.5 mL of a 100 mg /L internal standard Mix solution (Agilent Technologies, USA) was added into the filtrates and then diluted to a final volume of 50 mL using ultra-pure water. The samples were then analyzed for total Fe concentration via an ICP-MS system. Fish tissues in the control were also digested in the same way.

2.2.4 Histopathology of liver tissue

Two randomly selected fish were removed from each of the triplicate treatment beakers at 96h of exposure. Fish were euthanized in buffered MS222 and subsequently the liver tissues were dissected. The tissues were fixed in the Davidson's Fixative (95% Ethanol, Acetic acid, formalin and deionized water) in cassettes for 48 hours. Then the tissues were stored in 70% ethanol. Further, the tissues were dehydrated using graded ethanol series 80%, 90%, 95% and 100% ethanol for 60 mins each, then another 30 mins in 100% ethanol, followed by 60 mins in Xylene, and another 60 mins in fresh Xylene. The carcasses were subsequently transferred to a Tissue Embedding System, and the tissues were embedded in paraffin. The tissue blocks were sectioned into 6 μm thick ribbons with microtome. The ribbons were transferred to a water bath set at 45°C. Selected tissue sections were placed on slides, which were set vertical to air dry and then placed on a slide warmer set at 45 °C until completely dry. The slides were then stained using the hematoxylin and eosin (H&E) stain by the method of Shehand and Hrapchak (Sheehan and Hrapchak, 1980). The stained slides were mounted and covered with a coverslip. The slides were observed using a light microscopy on an Olympus BX40 microscope and photomicrographs were taken using an Olympus BX53 digital camera.

2.2.5 High-throughput transcriptomic sequencing

2.2.5.1 Total RNA isolation and illumina sequencing

Total RNAs were isolated from triplicates of liver tissue (each replicate consisted of tissues pooled from three fishes) at control and bare or CMC-FeS NPs treated zebrafish group. The tissue was homogenized in the TRIzol® Reagent and total RNA was extracted using RNeasy Mini Kit (Qiagen, Hilden, Germany) following the manufacturers protocol. The quantity and quality of RNA were examined by Thermo Scientific™ NanoDrop™ 8000 Spectrophotometer and Agilent 2100 Bioanalyzer (Agilent Technologies, Santa Clara, CA, U.S.). Only RNA with

OD 260/280 \geq 1.8 and RNA integrity number \geq 7 were selected for the following experiments. Equal quantities of high quality RNA from each tissue sample were pooled together for cDNA synthesis and sequencing.

After generating the clusters, library sequencing was performed on an Illumina HiSeq 4000 platform, to create paired-end reads with lengths of 150 bp.

2.2.5.2 Bioinformatics analyses

The quality control of RNA-Seq data was conducted by NGS QC Toolkit (Patel and Jain, 2012) with default parameters. Clean paired-end reads were aligned to the zebrafish reference genome sequence, GRCz10 version (Chen et al., 2014), using TopHat (Han et al., 2011a).

To identify differential expression genes (DEGs) between bare or CMC-FeS NPs treated group with control samples, the expression level for each transcript was calculated using the fragments per kilobase of exon according to the million mapped reads (FRKM) method. Cuffdiff (<http://cufflinks.cbc.umd.edu/>) (Trapnell et al., 2013) was used for the differential expression analysis. The DEGs between two samples were selected based on the following criteria: 1) the logarithmic of fold change was greater than 2, and 2) the false discovery rate (FDR) should be less than 0.05. To understand the functions of the differentially expressed genes, gene ontology (GO) functional enrichment and Kyoto encyclopedia of genes and genomes (KEGG) pathway analysis were carried out by Goatools (<https://github.com/tanghaibao/Goatools>) and KOBAS (<http://kobas.cbi.pku.edu.cn/home.do>) (Xie et al., 2011a). DEGs were significantly enriched in the GO terms and metabolic pathways when their Bonferroni-corrected P-value was less than 0.05.

2.2.5.3 Experimental validation by qRT-PCR

In order to validate the expression pattern of DEGs identified by RNA-Sequencing, we selected twelve genes from DEGs potentially associated with immune and inflammatory response, detoxification, oxidative stress, and DNA damage/repair for qPCR validation, including *flot2a*, *cp*, *stat2*, *tsc22d3*, *sgk1*, *sod3a*, *cyp1a*, *abcb4*, *krt18*, *pdia4*, *rad51b*, *orc1*. Total RNA was extracted using the TRIzol reagent following the manufacturer's instructions. The RNA quality was assessed using 1% agarose electrophoresis and by measuring the 260/280 nm absorbance ratios. After purification using DNase I (Promega) to remove genomic DNA contamination, the total RNA was reverse-transcribed into cDNA and the gene transcription levels were analyzed using a SYBR Green PCR kit (Toyobo, Osaka, Japan) on an ABI PRISM 7300 Sequence Detector system (Perkin-Elmer, Applied Biosystems). Primer sequences of the selected genes were designed using Primer 3 software (<http://frodo.wi.mit.edu/>) (Table 2.2). The relative gene transcription levels were calculated using the $2^{-\Delta\Delta CT}$ method; beta-actin was used as the reference gene and its transcription was constant among exposure groups. Comparing the relative expression level of twelve selected genes, most results of qPCR were consistent with the results of RNA-Seq. The Pearson's correlation of \log_{10} (fold-change) between qPCR and RNA-Seq was 0.80, indicating the accuracy and reliability of RNA-Seq based transcriptome analysis.

Table 2. 2 Sequences of primers for selected genes.

| Gene Name | Forward primer | Reverse primer |
|----------------|----------------------|------------------------|
| <i>flot2a</i> | CATTCATACGAGGCGAGCAG | CCTTATTCGAGGACGACGGA |
| <i>cp</i> | GGACTGGGAAATGAGGTGGA | GACAGTGCAGTAGCCATGTG |
| <i>stat2</i> | GTCGGAAATCTCGGCTATGC | CTTCTGGAGCTGGAACATGC |
| <i>tsc22d3</i> | GCCTTTCCAAGTCAAGCCAA | GCTCTGTTACAGGTCCGTCT |
| <i>sgk1</i> | GAAAGGGTAGCTTCGGCAAG | GAGTAATGCAGGCCCAACAAAG |
| <i>sod3a</i> | AGTAAACGCAGTGGGAATGC | CAGATGAGGCTTGGTGATGC |
| <i>cyp1a</i> | TGGAGCTAATTGGCACTGGA | TAGGCGCATGAGCAGATAACA |
| <i>abcb4</i> | TGGCCTGACGTTCTCTTTCT | CTCTCCAACCTGCCATTGCTC |
| <i>krt18</i> | GAGTGCAAGTGGTAGCACAG | CCAGACGGTCGTTCAAGTTC |
| <i>pdia4</i> | AGGTCCAGACCCTGAAACAG | ATACGCTGCATCTTCATCGC |
| <i>rad51b</i> | TAAGACAGCAGTCCTGCACA | GGGAACAGGAGTCATGGGAA |
| <i>orc1</i> | GGCAGCTCTTTCAGGTGATG | CACTGCCTTTCTGCTGGTTT |

2.3 Results and Discussion

2.3.1 Characterization of bare FeS NPs and CMC-FeS NPs

Transmission electron microscopy (TEM) was used to confirm size and elemental compositions of synthetic CMC-FeS NPs. As shown in **Fig. 2.1a**, the nanoparticles appear mainly spherical. **Fig. 2.1b** shows the size distribution of CMC-FeS, estimated with the ImageJ software. The mean particle size was 32.18 ± 5.25 nm, which is comparable to the CMC-FeS NPs synthesized by Gong et al. (2012). The mean hydrodynamic diameter of fresh made CMC-FeS NPs was 352.65 ± 10.68 nm, which grew to 398.50 ± 7.78 nm after 24h of aging as measured by DLS. The bare FeS NPs was observed as much larger particles. The DLS-based method was not applicable to the bare NPs because of the rapid gravity settling effect (He and Zhao, 2008). The zeta-potential of CMC-FeS were -48.40 ± 1.27 mv at 0h and -44.55 ± 5.02 mv at 24h (**Table 2.3**), indicating the stable dispersion of the CMC-FeS NPs. The highly negative surface of CMC-FeS confirmed that the attachment of CMC on the FeS nanoparticles induced strong electrostatic repulsion, thereby preventing the particles from agglomeration. However,

sonicated bare FeS NPs had a zeta potential of -26.85 ± 1.20 mV at 0h, it increased to 1.05 ± 1.12 mV at 24h (**Table 2.3**), indicating that the agglomeration of the NPs while aging.

At the 10 mg/L FeS dosage, the dissolved Fe concentration was both under 0.20 mg/L for bare and CMC-FeS NPs, indicating that the nanoparticles were essentially constant throughout the exposure period.

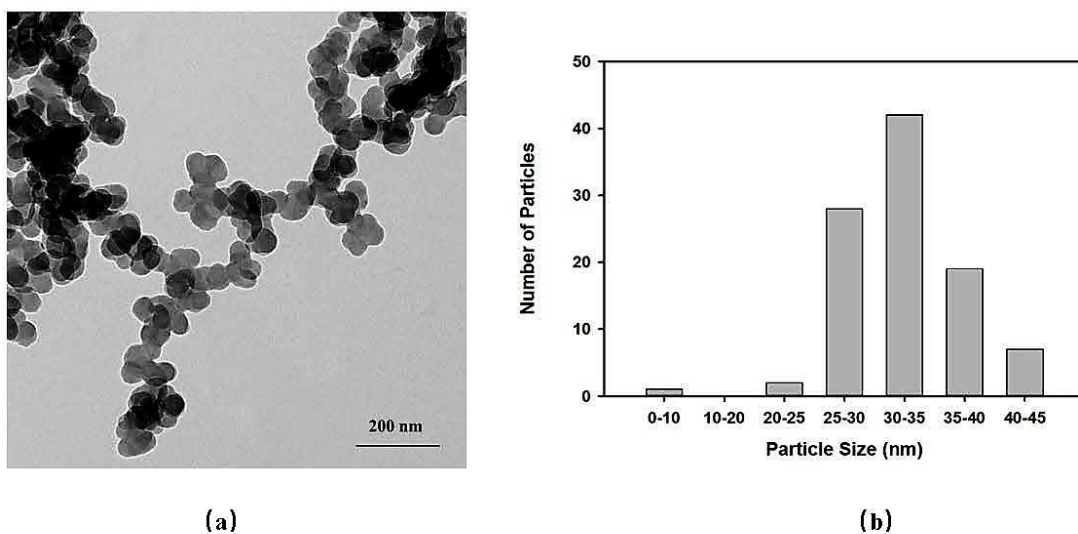


Figure 2. 1 Transmission electron microscopy (TEM) image (a) and the histogram of size distribution (b) of CMC-stabilized FeS nanoparticles (FeS = 10 mg/L, CMC = 0.001 wt.%). The mean particle size is 32.18 ± 5.25 nm. (Scale bar represents 200 nm)

Table 2. 3 Mean hydrodynamic diameters and zeta potential of freshly prepared and 24-h aged bare and CMC-FeS NPs.

| Samples | Aging time (h) | Hydrodynamic diameter (nm) | Zeta-potential (mV) |
|--------------|----------------|----------------------------|---------------------|
| Bare FeS NPs | 0 | ND | -26.85 ± 1.20 |
| | 24 | ND | 1.05 ± 1.12 |
| CMC-FeS NPs | 0 | 352.65 ± 10.68 | -48.40 ± 1.27 |
| | 24 | 398.50 ± 7.78 | -44.55 ± 5.02 |

2.3.2 Acute toxicity evaluation

CMC was used as a coating material for FeS NPs. There are several advantages to the use of CMC: (a) CMC are widely used in biomaterials, pharmaceutical formulation (FDA Inactive Ingredients Database), and food (FDA database of Select Committee on GRAS substances reviews); (b) CMC is claimed to be bioeliminable (Turaev, 1995) and has been approved by FDA for parenteral use; (c) CMC presents as an attractive candidate polymer due to a high carboxylate D S (degree of substitution) (0.8) compared to other polysaccharides (0.2–0.5), enabling the incorporation of high particle content and increased particle-forming properties (Ernsting et al., 2011). On an equal weight basis, CMC with a greater M.W. or higher D.S. can facilitate smaller nanoparticles formation at lower temperature. For instance, it is proposed that CMC forms a bulky and negatively charged layer via sorption of CMC molecules on the ZVI nanoparticles, it could accelerate nucleation of Fe atoms during the formation of zero valent iron (ZVI) nanoparticles and, subsequently, preventing the nanoparticles from agglomeration through electrosteric stabilization (He and Zhao, 2007). CMC (D.S. = 0.7) toxicity test was conducted using *Pseudomonas putida*, *Selenastrum capricornutum*, *Daphnia magna*, and *Brachydanio rerio*. In terms of *Brachydanio rerio*, no mortality was found at concentration of 2500 mg/L after 96h. And the subsequently, the acute toxicity of CMC intermediates to *Brachydanio rerio* was assessed using conventional methods. No toxicity was detected at 1000 mg/L; There were no toxicity detected on other organisms as well, therefore, authors claimed that biologically treated CMC does not exhibit toxicity (VanGinkel and Gayton, 1996). In our study, 0.001% (w/w) of the CMC was used to stabilize 10 mg/L FeS nanoparticles, the concentration of CMC can be converted to 10 mg/L, which is 250 times less than the CMC used in the study of (VanGinkel and Gayton, 1996), so no toxicity is expected for CMC toward zebrafish in our study. Therefore, CMC control toxicity on adult zebrafish is not necessary in our test.

The results showed that the CMC-FeS NPs were acutely toxic to zebrafish with a LC₅₀ concentration of 21.0 mg/L at a 96h static exposure. Consequently, the nanoparticle dosage at the LC₂₅ was used in the subsequent exposure experiments (LC₂₅ is the highest exposure concentration possible to ensure adequate live organisms for downstream gene expression analysis (Poynton et al., 2010). The exposure to LC₂₅ for 96 h resulted in no fish mortality in bare and CMC-FeS NPs treated group, and no visible difference in behavior between control and treated group was observed. However, the exposure to 100 mg/L of CMC-FeS NPs (the maximum tested concentration) caused 100% mortality in 12 h. Moreover, aggressive behavior was observed within the 1 h of treatment showing a sign of toxicity stress. For instance, the swimming speed and respiratory rate were increased and fish were trying to jump out of the solution. The surface respiration took place and ultimately the fish lost their balance and presented jerky movements and sank on the bottom of the beaker before death. Extravasation of the blood was observed in the anterior ventral surface of the body, behind the head of fish. But, no such behavioral changes and extravasation of blood were observed at lower dosages of CMC-FeS NPs (10 mg/L and 5 mg/L as Fe) and the pigment of color was normal in all the fish.

Total iron concentrations in the fish tissues after 96 h were determined to be 12.71 ± 1.63 mg/kg iron in the control group, and 28.16 ± 3.93 mg/kg for the CMC-FeS treated group, showing a 2.2 times Fe concentration increase after the exposure.

2.3.3 Histological analysis of liver tissue

It is generally accepted that chemicals/toxicants first elicit biological changes at the molecular level. Toxicant-induced dysregulation of gene expression may subsequently lead to biological changes at the cellular level. The liver as the key innate immune organ for

detoxification is very susceptible to damage. Typically, histological observation of key immune organ can reveal abnormal immune cells/tissues as well as in vivo molecular changes.

Our results indicated that accumulation of CMC-Fe NPs resulted in observable morphological alterations in liver tissue at the tested exposure concentrations and duration. The control group showed normal hepatocytes (**Fig. 2.2a**), and while the CMC-FeS NPs treated group showed cells with pyknotic nuclei and the presence of vacuolization suggesting early stages of apoptosis (**Fig. 2.2b**) and the tissues exhibited clear signs of toxic effects, thereby reducing the detoxification processes of zebrafish. This agrees with an earlier study where histopathological changes such as pyknosis occurred in zebrafish liver after exposure to AgNP due to oxidative stress and apoptosis (Choi et al., 2010).

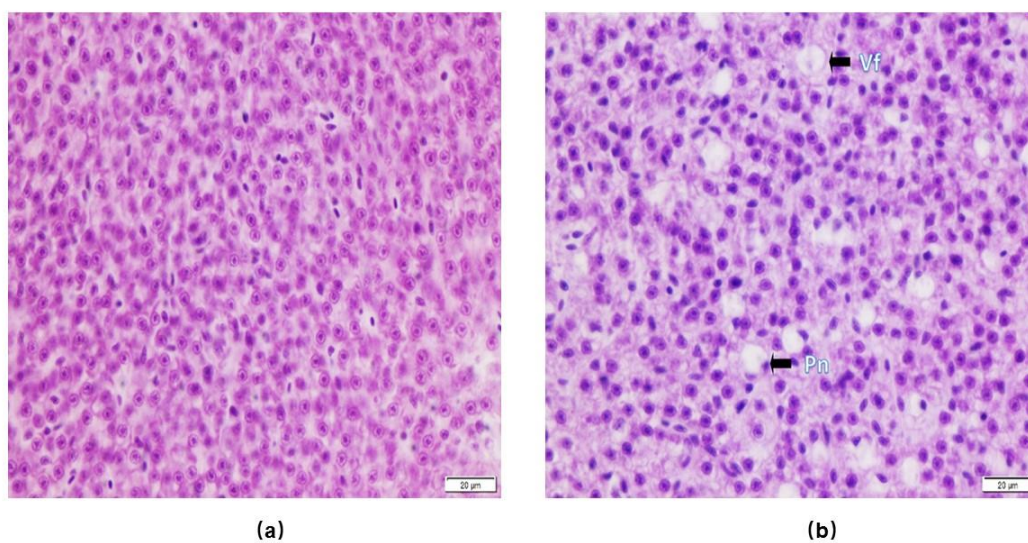


Figure 2. 2 Histological analysis of the liver of Zebrafish in control **(a)** and upon CMC-FeS exposure **(b)**.The liver of control zebrafish had normal hepatocytes, while the nanoparticle treated groups showed pyknotic nuclei (pn), and vacuole formation (vf). The scale bar represents 20 μm .

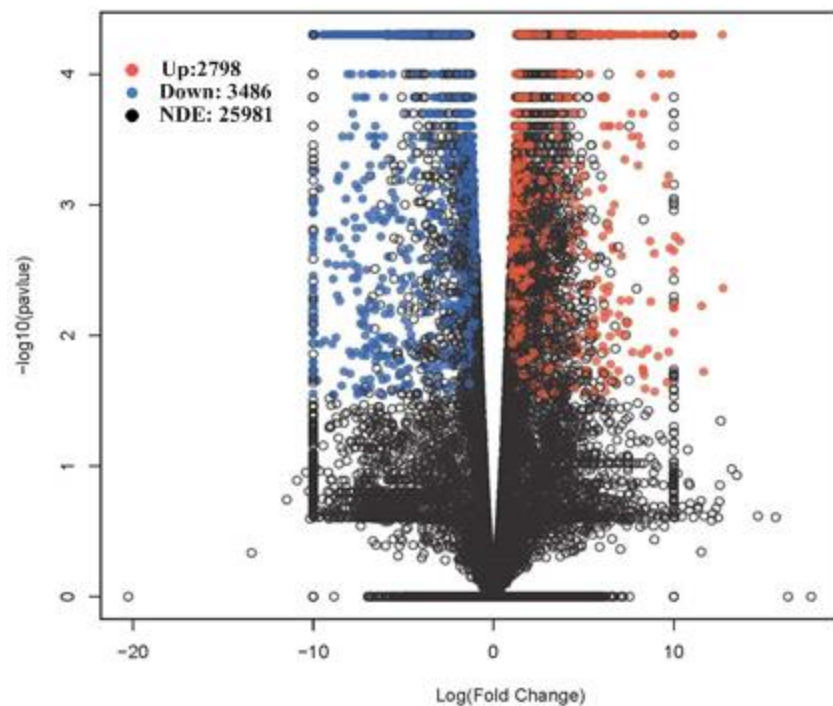
2.3.4 Transcriptomic analysis for bare and CMC-FeS NPs

The effect of bare and CMC-FeS NPs on zebrafish was then explored by screening the genes involved in toxicity and analyzing GO and KEGG pathways using RNA-seq technology. The results revealed that the exposure and/or accumulation of bare or CMC-FeS NPs induced dramatic alterations in global gene transcription profiles in zebrafish livers.

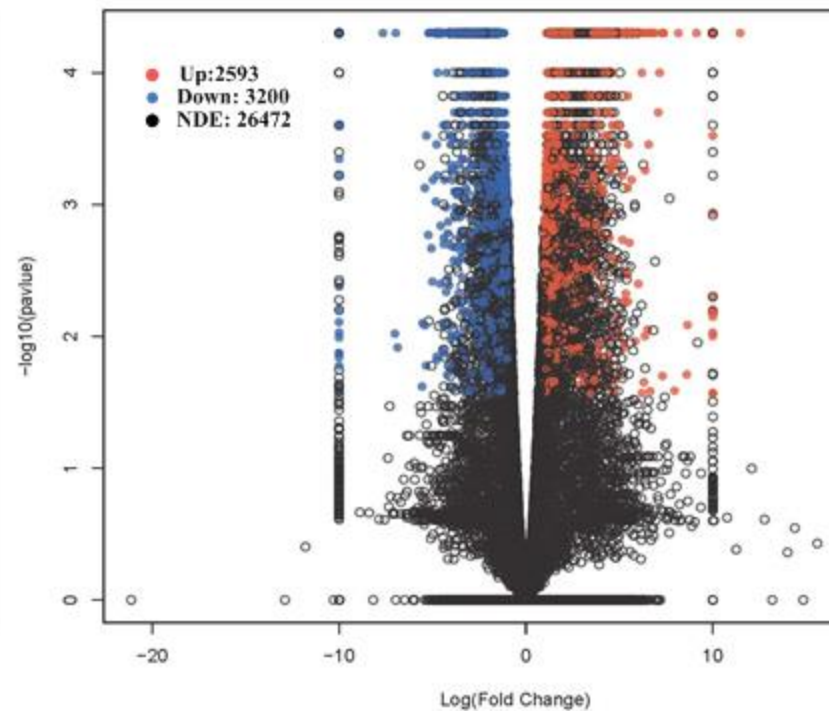
The differences in the gene regulatory pathways were analyzed with the liver tissue. It produced approximately 429,317,880 total clean reads from the 65.8 Gbp clean sequence data for all the biological replicates. More than 88% of the clean reads had quality scores over the Q30 value, and over 83% of the total reads were uniquely mapped to the reference genome for the liver (**Table 2.4**).

Table 2. 4 Summary of sequence data generated for zebrafish transcriptome and quality filtering.

| Samples | Clean reads | Mapped reads | Mapped rate (%) | Q30 percentage (%) |
|----------------|--------------------|---------------------|------------------------|---------------------------|
| Control-1 | 37,220,362 | 32,336,730 | 86.88 | 91.69 |
| Control-2 | 41,194,526 | 34,871,813 | 84.65 | 96.16 |
| Control-3 | 67,918,028 | 57,520,603 | 84.69 | 95.85 |
| FeS NPs-1 | 59,012,990 | 51,849,910 | 87.86 | 92.24 |
| FeS NPs-2 | 51,279,952 | 44,453,683 | 86.69 | 92.65 |
| FeS NPs-3 | 55,317,702 | 49,773,996 | 89.98 | 92.66 |
| CMC-FeS NPs-1 | 40,250,516 | 34,530,413 | 85.79 | 88.49 |
| CMC-FeS NPs-2 | 35,741,238 | 30,230,176 | 84.58 | 94.13 |
| CMC-FeS NPs-3 | 41,382,566 | 34,632,427 | 83.69 | 94.68 |



(a) FeS NPs VS. Control



(b) CMC-FeS NPs VS. Control

Figure 2. 3 Volcano plots for gene libraries of zebrafish liver showing variance in gene expression with respect to fold change and significance (P-value). **(a)** Expressed genes for untreated (control) and bare FeS NPs treated zebrafish, **(b)** Expressed genes for untreated and CMC-coated FeS NPs treated zebrafish. Each dot represents an individual gene: Red dots refer to the up-regulated DEGs, Blue dots to the down-regulated DEGs, and black dots to not differentially expressed genes (NDE).

A total of 6,284 DEGs (up-regulated DEGs: 2,798, 44.5%, down-regulated DEGs: 3,486, 55.5%) in the livers were found for the group exposed to bare FeS NPs, compared to 5,793 DEGs (up-regulated DEGs: 2,593, 44.8%, down-regulated DEGs: 3,200, 55.2%) identified significantly expressed for CMC-FeS NPs treated group (**Figure 2.3**). The 8.5% more DEGs for the bare FeS NPs treated group were identified suggesting that livers are more susceptible to the bare FeS NPs than CMC-FeS NPs.

Furthermore, a great proportion of overlap were found for up and down regulated DEGs in both treatments (1,871 shared up-regulated DEGs and 2,639 shared down-regulated DEGs) in the livers (**Figure 2.4**), indicating that the two treatments shared some regulatory mechanisms beyond the coating effects.

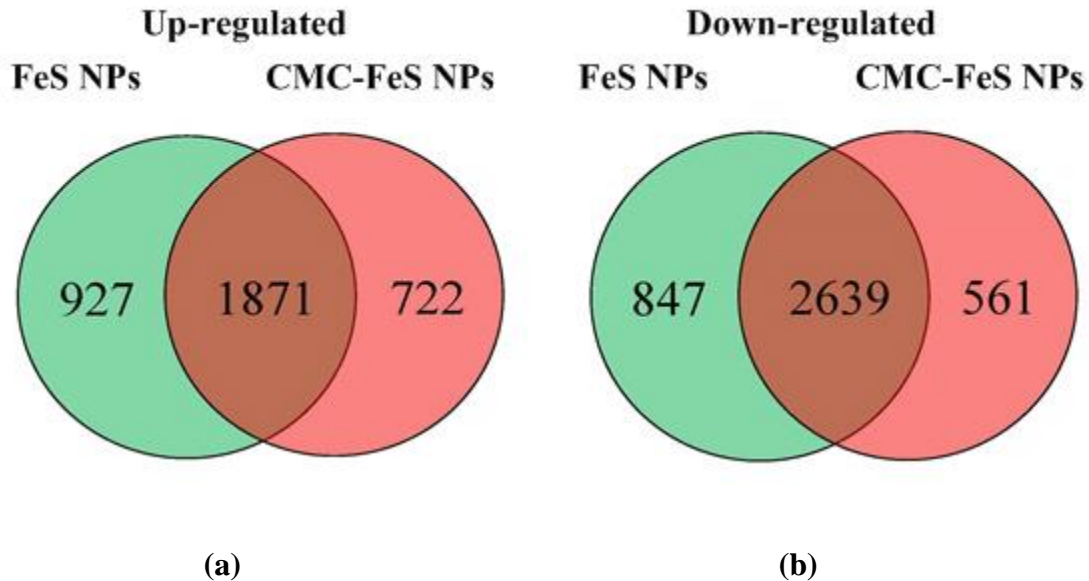


Figure 2. 4 Venn diagram showing number of genes identified with up- or down-regulated expression ($P < 0.05$) in zebrafish livers upon exposure to bare and CMC-coated FeS nanoparticles. (a) Overlap of up-regulated DEGs, (b) Overlap of down-regulated DEGs.

When nanoparticles are introduced to organisms, NPs would trigger gene expression regulation, which are known to be induced during oxidative stress and other stress conditions (Simon et al., 2013). Although both forms of FeS NPs with 10 mg/L of total Fe did not exert cause mortality to the zebrafish, they were still capable of triggering gene regulations related to immune and inflammation response, ER stress and unfolded protein response, oxidative stress and antioxidant response, impacts on mitochondria energy metabolism, disruption of DNA damage and repair, and heat shock pathways.

A total of 58 and 47 representative genes in livers were identified for bare and CMC-coated FeS NPs treatments, respectively, involving the mitochondria energy metabolism, mitochondria dysfunction pathway, immune and inflammation response, ER stress and unfolded protein response, oxidative stress and antioxidant response, DNA damage and repair and apoptosis pathway. It is noteworthy that the representative genes for the immune and inflammation response, oxidative stress and antioxidant response and mitochondria dysfunction pathway were all upregulated for both treatments, whereas all the genes for the DNA damage and repair were downregulated. Moreover, the changes related to the DNA damage and repair were more pronounced under the exposure to bare FeS NPs as shown in **Fig. 2.5**, suggesting that the CMC can alleviate the toxicity of bare FeS NPs.

Interestingly, our results indicated that bare and CMC-FeS NPs can cause up-regulation of some biomarker genes for inflammation and oxidative stress. The *cp* gene, coding for ceruloplasmin, is an inflammatory-linked gene that was found expressed at a higher level of 14.2-fold and 18.5-fold more in the bare and CMC-FeS NPs treated group compared with the control, respectively. Ceruloplasmin, as an acute phase protein, is synthesized in the liver responding to the acute phase of an inflammation and it also plays a vital role in iron

detoxification; *cp*, also considered as a metalloprotein gene, was found to involve the primary functions of all of the encoded proteins concerning metal ion binding and metal detoxification in birds (Watson et al., 2017), as such, it is considered as an indicator of acute inflammation in birds (Chamanza et al., 1999). Furthermore, *stat2*, a well-known essential and specific positive effector of type I interferons (IFN) signaling, was over expressed 16.8-fold and 12.6-fold respectively in the bare and CMC-FeS NPs treated groups; IFNs are multifunctional cytokines that modulate immune responses and cellular functions (Li et al., 2010b), and activation of *stat2* can trigger inflammation response accordingly. The third differentially expressed gene, *tsc22d3*, encoding a leucine zipper transcription factor, was found up regulated 10.7-fold in CMC-FeS NPs treated group. Strikingly, over expression of *tsc22d3* (32.6-fold) were identified in the bare FeS NPs treated group indicating a more critical stress condition upon exposure. Several studies showed that glucocorticoids (GCs) could induce *tsc22d3*, in turn, *tsc22d3* plays a very important role to regulate the anti-inflammatory and immunosuppressive action of GCs (Ayroldi and Riccardi, 2009). Regulation of *tsc22d3* gene was reported when Caco-2 cells were exposed to 5 nm AuNPs (300 μ M, 72 h) where inflammation stress conditions were found (Bajak et al., 2015). Moreover, multiple immune sensor genes, e.g. *crp*, *b2m* and *b2ml* were up-regulated. To our surprise, *crp* was found extremely over expressed (129.5-fold) in the bare FeS NPs treated group, compared to a 18.2-fold change in the CMC-FeS NPs treated group, again showing a more pronounced toxicity under bare FeS NPs; The up-regulation of these biomarker genes indicated the inflammation response and iron detoxification effect when adult zebrafish was exposed to both FeS NPs.

In addition, *pdia4*, the protein product of an endoplasmic reticulum (ER) chaperones, was found down regulated 2.3 and 5-fold for bare and CMC coated FeS NPs in our study, showing

the evidence for decreased ER function due to stress. A previous report indicated that ER stress in PC12 cells induced by over-expression of β -amyloid precursor protein are also associated with the overexpression of *sgk1* (Copanaki et al., 2007). This finding was consistent with our result that *sgk1* was found over expressed 4.7 and 3.7-fold in the bare and CMC-FeS treated group. Similar finding was reported for zebrafish hepatic inflammation when exposed to Tris (1,3-dichloro2-propyl) Phosphate (TDCIPP) (Liu et al., 2016). It was reported that ER stress can directly induce toll-like receptors (TLRs) and synergize with TLRs to cause inflammatory responses or/and related disease in the liver (Lawless and Greene, 2012). *tlr3* was found over-expressed 27-fold in the bare FeS treated group, but it was not display differentially expressed in the CMC-FeS NPs group, clearly showing the intensified stress under bare FeS NPs. Collectively, up-regulation of inflammatory biomarker genes and induced ER stress strongly suggested that inflammatory response did occur in zebrafish liver upon the both FeS exposure, however, CMC coated FeS exerted less stress than the bare NPs.

Inflammation triggers an increased production of reactive oxygen species (ROS). If not effectively removed by antioxidant defenses, ROS can lead to oxidative stress and damage to cellular macromolecules such as nucleic acids, lipids and proteins (Halliwell and Gutteridge, 2015). Thus, inflammation and oxidative stress are tightly linked.

Oxidative stress has been proposed as a possible mechanism involved in the toxicity of nanoparticles (Nel et al., 2006). In our study, the bare and CMC-FeS NPs exposure increased the expression of several oxidative stress related genes such as *sod3a* (29.6 and 19.8-fold for bare and CMC-FeS NPs, respectively) and *cat* (38 and 5.4-fold for bare and CMC-FeS NPs respectively), suggesting the production of ROS. The *cat* gene induction was considered as an indicator of ROS production when zebrafish were exposed to uranium (Lerebours et al., 2009).

The up-regulation of gene expression for constituents of mitochondrial dysfunction pathway (genes including *mt-nd4*, *mt-nd5*, *mt-cyb*, *cox4l1*, *cox6b1*, *mt-co2* and *mt-co3*) further suggested the production of ROS in both FeS NPs treated group. The results agree with a previous study showing the alteration of these mitochondrial dysfunction pathway genes when zebrafish embryos were exposed to Ag nanoparticles, bulk Ag and Ag⁺ by transcriptome analysis (van Aerle et al., 2013). Another stress indicator gene, cytochrome P450 1A (*cyp1a*) was found up regulated upon the bare and CMC-FeS exposure, indicating detoxification of the stressor. Concurrently, *abcb4* (ATP-binding cassette, sub-family B (MDR/TAP), member 4) was significantly up-regulated 21.1-fold and 14.2-fold in bare and CMC-FeS NPs treated group. The ATP-binding cassette (ABC) superfamily of genes encode membrane proteins that transport a diverse set of substrates across membranes. These genes play important roles in protecting organisms from xenobiotics (Dean and Annilo, 2005). It was reported that *abcb4* could affect bioavailability of chemicals to zebrafish embryos (Dean and Annilo, 2005) and adult tissue (Lu et al., 2015). The ATP-binding cassette superfamily of genes was also found over-expressed in liver and gill of zebrafish when exposed to uranium (Lerebours et al., 2009). Meanwhile, another gene family member, *abcb11b*, was induced in liver, highlighting the role of liver in the detoxification process.

Many studies have suggested the toxicity of iron-based nanoparticles are associated with ROS induced oxidative stress, which leads to DNA damage, tissue damage and cell death (Allabashi et al., 2009; Keenan et al., 2009; Wu et al., 2014). The *rad51* play important roles in the maintenance of genomic integrity through recombinational repair (Yokoyama et al., 2004). In this work, DNA damage and repair related genes *rad51* and *chek1* were found 5.4 and 7.2 time more down regulated in the bare FeS NPs group compared to the CMC-coated FeS NPs

group as a result for excessive production of ROS. Moreover, *fas* was identified 77.2-fold upregulated in the bare FeS NPs group but didn't show any significant expression in the CMC-coated FeS NPs group, indicating a severe apoptosis induction with the bare FeS treatment. Similarly, the origin recognition complexes (*orc1*, *orc3* and *orc5*), which are essential proteins for DNA replication, were found down regulated, showing the adverse effect on the cell cycle progression (Lucifò et al., 2013). The significance of the very pronounced increase in *krt18* (17.3 and 12.5-fold in bare and CMC-FeS NPs groups respectively), hepatotoxicity biomarker gene (Liu et al., 2016), further implied an apparent hepatotoxicity under FeS NPs exposure.

Taken together, bare FeS NPs could induce more pronounced toxicity than it with CMC coating, in other words, coating FeS NPs with CMC could alleviate its impact on aquatic organisms.

Histological evidence of liver stress was confirmed by exploring the DEGs under the CMC-FeS exposure. Over expression of *flot2a* (5-fold), which is encoding flotillin 2, a protein previously proposed as involved in nanoparticles transport into cell

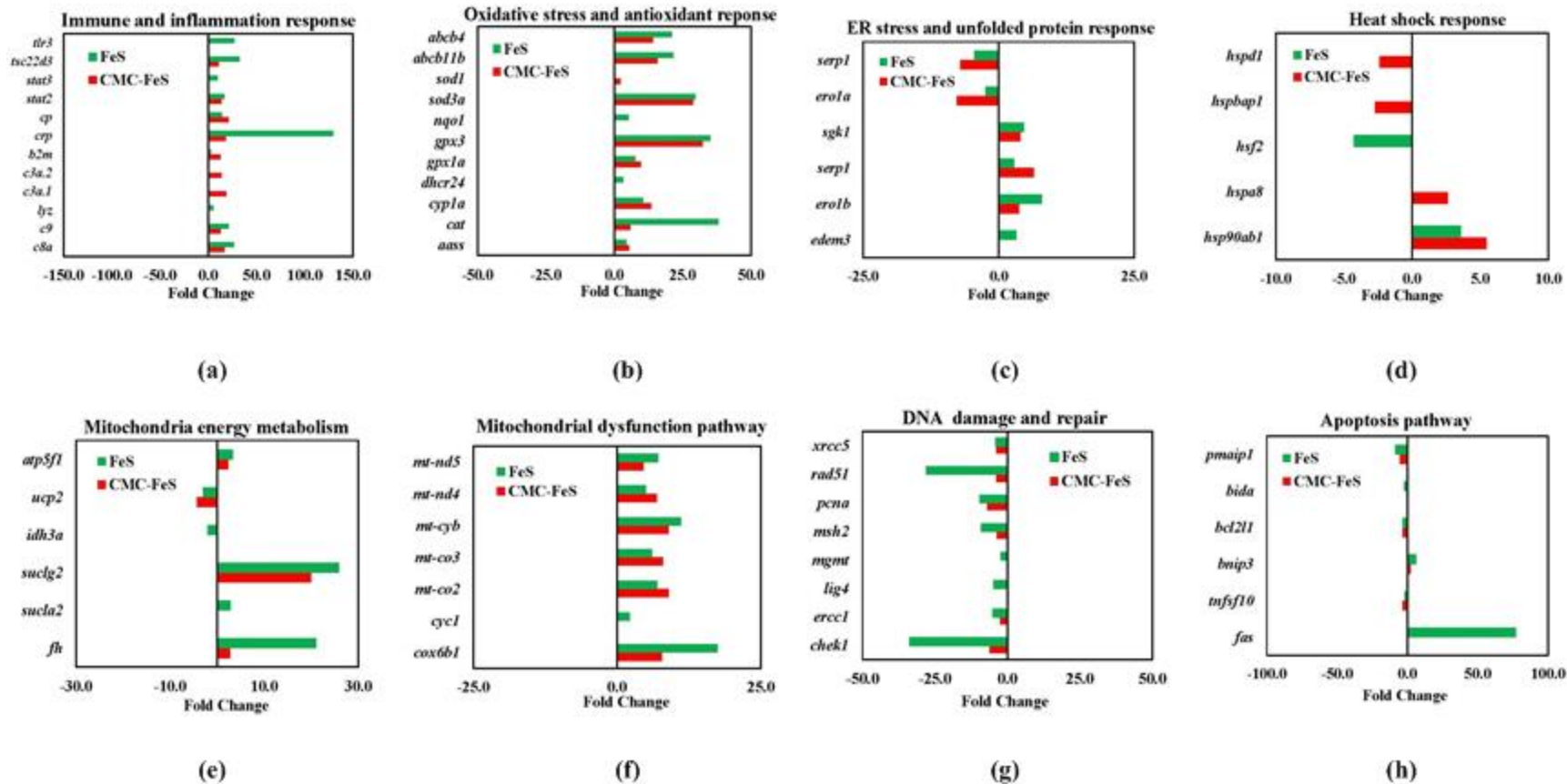


Figure 2. 5 Fold changes of representative genes in zebrafish livers in relation to: (a) immune and inflammation response, (b) oxidative stress and antioxidant response, (c) ER stress and unfolded protein response, (d) heat shock response, (e) mitochondria energy metabolism pathways, (f) mitochondria dysfunction pathway, (g) DNA damage and repair, and (h) apoptosis pathway upon treatments with bare or CMC-coated FeS NPs for 96h (Data shown having fold change < -2 and > 2 at P<0.05).

(Freese et al., 2013; Kasper et al., 2013; Poynton et al., 2012), indicated the nanoparticles were taken up by endocytosis in zebrafish liver cells. The same gene family member *flot1* was found over expressed in liver of fathead minnow when exposed to PVP-coated Ag nanoparticles but not AgNO₃ (Garcia-Reyero et al., 2014). The expression pattern of this gene may provide the insight for the nanoparticle absorption and the cellular uptake mechanism of FeS NPs.

To identify the effects on the transcriptomic pathways, the subset of the genes that were significantly affected by the bare and CMC coated FeS NPs treatment were subjected to the gene ontology (GO) analysis using the Goatools functional enrichment tool. The GO analysis was performed to identify GO pathways with three GO categories: cellular components, biological processes and molecular functions. The basic GO unit is the GO term. Every GO term belongs to a particular category. GO terms with the Bonferroni-corrected P-values < 0.05 were defined as being significantly enriched in DEGs. The majority of the responsive GO terms were found in the biological processes, followed by the molecular functions and cellular components both FeS NPs treatment in zebrafish (**Table 2.5**).

Then we plotted the histogram of the percentage of DEGs in the livers falling into the GO categories for the groups treated with bare or CMC-coated FeS NPs (**Figure 2.6**). Moreover, the GO terms for both treatment followed the same pattern, the biological processes were the most prevalent, and genes associated with the cellular process (GO:0009987), metabolic process (GO:0008152) and single-organism metabolic process (GO:0044699) were most enriched. The most represented DEGs molecular functions were involved in binding (GO:0005488), catalytic activity (GO:0003824) and heterocyclic compound binding (GO:1901363). For cellular components, the cell part (GO:0044464), intracellular organelle part (GO:0043229) and

membrane-bounded organelle (GO:0043227) were the most significantly affected DEGs categories.

Table 2. 5 GO enrichment statistics for bare and CMC coated FeS NPs

| Samples | GO enrichment number | Biological Process | Cellular Component | Molecular Function |
|-------------|----------------------|--------------------|--------------------|--------------------|
| FeS NPs | 2429 | 1453 (59.8%) | 282 (11.6%) | 694 (28.6%) |
| CMC-FeS NPs | 2167 | 1392 (64.2%) | 265 (12.2%) | 510 (23.6%) |

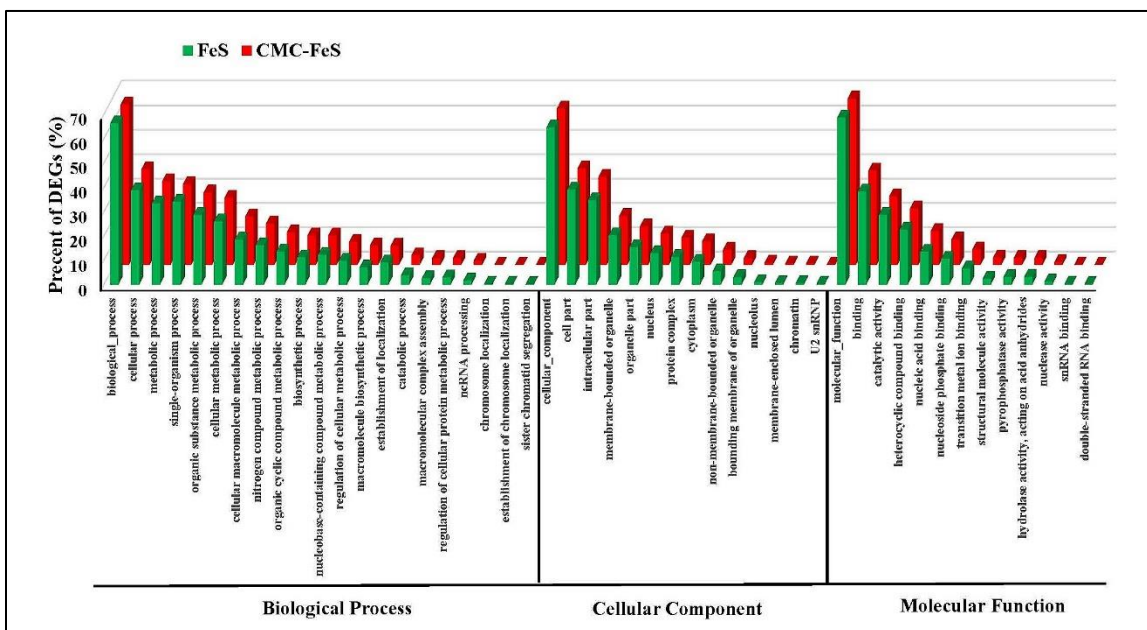


Figure 2. 6 Gene ontology (GO) category patterns of the differentially expressed genes in livers of zebrafish upon exposure to treatments with bare or CMC-coated FeS NPs for 96h. The GO was assigned into three categories: biological process, cellular component and molecular function.

The KEGG pathway analysis also provides evidence for toxic effects within liver tissue. Several KEGG pathways were significantly altered. The high degree of common KEGG pathways (42 up-regulated and 31 down regulated KEGG pathways are common with both treatments) in the livers for the two forms of FeS NPs suggests a very significant overlap in the mechanisms of toxicity of the nanoparticles (**Table 2.6**). The complement and coagulation cascades, related to fish immunity were also found to be significantly upregulated, Cell cycle

was found significantly down regulated in bare FeS NPs group, which is in line with our findings for CMC-FeS treated group.

Table 2. 6 Up or down-regulated and common KEGG pathways statistics for bare and CMC coated FeS NPs treated groups

| KEGG pathways | FeS NPs treated | CMC-FeS NPs treated | Common pathways |
|-----------------------|------------------------|----------------------------|------------------------|
| Up-regulated | 63 | 46 | 42 |
| Down-regulated | 34 | 37 | 31 |

Overall, the comparison of transcriptome profiling indicated that CMC coating can alleviate FeS NPs toxicity over the liver tissue, which may be associated with the characteristics of the NPs.

The most significantly enriched KEGG pathway in CMC-FeS NPs treated group was ribosome. Some of the most pronounced changes were observed for the ribosomal proteins (e.g. *rpl10*, *rpl10a*, *rpl13*, *rpl14*, *rpl15*, *rpl18*, *rpl18a* ect.). Upregulation of these genes was considered as a modifying the primary metabolism, such as protein biosynthesis, and it is one of the key strategies that cells use to tackle stress. These results align well with previous literatures that reported disruption to protein biosynthesis pathway in a range of organisms following exposure to Ag nanoparticles and Ag⁺ (Nair and Choi, 2011; Powers et al., 2011; van Aerle et al., 2013). When Bluntnout bream (*Megalobrama amblycephala*) were subjected to nitrite (15 and 30 mg/L), ribosome was found to be the most significantly enriched KEGG pathway (Sun et al., 2014).

The complement and coagulation cascades pathway, related to the immune system response, was the second significantly up-regulated pathway that showed gene expression changes in the CMC-FeS NPs treated group. The activation of the complement cascade can be triggered by different signals involving various proteins. The protein C3 is always activated when this

cascade is activated. Its activation represents a key event of the complement cascade, which will cause elimination of the nanoparticles that triggered the activation (Vauthier et al., 2011). In this work, *c3* was found over expressed upon the CMC-FeS NPs exposure. Moreover, the *f2* gene, which plays an important role in blood clotting, was dramatically up regulated (14.4-fold), resulting in increased coagulation. The over expression of *c3* and *f2* indicated an immune system response upon the CMC-FeS NPs exposure. This pathway was found to be significantly altered in rats during exposure to copper nanoparticles (Liao and Liu, 2012), and it was also affected in bluntnout bream upon nitrite exposure (Sun et al., 2014).

The cell cycle pathway was the most significant down-regulated transcriptomic regulation KEGG pathway in CMC-FeS NPs treated group. The nanoparticles influenced the cell cycle pathway by down regulating some of the key genes involved, such as cyclin A and cyclin B (*ccna1*, *ccna2*, *ccnb1*, *ccnb2*, *ccnb3*) coding cyclins, and cyclin-dependent kinases (CDK) (*cdk1*, *cdk7*, *cdk8*, *cdk9*, *cdk10*). The cyclins function in the regulation of cell cycle progression and are associated with CDKs, which regulates cell growth, survival, differentiation and oncogenesis. Cell-cycle progression is well connected to the regulation of DNA damage repair (Panigrahi and Mai, 2005) and down regulation of cell cycle pathways suggesting a possibility of cell death through apoptosis (Frohlich, 2013). Other cell cycle regulators, origin recognition complexes (ORC) (*orc1*, *orc3* and *orc5*) and mini-chromosome maintenance protein (MCM) complexes (*mcm10*, *mcm2* and *mcm5*), which are essential proteins for DNA replication, were all down-regulated, again indicating cell cycle progression disturbance under the nanoparticle exposure. This is consistent with the previous study that the suppression of cell cycle regulators was accompanied by the downregulation of a number of genes directly involved in the process of

DNA replication (MCM10, ORC1) when tumor cells were subjected to fullerene for 48 h (Lucafò et al., 2013).

More DEGs were involved in the regulation of KEGG pathways in the bare FeS NPs group, again indicating a more stressed condition with bare FeS treatment. The ten most up and down regulated KEGG pathways are listed in **Table 2.7** and **Table 2.8**.

Table 2. 7 Top 10 differentially up or down regulated KEGG pathways in CMC-FeS treated zebrafish compared with the control.

| # | Pathways | Number of DEGs | P-Value | Pathway ID |
|-----------------------|--|----------------|----------|------------|
| Up-regulated | | | | |
| 1 | Ribosome | 76 | 1.38E-28 | ko03010 |
| 2 | Complement and coagulation cascades | 35 | 3.18E-13 | ko04610 |
| 3 | Glycine, serine and threonine metabolism | 22 | 2.42E-08 | ko00260 |
| 4 | PPAR signaling pathway | 23 | 5.66E-07 | ko03320 |
| 5 | Peroxisome | 27 | 2.00E-06 | ko04146 |
| 6 | Staphylococcus aureus infection | 15 | 9.22E-06 | ko05150 |
| 7 | Tryptophan metabolism | 18 | 1.14E-05 | ko00380 |
| 8 | Glyoxylate and dicarboxylate metabolism | 13 | 6.84E-05 | ko00630 |
| 9 | Glycerolipid metabolism | 18 | 7.59E-05 | ko00561 |
| 10 | Fat digestion and absorption | 13 | 1.87E-04 | ko04975 |
| Down-regulated | | | | |
| 1 | Cell cycle | 48 | 3.05E-16 | ko04110 |
| 2 | DNA replication | 23 | 2.34E-12 | ko03030 |
| 3 | Pyrimidine metabolism | 35 | 6.35E-12 | ko00240 |
| 4 | Cell cycle - yeast | 30 | 2.81E-11 | ko04111 |
| 5 | Spliceosome | 36 | 5.47E-10 | ko03040 |
| 6 | RNA transport | 37 | 2.41E-09 | ko03013 |
| 7 | RNA degradation | 24 | 1.10E-07 | ko03018 |
| 8 | Meiosis - yeast | 21 | 3.81E-07 | ko04113 |
| 9 | Purine metabolism | 36 | 3.92E-07 | ko00230 |
| 10 | Ubiquitin mediated proteolysis | 30 | 8.64E-07 | ko04120 |

Table 2. 8 Top 10 differentially up or down regulated KEGG pathways in bare FeS NPs treated zebrafish compared with the control.

| # | Pathways | Number of DEGs | P-Value | Pathway ID |
|-----------------------|--|----------------|----------|------------|
| Up-regulated | | | | |
| 1 | Complement and coagulation cascades | 38 | 2.73E-08 | ko04610 |
| 2 | Glycine, serine and threonine metabolism | 28 | 5.79E-07 | ko00260 |
| 3 | Tryptophan metabolism | 29 | 8.27E-07 | ko00380 |
| 4 | PPAR signaling pathway | 32 | 1.89E-06 | ko03320 |
| 5 | Peroxisome | 40 | 2.16E-06 | ko04146 |
| 6 | Fatty acid degradation | 25 | 2.82E-06 | ko00071 |
| 7 | Fatty acid metabolism | 28 | 9.01E-06 | ko01212 |
| 8 | Fat digestion and absorption | 22 | 9.86E-06 | ko04975 |
| 9 | Glycerolipid metabolism | 29 | 1.11E-05 | ko00561 |
| 10 | Glycerophospholipid metabolism | 38 | 5.49E-05 | ko00564 |
| Down-regulated | | | | |
| 1 | Cell cycle | 61 | 9.04E-16 | ko04110 |
| 2 | DNA replication | 30 | 3.35E-13 | ko03030 |
| 3 | Cell cycle - yeast | 41 | 1.42E-12 | ko04111 |
| 4 | Spliceosome | 53 | 1.70E-12 | ko03040 |
| 5 | RNA transport | 53 | 5.49E-11 | ko03013 |
| 6 | Pyrimidine metabolism | 41 | 6.60E-10 | ko00240 |
| 7 | Nucleotide excision repair | 25 | 4.71E-09 | ko03420 |
| 8 | RNA degradation | 34 | 6.42E-09 | ko03018 |
| 9 | Homologous recombination | 18 | 1.50E-07 | ko03440 |
| 10 | Meiosis - yeast | 28 | 1.85E-07 | ko04113 |

CMC as lager M.W. polyelectrolytes was claimed to inhibit close contact between particles and gram-negative *E. coli*. cells by electrosteric repulsion, consequently exerting less toxicity (Dong et al., 2016). Others indicated that CMC coating could decrease toxicity and oxidizing capacity of nano ZVI (NZVI) towards the bacteria *Agrobacterium* sp. PH-08 as compared with the uncoated counterpart. However, they observed that CMC enhanced the physical contact of NPs with bacteria, the possible reason for mitigating NZVI toxicity they claimed was that stabilization might alter surface reactivity and change iron-cell interaction. Also they suggested CMC might act as a radical scavenger resulting in less oxidation stress by detecting less ROS generation from iron corrosion (Zhou et al., 2014). CMC as a radical scavenger statement was

reported elsewhere by several studies ($\cdot\text{OH} + \text{CMC} \rightarrow \text{H}_2\text{O} + \text{CMC}$) (Joo and Zhao, 2008; Wach et al., 2005). In our study, CMC coating decreases the zeta potential of bare FeS NPs by forming negatively charged surface and CMC-FeS NPs showed less toxicity on zebrafish liver compared to bare FeS NPs by RNA-seq analysis. The most plausible explanation is CMC might scavenge the excess oxidants, offsetting FeS-cell physical proximity induced redox damage. In terms of contacts of CMC-FeS NPs with cells, more experiment should be performed to further visualize the difference. Moreover, the proposed scavenge mechanism is needed for further assessed.

In terms of subsequent alteration of CMC-FeS NPs in the environment, CMC degradation and NP behavior are considered. CMC degrades completely at low rate in the environment. It was reported that CMC goes through 3 phases of degradation, it took 110 days for CMC to be completely degraded in a semicontinuous activated sludge (SCAS) test (VanGinkel and Gayton, 1996). After degradation of CMC, NPs are expected to either aggregate and precipitate in the sediment or become coated with natural organic matter (NOM) (Li, 2011).

Several members of genes involved in responses to immune and inflammatory response, detoxification, oxidative stress, and DNA damage/repair in CMC-FeS NPs were selected for qPCR validation. As an internal gene, the beta-actin was used. Under the given experimental conditions, the internal gene showed to be not affected by exposure to the nanoparticles (data not shown). Generally, as shown in **Fig. 2.7**, the gene expression levels and trend of regulation (increase/decrease) detected with RNA-seq and qualification based on qPCR are in agreement with each other.

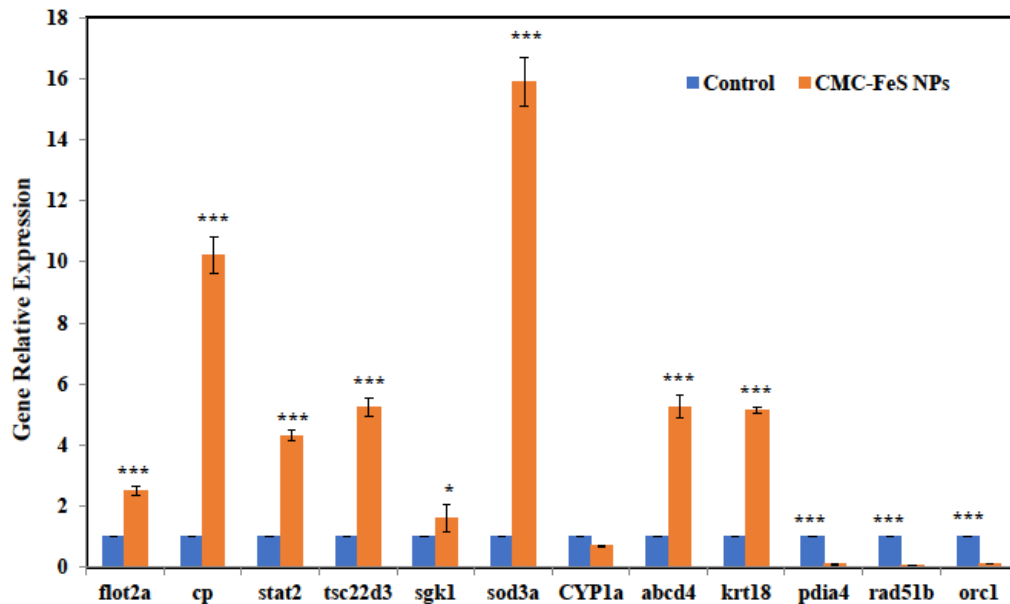


Figure 2. 7 Validation of liver tissue transcriptome results by qRT-PCR using twelve selected differentially expressed genes in CMC-FeS treated zebrafish. The qRT-PCR fold changes are relative to the control samples and normalized by changes in beta-actin values. The averages of three relative quantities of biological replications were used in a two-tailed Student's t test with a 95% confidence level ($P < 0.05$) to determine the gene expression significance.

2.4 Conclusions

This is the first description of the relevance of major transcriptional changes associated with biological networks alternation that provides both global and specific information on coordinated adaptive response to acute toxicity of CMC-FeS in the liver of zebrafish. Toxicity and transcriptome sequencing analyses demonstrated that the transcriptional activity associated with stress remained significant throughout the study. The findings were further supported by histological evidence, which may be used as a reference for phenotype-anchoring points for certain classes of genes in future studies. Since many differentially expressed genes are associated with immune and inflammatory response, detoxification, oxidative stress, and DNA damage/repair, our results indicated that exposure to CMC-FeS at LC_{25} for 96 h caused

significant DNA and protein damage due to the nanoparticle induced oxidative stress. The oxidative stress caused major cellular and tissue injury, which was evident from the histological of NP-exposed liver and aligned well with changes in the altered expression of genes associated with hepatotoxicity. Further comparison of transcriptome profiling of bare and CMC coated FeS NPs showed that coating could mitigate the FeS NPs toxicity. The findings of this study provided insights into the genotoxicity and the toxicological mechanism caused by stabilized nanoparticles, which are useful for the assessment of the potential toxicity of CMC-FeS and possibly other stabilized nanoparticles.

Chapter 3 Effects of Surface Coating of Magnetite Nanoparticles on Cellular Uptake, Toxicity and Gene Expression Profiles in Adult Zebrafish

3.1 Introduction

Engineered magnetite nanoparticles (Fe_3O_4 NPs) have been widely studied or used in a number of fields including medical and environmental remediation areas due to their special physicochemical properties. For instances, a recent review by Revia and Zhang (2016) provided a detailed account of Fe_3O_4 NPs used for cancer diagnosis, treatment, and treatment monitoring; whereas Sharifi et al. (2015) and Wu et al. (2015) reported applications of superparamagnetic iron oxide nanoparticles (SPIONs) for in vivo molecular and cellular imaging, cell tracking, and drug delivery. In the environmental cleanup field, Fe_3O_4 NPs have attracted attention for adsorption of trace contaminants from water and for in situ immobilization of toxic chemicals in soil and groundwater due to their high adsorption capacity and paramagnetic properties that enable the NPs to be easily separated from the environmental media (Su, 2017). For instance, Fe_3O_4 NPs are used for pollutant removal and mitigation of organics. Hernandez et al. (2015) reported degradation of methylene blue by Fe_3O_4 NPs; Li et al. (2015) claimed the effective removal of trace perfluorooctane sulfonates from water by mesoporous $\text{Fe}_3\text{O}_4@\text{SiO}_2@\text{CTAB}-\text{SiO}_2$; Ruan et al. (2015) used magnetite as a heterogeneous activator in degradation of trichloroethylene by persulfate. Fe_3O_4 NPs were also found effective for removal of metalloids. An et al. (2011) prepared a new class of starch-bridged magnetite NPs and observed unusually high adsorption capacity toward arsenate. Others reported that engineered Fe_3O_4 NPs can also

remove heavy metal cations (e.g. Hg(II), Cr (VI), Cu(II), Pb(II) and Co(II)) (Shan et al., 2015; Villacís-García et al., 2015; Wanna et al., 2016), radionuclides (e.g. Sr(II), Th(IV) and U(VI)) (Ding et al., 2015; Tan et al., 2015), and rare earth elements (e.g. La, Ce, Pr and Nd) (Basualto et al., 2015). In addition, Fe₃O₄ nanocomposites have also been studied as antimicrobial agents for water disinfection (Pina et al., 2014).

However, bare or non-stabilized Fe₃O₄ NPs tend to form large aggregates, impeding their delivery and performances. To prevent the particle aggregation, various stabilizers or coating agents are often employed. Numerous studies have been conducted on modifying surface properties of SPIONs for medical uses, and it has been shown that the appropriate surface coating can facilitate size control, adsorption capacity, transportability/deliverability and biocompatibility of the materials (Gupta and Gupta (2005). For instance, An et al. (2011) reported starch-bridged Fe₃O₄ NPs offered 5 times higher adsorption for As(V) than bare Fe₃O₄ NPs within 1h in simulated ion exchange brine. Liang et al. (2012) reported that starch-stabilized Fe₃O₄ NPs offered a 2.2 times greater As(V) uptake capacity than conventional non-stabilized Fe₃O₄ NPs. Furthermore, the researchers found that the stabilized NPs are deliverable into a sandy loam soil and may facilitate in situ immobilization of As(V) in soil (Liang and Zhao, 2014). Recently, Pan et al. (2017) modified the surface of Fe₃O₄ NPs by coating the particles with stearic acid (SA), oleic acid (OA), and octadecylphosphonic acid (ODP), and achieved improved capacity for U(VI) adsorption.

As uses of Fe₃O₄ NPs continue to grow, however, the potential environmental health impacts remain poorly understood. In particular, the fate and health risks of stabilized Fe₃O₄ NPs are of greater concern due to their much smaller size and environmental mobility. The uses of stabilizers or surface coatings on Fe₃O₄ NPs can not only prevent particle aggregation, but also

regulate surface physical and chemical properties (e.g., particle size, surface charge, and functionalities) and affect the particle dissolution and environmental fate and transport behavior (He et al., 2009). Therefore, the surface coating is expected to play critical roles in assessing the environmental impacts and toxicity of NPs.

Several studies have addressed the toxicity of coated Fe₃O₄ NPs. For instance, the genotoxicity of Fe₃O₄ NPs was evaluated with different surface coatings (PEG or polyethylene glycol, PEI or polyethylenimine) using three standard genotoxicity assays. The results suggested that the mutagenicity of Fe₃O₄ NPs varies with different surface coatings. PEG-coated Fe₃O₄ NPs exhibited mutagenic activity but no chromosomal and clastogenic abnormalities; while PEI-coated Fe₃O₄ NPs showed no genotoxicity in all three assays (Liu et al., 2014). Fe₃O₄ NPs coated with a dopamine-based ligand were found less toxic to RAW264.7 cells even though the particle dispersibility was increased in aqueous solutions (Wang et al., 2015). Sulfhydryl-modified Fe₃O₄@SiO₂ core/shell NPs showed low toxicity in mouse fibroblast (L-929) cell lines and no hemolytic activity, indicating good biocompatibility of this nanocomposite (Guo et al., 2015). Dimercaptosuccinic acid (DMSA)-coated Fe₃O₄ NPs were found non-toxic but accumulated in the spleen, liver and lung tissues in rats (Ruiz et al., 2015). Superparamagnetic Fe₃O₄ core-shell nanostructure microspheres showed good biocompatibility in the in vitro cytotoxicity tests (Yu et al., 2016). In another study, bare superparamagnetic iron oxide nanoparticles (SPIONs) were found nontoxic to cells via cell viability assays (Mbeh et al., 2015a); however, SPIONs coated with positively ($-\text{NH}_3^+$) or negatively ($-\text{COO}^-$) charged shells alternated biocompatibility as their surface charge changed, negatively charged SPIONs are more biocompatible than both the positively charged SPIONs and the bare SPIONs (Mbeh et al., 2015b). Moreover, Berry et al. (2003) found that dextran-coated Fe₃O₄ NPs could cause cell death and reduce cell proliferation

similar to that caused by uncoated iron oxide particles at 50 $\mu\text{g/mL}$, though dextran-coated Fe_3O_4 NPs showed more prominent membrane disruptions. Mahmoudi et al. (2010) reported that uncoated magnetite particles induce greater toxicity than the polyvinyl alcohol (PVA)-coated particles on a mouse fibroblast cell line. Based on the latest information, it is evident that the coatings on Fe_3O_4 NPs can greatly affect the toxic effects of the nanoparticles. Nonetheless, most of the Fe_3O_4 NPs toxicity studies are conducted within biomedical fields, and very limited toxicity information is available related to coatings used in the environmental remediation settings (e.g. starch).

In recent years, gene expression analysis has gained more interest in toxicological studies. This is due to the fact that gene regulation would be initiated when cells are subjected to toxicant exposure to protect cellular structures and repair damage (Causton et al., 2001). Studying gene expression profile can provide toxicity information of contaminants and predict their potential effects at higher biological levels (Garcia-Reyero et al., 2008). In addition, it can also provide a sensitive detectable endpoint for toxicity, and thus can serve as an early warning sign of a particular material. RNA-seq using the next-generation sequencing (NGS) has been widely used to serve this purpose. Namely, it could be used to study the effects of chemicals or pollutants on organisms with the benefit of the increased sensitivity.

In this study, we used zebrafish (*Danio rerio*) as a model organism to evaluate *in vivo* toxicity of bare and starch-coated Fe_3O_4 NPs in an aquatic environment. Zebrafish is known to be sensitive to various environmental pollutants, and has close homology with the human genome (Westerfield, 2000b). To our knowledge, this is the first toxicological study on the toxic effects of starch-coated Fe_3O_4 NPs on zebrafish. We selected gill and liver as the external and internal target organs to test the toxic effects via the latest RNA-seq technique. Our aim was to

investigate the coating effects on cellular uptake, toxicity and gene expression profiles on zebrafish during aqueous exposure of Fe₃O₄ NPs. We therefore characterized the nanoparticle properties and measured tissue burden, evaluated the Differentially Expressed Genes (DEGs) profiles as well as gene ontology (GO) and Kyoto encyclopedia of genes and genomes (KEGG) pathways to study the underlying molecular mechanisms of coating effects on toxicity of Fe₃O₄ NPs in the fish.

3.2 Materials and Methods

3.2.1 Chemicals

A potato starch (hydrolyzed for electrophoresis) and Ferrous sulfate heptahydrate (FeSO₄ · 7H₂O) was obtained from Acros Organics (Pittsburgh, PA, USA). Ferric chloride (FeCl₃), hydrogen peroxide (H₂O₂) and sodium hydroxide (NaOH) were obtained from Fisher Scientific (Pittsburgh, PA, USA). Hydrochloric acid and nitric acid were purchased from Mallinckrodt Chemical (St. Louis, MO, USA). All chemicals are of the ACS reagent grade.

3.2.2 Synthesis and characterization of Fe₃O₄ NPs and starch-Fe₃O₄ NPs

Fully stabilized Fe₃O₄ NPs were prepared in 1000 mL flask using the starch as a stabilizer and under nitrogen purging/mixing following the method by Liang et al. (2012). First, a 1 wt.% of a starch stock solution was prepared by adding 5 g of starch into 500 mL deionized water. To assure completion dissolution of starch, the solution was heated to the boiling point under magnetic stirring, and kept boiling for 15 min, and then cooled to room temperature. In the meantime, a ferrous-ferric stock solution was prepared at an Fe²⁺: Fe³⁺ molar ratio of 1:2 by dissolving 0.1655 g of FeSO₄ · 7H₂O and 0.1935 g of FeCl₃ in deoxygenated deionized water.

Then, 956 mL of the Fe^{2+} - Fe^{3+} stock solution was mixed with 40 mL of the stabilizer stock solution to yield a mixture of 996 mL containing 100 mg/L Fe and 0.04 wt.% of starch. Then, 4 mL of a 2 M NaOH solution was injected in one shot into the mixture to raise the pH of the solution to ~ 11 under N_2 purging. The color change from clear to black indicates the formation of the magnetite nanoparticles. The nanoparticles were then allowed to grow for 24 h under N_2 purging at room temperature. Then, the suspension pH was lowered to 6.8 ± 0.4 by adding < 1 mL of 2 M hydrochloric acid. For comparison, bare Fe_3O_4 NPs were prepared without starch in otherwise identical conditions.

The morphology of the resulting Fe_3O_4 NPs was determined by Transmission Electron Microscopy (TEM) at a 200 KV accelerating voltage (JEM-2100, JEOL, Tokyo, Japan). The hydrodynamic diameter and zeta potential (ζ) of the particles were determined by dynamic light scattering (DLS) analysis using a Malvern Zetasizer Nano ZS (Malvern Instruments, Worcestershire, U.K.).

To measure the amount of dissolved Fe ions in the Fe_3O_4 NPs suspension, the suspensions were filtered at time zero and 24 h of preparation using a 25 nm Millipore membrane filter (Millipore Corp., Billerica, MA, USA), and the filtrates were analyzed for dissolved Fe using an Agilent 7500 cx ICP-MS (Agilent Technologies, USA) equipped with an Octopole Reaction System (ORS).

3.2.3 Zebrafish exposure to magnetite nanoparticles

All procedures involving the handling and treatment of fish used during this study were approved by the Animal Care and Use Committee at Heilongjiang River Fisheries Research Institute (ACUC-HRFRI). All experiments were conducted in accordance with the relevant guidelines and regulations.

The zebrafish (*Danio rerio*) were obtained from the Heilongjiang River Fisheries Research Institute Zebrafish Facilities. Adult zebrafish of both sexes with an average age of 6 months (average weight = 0.61 ± 0.10 g, and average length = 44.27 ± 2.77 mm) were selected for the study. The fish were fed daily with commercial fish food and maintained in aquaria at a temperature of 25 ± 1 °C with a 14h:10h light and dark cycle for four weeks before use. Before each intended exposure, the fish were removed from the aquaria and placed in static tanks and fasted for 24 h.

The zebrafish were randomly assigned to 6 groups (10 fish each), which were exposed to bare or starch-coated Fe₃O₄ NPs for 7 days in 1 L beaker containing 1 L of a test suspension. The suspensions were replaced every 24 h with freshly prepared NP suspensions of the same concentration simulating a scenario of continued exposure to high strength of Fe₃O₄ NPs. Three more groups (10 fish each) were used as no-dose controls. Each treatment was run in triplicate under the same conditions and under the natural light/dark cycles. To avoid water contamination and interference of fish food, the fish were not fed during the exposure experiments.

After 7 days of exposure, the zebrafish were sampled and rinsed with DI water three times to remove the nanoparticles on fish surface for further testing.

3.2.4 Accumulations of NPs in fish tissue

After 7 days of exposure, three zebrafish were removed from each of the replicate testing beakers including the control, and then euthanized with tricaine methanesulfonate (MS222). The carcasses were weighed 0.41 ± 0.10 g and then digested for analyzing the Fe content. The digestion was performed in a MarXpress microwave system (CEM, USA). A homogenized tissue sample was transferred into a PTFE (polytetrafluoroethylene) vessel. Then, 5 mL HNO₃, 2 mL

H₂O₂ and 3 mL ultra-pure water were added, and then the temperature was ramped to 185 °C in 10.5 min, and kept at this temperature for 14.5 min. After cooling to room temperature, the samples were filtered using 0.45 µm filter. Finally, 0.5 mL of a 100 mg /L internal standard Mix solution (Agilent Technologies, USA) was added into the filtrates and then diluted to a final volume of 50 mL using deionized water. The samples were then analyzed for total Fe concentration via an ICP-MS system. Fish tissues in the control were also digested in the same way.

3.2.5 High-throughput transcriptomic sequencing

3.2.5.1 Total RNA isolation and Illumina sequencing

Total RNAs were isolated from triplicates of gill and liver tissues (each replicate consisted of tissues pooled from three fishes). Both control and treated zebrafish tissues were homogenized in the TRIzol® Reagent and the total RNA was extracted using the RNeasy Mini Kit (Qiagen, Hilden, Germany) following the manufacturers protocol. The quantity and quality of RNA were examined by Thermo Scientific™ NanoDrop™ 8000 Spectrophotometer and Agilent 2100 Bioanalyzer (Agilent Technologies, Santa Clara, CA, U.S.). Only RNA with OD 260/280 \geq 1.8 and RNA integrity number \geq 7 were selected for the subsequent experiments. Equal quantities of high quality RNA from each tissue sample were pooled together for cDNA synthesis and sequencing.

After generating the clusters, the library sequencing was performed on an Illumina HiSeq 4000 platform to create paired-end reads with lengths of 150 bp.

3.2.5.2 Bioinformatics analyses

The quality control of RNA-Seq data was conducted by NGS QC Toolkit (Patel and Jain, 2012) with default parameters. Clean paired-end reads were aligned to the zebrafish reference genome sequence, GRCz10 version (Chen et al., 2014), using TopHat (Han et al., 2011a).

To identify differential expression genes (DEGs) between two different samples, the expression level for each transcript was calculated using the fragments per kilobase of exon according to the million mapped reads (FRKM) method. Cuffdiff (<http://cufflinks.cbc.umd.edu/>) (Trapnell et al., 2013) was used for the differential expression analysis. The DEGs between two samples were selected based on the following criteria: 1) the logarithmic of fold change was greater than 2, and 2) the false discovery rate (FDR) should be less than 0.05. To understand the functions of the differentially expressed genes, gene ontology (GO) functional enrichment and Kyoto encyclopedia of genes and genomes (KEGG) pathway analysis were carried out by Goatools (<https://github.com/tanghaibao/Goatools>) and KOBAS (<http://kobas.cbi.pku.edu.cn/home.do>) (Xie et al., 2011a). DEGs were significantly enriched in the GO terms and metabolic pathways when their Bonferroni-corrected P-value was less than 0.05.

3.2.5.3 Validation by qRT-PCR

In order to validate the expression patterns of DEGs identified by RNA-Sequencing, we selected twelve genes from the DEGs potentially associated with mitochondria energy metabolism, mitochondria dysfunction pathway, immune and inflammation response, ER stress and unfolded protein response, oxidative stress and antioxidant response, DNA damage/repair and apoptosis for qPCR validation, including *abcb4*, *fen1*, *sgk1*, *tsc22d3*, *irf7*, and *stat2* for gill, and *cyp1a*, *tsc22d*, *tp53*, *chek1*, *pdia4*, and *suclg2* for liver. Total RNA was extracted using the TRIzol reagent following the manufacturer's instructions. The RNA quality was assessed using

1% agarose electrophoresis and by measuring the 260/280 nm absorbance ratios. After purification using DNase I (Promega) to remove genomic DNA contamination, the total RNA was reverse-transcribed into cDNA and the gene transcription levels were analyzed using a SYBR Green PCR kit (Toyobo, Osaka, Japan) on an ABI PRISM 7300 Sequence Detector system (Perkin-Elmer, Applied Biosystems). Primer sequences of the selected genes were designed using the Primer 3 software (<http://frodo.wi.mit.edu/>) (Table 3.1). The relative gene transcription levels were calculated using the $2^{-\Delta\Delta CT}$ method (Livak and Schmittgen, 2001); beta-actin was used as the reference gene and its transcription was constant among the exposure groups. Comparing the relative expression levels of twelve selected genes revealed that most the qPCR results were consistent with the results of RNA-Seq (Fig. 3.7). The Pearson's correlation of \log_{10} (fold-change) between qPCR and RNA-Seq was 0.80, indicating that the RNA-Seq based transcriptome analysis was accurate and reliable.

Table 3. 1 Sequences of primers for selected genes in qPCR validation.

| Tissue | Genes | Forward primer | Reverse primer |
|--------------|----------------|----------------------|----------------------|
| Gill | <i>abcb4</i> | TGGCCTGACGTTCTCTTTCT | CTCTCCAAGTCCATTGCTC |
| | <i>fen1</i> | AGCTGACGCATCAACAGTTC | GAGCAGGGTGCTTATTTGGG |
| | <i>sgk1</i> | GAAAGGGTAGCTTCGGCAAG | GAGTAATGCAGGCCCAAG |
| | <i>tsc22d3</i> | GCCTTTCCAAGTCAAGCCAA | GCTCTGTTACAGGTCCGTCT |
| | <i>irf7</i> | GCAGAGCACAAATGCCAAAC | TGTGTTTCCAAGGGATCCGA |
| | <i>stat2</i> | GTCGGAAATCTCGGCTATGC | CTTCTGGAGCTGGAACATGC |
| Liver | <i>cyp1a</i> | TGGAGCTAATTGGCACTGGA | TAGGCGCATGAGCAGATACA |
| | <i>tsc22d3</i> | GCCTTTCCAAGTCAAGCCAA | GCTCTGTTACAGGTCCGTCT |
| | <i>tp53</i> | GCCTGCTGGCCATTTGATAA | GCTGTGGTGCTTCATATGGG |
| | <i>chek1</i> | TTCTTTGGGCACAGTGTGG | CAGAGTACCACACAGACGGT |
| | <i>pdia4</i> | AGGTCCAGACCCTGAAACAG | ATACGCTGCATCTTCATCGC |
| | <i>suclg2</i> | ACCAAACAGACGCCTAAGGA | CATTACACGAGCGGTCCATC |

3.3 Results and Discussion

3.3.1 Particle characterization

Transmission electron microscopy (TEM) was used to confirm size and elemental compositions of bare and starch-coated Fe₃O₄ NPs. **Figures 3.1a and 3.1c** show that bare Fe₃O₄ NPs existed as much larger aggregates than the starch-coated Fe₃O₄ NPs. Physically, the bare NPs settled by gravity within a few minutes while the starch-coated NPs remained well dispersed in water without sedimentation during the course of the study. **Figures 3.1b and 3.1d** show the size distributions of the bare and starched Fe₃O₄ NPs, which was processed using the ImageJ software, giving a mean particles size of 20.92 ± 7.48 nm for bare NPs and 4.26 ± 0.84 nm for starched NPs. The mean hydrodynamic diameter of freshly made starch-Fe₃O₄ NPs was 217.90 ± 8.20 nm, which grew to 225.00 ± 0.57 nm after 24 h of aging (**Table 3.2**). The DLS-based method was not applicable to the bare NPs because of the rapid gravity settling effect (He and Zhao, 2008). **Table 3.2** also gives zeta potential of the bare Fe₃O₄ NPs (13.45 ± 0.21 mV at 0 h and 15.00 ± 0.57 mV at 24 h) and starch-Fe₃O₄ NPs (-0.23 ± 0.14 mV and -0.25 ± 0.12 mV at 24 h), indicating that the starch coating greatly suppressed the surface potential of the nanoparticles. The nearly zero surface potential also indicates that steric stabilization is the key mechanism for starch-stabilized NPs. In all cases, the dissolved Fe was less than 0.40% during the experiments, indicating that the nanoparticles were essentially constant throughout the exposure period.

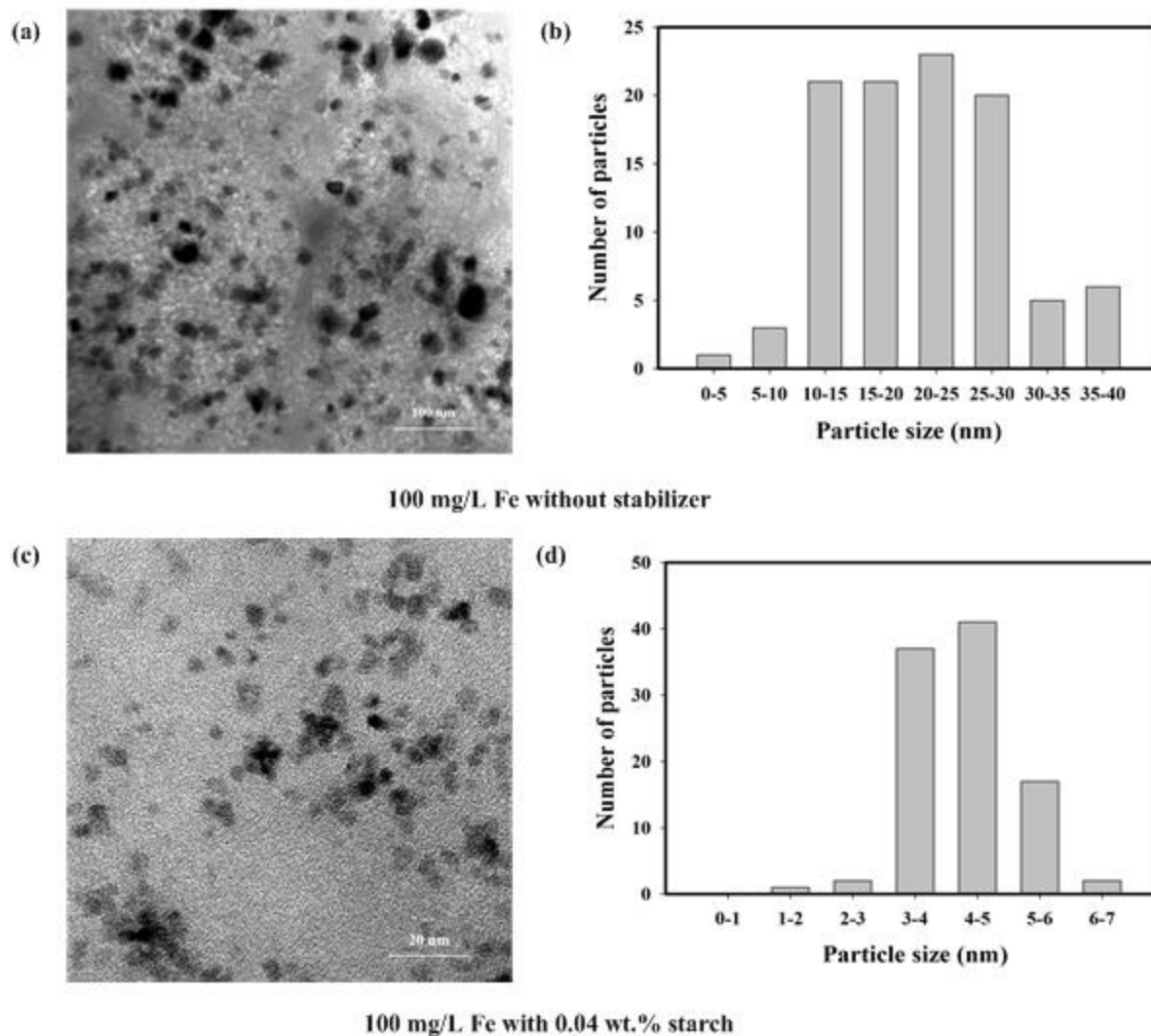


Figure 3. 1 Transmission electron microscopy images and histograms showing size distributions of bare and starch-stabilized Fe₃O₄ NPs (total Fe = 100 mg/L, starch = 0.04 wt.%): (a) TEM image of bare Fe₃O₄ NPs, (b) Histogram of bare Fe₃O₄ NPs size (mean size = 20.92 ± 7.48 nm), (c) TEM image of starch-coated Fe₃O₄ NPs, and (d) Histogram of starch-coated Fe₃O₄ NPs size (mean size = 4.26 ± 0.84 nm).

Table 3. 2 Mean hydrodynamic diameters and zeta potential of freshly prepared and 24-h aged Fe₃O₄

| Samples | Aging time (h) | Hydrodynamic diameter (nm) | Zeta-potential (mV) |
|---|----------------|----------------------------|---------------------|
| Bare Fe ₃ O ₄ NPs | 0 | ND | 13.45 ± 0.21 |
| | 24 | ND | 15.00 ± 0.57 |
| Starch-Fe ₃ O ₄ NPs | 0 | 217.90 ± 8.20 | -0.23 ± 0.14 |
| | 24 | 225.00 ± 0.57 | -0.25 ± 0.12 |

ND: Not detectable.

3.3.2 Tissue burden

During the course of the experiments, no fish mortality was observed. Starch, as one of the most abundant naturally occurring polysaccharides, was used to coat Fe₃O₄ NPs here. Starch consists of long-chain polymer of d-glucose. It has been applied experimentally as a drug carrier because it is biocompatible, biodegradable, and nontoxic (Cole et al., 2011). Starch at concentration of 500 mg/L and 1000 mg/L were evaluated for its toxicity to zebrafish embryos as a control for capping Ag NPs, it was claimed that starch treated zebrafish embryos without adding NPs appeared normal (Asharani et al., 2008). In our study, 0.04 wt.% of starch was used to stabilize 100 mg/L of total Fe in 1L of Fe₃O₄ NPs suspension, the starch concentration in terms of mg/L is 40 mg/L, 12.5 times less than the lower concentration of starch used in Asharani et al. (2008) study, again suggesting no toxicity could be expected from starch in our context. Therefore, no starch control was performed on adult zebrafish.

The total iron concentrations in the fish bodies after 7 days of exposure were determined to be 12.71 ± 1.63 mg/kg for the control group, and 253.50 ± 15.03 and 188.17 ± 18.42 mg/kg for the groups exposed to bare and starched Fe₃O₄ NPs, respectively. Evidently, the total Fe content was 19.9 and 14.8 times higher upon exposure to the NPs compared to control, indicating significant accumulation of the nanoparticles in the fish.

Bare Fe₃O₄ NPs induced more bioaccumulation of iron than starch-coated Fe₃O₄ NPs in the zebrafish carcasses, indicating the characteristics of Fe₃O₄ NPs play an important role in the bioaccumulation of the particles. The larger particle size of bare Fe₃O₄ NPs rendered nanoparticles more easily caught/immobilized in various body parts of the zebrafish than starch-coated Fe₃O₄ NPs that are much more transportable. Zhao and Wang (2010) reported that

aggregated NPs may get stuck in the guts of zebrafish and remained therein for prolonged times if the zebrafish are not subsequently fed. Moreover, the positively charged surface of bare Fe₃O₄ NPs are more prone to interacting to negatively charged groups than starch-coated Fe₃O₄ NPs. In fact, the starch coating not only suppressed the surface potential, but also prevents from attaching to a collector surface due to steric hindrance. Therefore, the uptake routes and locations of the forms of Fe₃O₄ NPs can be quite different. It should be noted that although the accumulated iron in the zebrafish reached ppm levels, no mortality was observed throughout the experiments, suggesting that important mechanisms against nanoparticles-induced stress and gene regulations were implemented to resist the impacts.

3.3.3 Transcriptomic analysis

The characterization of gene expression is a powerful approach to identify the differences of the transcriptional machinery between tissues and diverse statuses of cells (Dermitzakis, 2008). Great efforts have been made for investigating the RNA-seq transcriptome across tissues and individuals in humans (Dermitzakis, 2008), rats (Yu et al., 2014) and mice (Li et al., 2017), aiming to explore tissue-specific gene expression for many diseases and drug effects. In this work, we constructed a comprehensive transcriptome map of zebrafish, by describing the gene-expression profiles in two tissues, namely, gill and liver, to study the coating effects on Fe₃O₄ NP toxicity. The results revealed that the exposure to, and/or accumulation of, both bare and starched Fe₃O₄ NPs induced dramatic alterations in global gene transcription profiles in the zebrafish gills and livers.

The differences in the gene regulatory pathways were analyzed in the gill and liver tissues. It produced approximately 353,815,682 and 443,471,696 total clean reads from the 48.4 Gbp to 59.9 Gbp clean sequence data for all the biological replicates in gills and livers, respectively.

More than 92.5% for gills and 91.7 % for livers of the clean reads had quality scores over the Q30 value, and over 70.5% and 84.1% of the total reads were uniquely mapped to the reference genome of gills and livers, respectively (**Table 3.3**).

Table 3. 3 Summary of sequence data generated for zebrafish gill and liver transcriptome and qualify filtering.

| Tissue | Samples | Clean reads | Mapped reads | Mapped rate (%) | Q30 percentage |
|---------------|---|--------------------|---------------------|------------------------|-----------------------|
| Gill | Control-1 | 49,407,074 | 39,343,834 | 79.63 | 92.52 |
| | Control-2 | 35,405,116 | 24,947,315 | 70.46 | 96.65 |
| | Control-3 | 38,979,898 | 27,710,493 | 71.09 | 96.73 |
| | Fe ₃ O ₄ NPs-1 | 35,922,180 | 30,633,991 | 85.28 | 94.49 |
| | Fe ₃ O ₄ NPs-2 | 39,978,656 | 32,669,360 | 81.72 | 93.56 |
| | Fe ₃ O ₄ NPs-3 | 37,208,210 | 31,412,195 | 84.42 | 96.78 |
| | Starch-Fe ₃ O ₄ NPs-1 | 38,310,062 | 30,045,634 | 78.43 | 93.51 |
| | Starch-Fe ₃ O ₄ NPs-2 | 35,888,500 | 27,870,614 | 77.66 | 92.59 |
| | Starch-Fe ₃ O ₄ NPs-3 | 42,715,986 | 33,927,956 | 79.43 | 96.73 |
| Liver | Control-1 | 37,220,362 | 32,336,730 | 86.88 | 91.69 |
| | Control-2 | 41,194,526 | 34,871,813 | 84.65 | 96.16 |
| | Control-3 | 67,918,028 | 57,520,603 | 84.69 | 95.85 |
| | Fe ₃ O ₄ NPs-1 | 39,871,588 | 33,200,287 | 83.27 | 94.89 |
| | Fe ₃ O ₄ NPs-2 | 38,703,156 | 32,549,818 | 84.10 | 94.47 |
| | Fe ₃ O ₄ NPs-3 | 65,601,590 | 56,514,254 | 86.15 | 95.99 |
| | Starch-Fe ₃ O ₄ NPs-1 | 43,487,576 | 38,410,938 | 88.33 | 94.98 |
| | Starch-Fe ₃ O ₄ NPs-2 | 37,744,450 | 32,153,841 | 85.19 | 94.68 |
| | Starch-Fe ₃ O ₄ NPs-3 | 71,730,420 | 63,776,897 | 88.91 | 96.29 |

To inspect the gene regulations arising from the coating effects of Fe₃O₄ NPs, we identified the number of up/down regulated DEGs per treatment group, and the overlap between up or down regulated DEGs of two treatment groups within the gills and livers.

A total of 1,733 DEGs (up-regulated DEGs: 1026, 59%, down-regulated DEGs: 707, 41%) in the gills were found for the group exposed to bare Fe₃O₄ NPs, whereas, only 501 DEGs (up-regulated DEGs: 203, 41%, down-regulated DEGs: 298, 59%) were significantly expressed for starch-Fe₃O₄ NPs treated group (**Figures 3.2a and 3.2b** and **Figures 3.3**) compared with the control, i.e., around 3.5 times more DEGs were identified in the gills of bare Fe₃O₄ NPs. The striking differences in gene expression between two different treatment indicates an elevated stress condition under the bare Fe₃O₄ NPs exposure compared to starch-coated Fe₃O₄ NPs.

Furthermore, more DEGs (5,345 DEGs for bare Fe₃O₄ NPs and 6,529 DEGs for starch-Fe₃O₄ NPs) with a greater proportion of overlap (**Figs. 3.2c and 3.2d** and **Fig. 3.3**) were identified for both treatments in the livers, indicating that the two treatments also shared some regulatory mechanisms beyond the coating effects. However, the 22% more DEGs for the starch-Fe₃O₄ NPs treated group suggests that livers are more susceptible to the starch-coated Fe₃O₄ NPs. Indeed, about 3 and 13-fold more DEGs were found in livers than in gills when exposed to bare and starch-coated Fe₃O₄ NPs, respectively. A large set of genes altered their expressions in both tissues, indicating that the exposure caused complex genomic responses and related pathways regulations.

Fish gills directly contact with pollutants in the aquatic environment. Gills have extensive surface area, small diffusion distances, and large quantities of membrane proteins exposed to the environmental media. As a result, gill tissues are particularly sensitive to damage by aquatic toxins (Handy, 2011). In this study, gills expressed less complex transcriptomes, whereas livers harbored more complex transcriptomes.

Differential gene expression analyses revealed that more DEGs in gills were identified for the group treated with bare Fe₃O₄ NPs than that with starch-coated NPs (**Fig. 3.2 and 3.3**). These

results suggest that two forms of the Fe₃O₄ NPs interact with the gills in a different manner, which agrees with the assertion that surface modification of nanoparticles may change their bioavailability to aquatic organisms (Johnson et al., 2009; Kim et al., 2009). Very little overlap was found among the sets of genes affected by the NPs, indicating that there is very little in the way of a “generic particle” response at the gill. It can be explained by the nature of the mucus layer which covers the epithelial cells of the gills. This mucus layer contains glycoproteins enriched in sialic acid, carboxylic acid and sulfated functional groups, making the mucus a viscous layer of polyanions (Handy et al., 2008). While the positively charged bare Fe₃O₄ NPs undergo strong electrostatic interactions with the mucus layer, the starch-coated, nearly neutrally charged Fe₃O₄ NPs would have negligible or repulsive interactions with the mucus layer. This finding is in line with the conclusion of previous studies where more cationic Au nanoparticles accumulated in fish gills than neutral and anionic NPs (Zhu et al., 2010). The accumulation of the more poly-dispersed and more positively charged bare Fe₃O₄ NPs in the gills may increase the Na⁺/K⁺-ATPase activity and subsequently trigger the gill membrane damage and increase epithelial permeability in zebrafish. This assertion is supported by the observation by Bessemer et al. (2015), who reported bare ZnO NPs aggregates with a positive zeta potential caused tissue damage and increased the Na⁺/K⁺-ATPase activity in *Catostomus commersonii*'s gills. Moreover, it was reported larger NPs are likely to be more easily trapped in the mucus layer of the gill (Sanderson et al., 1996; Tao et al., 1999). Therefore, the greater impacts of bare Fe₃O₄ NPs over starch-coated Fe₃O₄ NPs are attributed to the higher accumulation in the fish gills and the associated genetic alterations. The results also provide strong evidence that the starch coating can greatly alleviate the toxicity of Fe₃O₄ NPs in the gill tissue.

In contrast, a large number of DEGs overlapped for the livers in response to the two forms of Fe₃O₄ NPs, reflecting the liver gene response shared similar mechanisms upon the two different treatments. The liver is known to be a critical target for xenobiotic-induced toxicity, and it is also a storage organ for iron (the proteins, ferritin and hemosiderin) (Zhao et al., 2016). Although both forms of Fe₃O₄ NPs did not cause mortality, they were still capable of triggering gene regulations (**Fig. 3.2 and 3.3**) related to immune and inflammation response, ER stress and unfolded protein response, oxidative stress and antioxidant response, impacts on mitochondria energy metabolism, disruption of DNA damage and repair, and heat shock pathways. Earlier, Karlsson et al. (2009) studied the human cell line A549 and found that Fe₃O₄ NPs (20-30 nm, 80 g/mL) may cause cell death, mitochondrial damage, DNA damage, and oxidative DNA lesions. Another study that used human brain cell cultures found that exposure to Fe₃O₄ NPs for 4-48 h affected the mitochondrial function without altering the cell membrane integrity and morphology, and several days of exposure to low concentrations of Fe₃O₄ NPs altered the growth and cell proliferation (Coccini et al., 2017). One more study demonstrated that *in vitro* Fe₃O₄ NPs coated with polyvinylpyrrolidone decreased neuron viability, triggered oxidative stress, and activated JNK- and p53-mediated pathways to regulate cell cycle and apoptosis (Wu et al., 2013). Overall, the body of evidence supports our findings that Fe₃O₄ NPs could elicit similar toxicity effect on zebrafish.

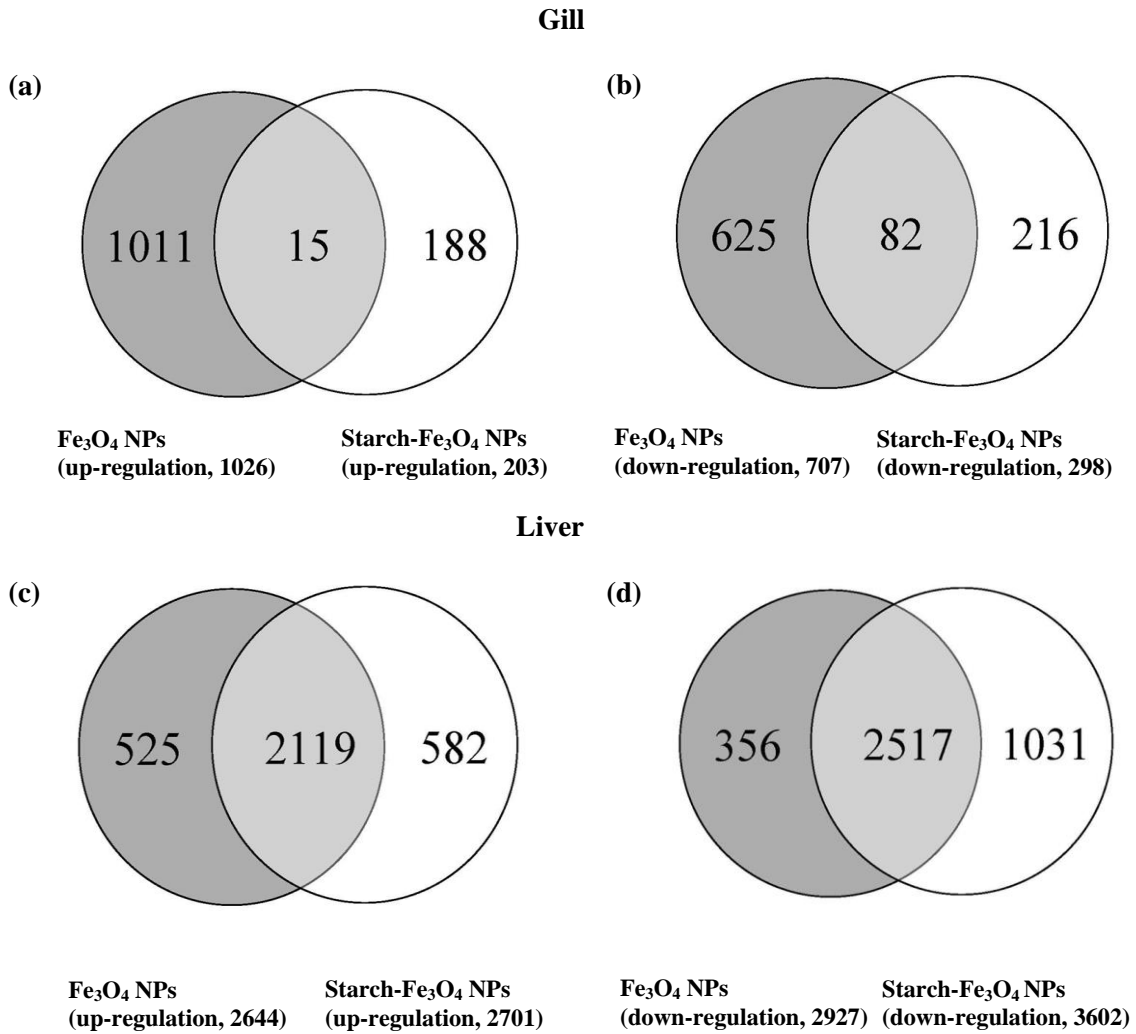


Figure 3. 2 Venn diagram showing number of genes identified with up- or down-regulated expression ($P < 0.05$) in zebrafish gills and livers upon exposure to bare and starch-coated Fe₃O₄ nanoparticles. **(a)** Up-regulated DEGs in gills, **(b)** Down-regulated DEGs in gills, **(c)** Up-regulated DEGs in livers, and **(d)** Down-regulated DEGs in livers.

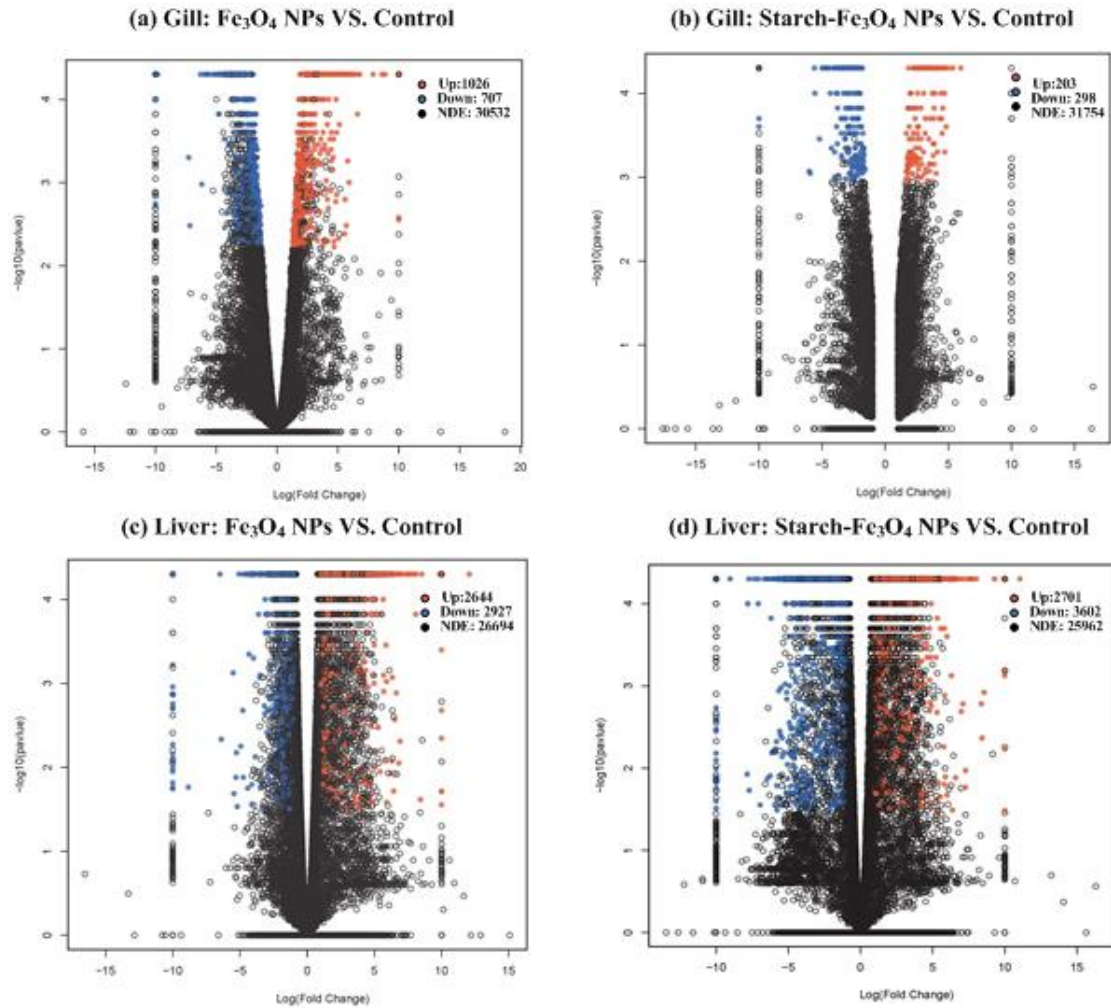


Figure 3.3 Volcano plots for gene libraries of zebrafish showing variance in gene expression with respect to fold change and significance (P-value). (a) Expressed genes in gill for untreated (control) and bare Fe_3O_4 NPs treated zebrafish, (b) Expressed genes in gill for untreated and starch-coated Fe_3O_4 NPs treated zebrafish, (c) Expressed genes in liver for untreated and bare Fe_3O_4 NPs treated zebrafish, and (d) Expressed genes in liver for untreated and starch-coated Fe_3O_4 NPs treated zebrafish. Each dot represents an individual gene: Red dots refer to the up-regulated DEGs, Blue dots to the down-regulated DEGs, and black dots to not differentially expressed genes (NDE).

Figures 3.4 and **3.5** compare the effects of bare and starch-coated Fe_3O_4 NPs on the immune and inflammation response, oxidative stress and antioxidant response, ER stress and unfolded protein response, mitochondria and unfold protein response, DNA damage and repair and

apoptosis pathways in the gills and livers of the zebrafish. The results indicate that the starch coating could alter the toxicity of Fe₃O₄ NPs in both tissues, and the toxicity is tissue-dependent.

Interestingly, a total of 17 representative genes in the gills were significantly expressed for bare Fe₃O₄ NPs treated group in relation to the immune and inflammation response, oxidative stress and antioxidant response, ER stress and unfolded protein response, mitochondria and unfold protein response, DNA damage and repair and apoptosis pathways, while only 3 genes were significantly expressed for the starch-coated Fe₃O₄ NPs treated group, which are related to immune and inflammation response, oxidative stress and antioxidant response (**Fig. 3.4**). This observation indicates that the starch coating remarkably mitigated the toxic effects of Fe₃O₄ NPs on the gills. Moreover, for the case of bare Fe₃O₄ NPs, 13 genes were found upregulated and 4 genes downregulated. For both groups, the major genes regulated were related to immune and inflammation response, indicating that the zebrafish were under significant oxidative stress.

A total of 55 and 64 representative genes in livers were identified for bare and starch-coated NP treatments, respectively, involving the mitochondria energy metabolism, mitochondria dysfunction pathway, immune and inflammation response, ER stress and unfolded protein response, oxidative stress and antioxidant response, DNA damage and repair and apoptosis pathway. It is noteworthy that the representative genes for the immune and inflammation response were all upregulated for both treatments, whereas all the genes for the DNA damage and repair were downregulated. Moreover, the changes related to the DNA damage and repair and the apoptosis pathway were more pronounced under the exposure to starch-coated Fe₃O₄ NPs as shown in **Figure 3.5**, suggesting that the starch can cause most of the changes in gene expressions observed.

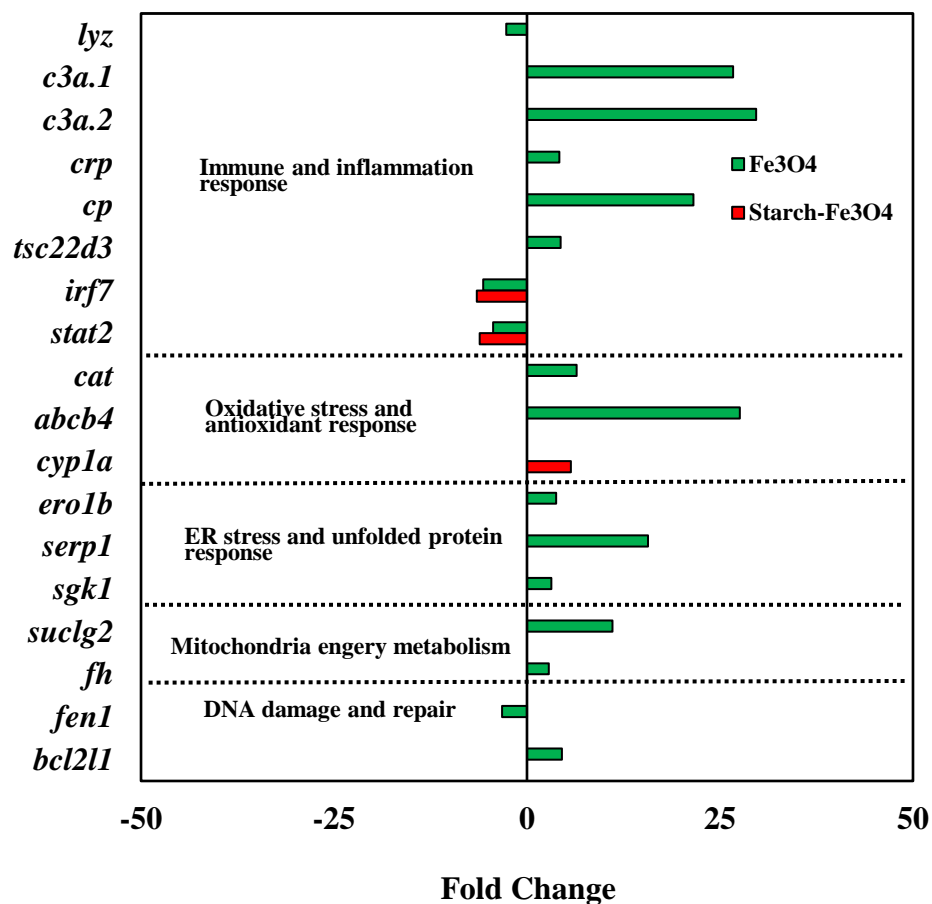


Figure 3. 4 Representative genes in zebrafish gills involved in immune and inflammation response, oxidative stress and antioxidant response, ER stress and unfolded protein response, mitochondria energy metabolism pathways, DNA damage and repair and apoptosis upon exposure to bare and starch-coated Fe₃O₄ NPs for 7 days (Data shown having fold change < -2 and > 2 at P<0.05).

Oxidative stress is a crucial factor in NP-induced toxicity (Nel et al., 2006). A possible role of oxidative stress is the induction and mediation of DNA damage and apoptosis (Simonian and Coyle, 1996). In this study, diverse DEGs related to immune, oxidative stress and antioxidant response were identified in livers and most of them were found up-regulated in both treatment cases, indicating an oxidative stress condition. Strikingly, the stress indicator gene, cytochrome P450 1A (*cyp1a*) was found ~50-fold and 76-fold up-regulated in the livers under bare and

starch-coated Fe₃O₄ NPs exposure, respectively, indicating significant detoxification of the stressor. Many researchers have suggested using the *cyp1a* gene as a fish biomarker for monitoring the antioxidant defense system (Chae et al., 2009; Pham et al., 2012). Evidently, this gene could serve the same purpose when evaluating the Fe₃O₄ NPs toxicity as well.

The significantly expressed gene, *tsc22d3*, encoding a leucine zipper transcription factor, was found ~30-fold and 46-fold overexpressed under bare and starch-coated Fe₃O₄ NPs, respectively, showing an inflammation stress condition (Bajak et al., 2015). Several studies showed that *tsc22d3* is induced by glucocorticoids (GCs), and plays a vital role as a mediator in the anti-inflammatory and immunosuppressive action of GCs (Ayroldi and Riccardi, 2009). The up-regulation of these biomarker genes indicate the inflammation response and possible iron detoxification effect when the adult zebrafish were exposed to the Fe₃O₄ NPs.

The DEGs regulation for constituents of the mitochondrial dysfunction pathway (genes including *mt-nd4*, *mt-nd5*, *mt-cyb*, *cox17*, *cox6a1*, *mt-co2* and *mt-co3* ect.) further suggested the production of reactive oxygen species (ROS) upon the exposure to the Fe₃O₄ NPs. Inflammation triggers an increased production of ROS, which, if not effectively removed by the antioxidant defenses, can induce oxidative stress and impair cellular macromolecules such as nucleic acids, lipids and proteins (Halliwell and Gutteridge, 2015). Thus, inflammation and oxidative stress are tightly linked. The overexpression of the hepatotoxicity biomarker gene, *krt18*, in both groups further confirms an apparent hepatotoxicity (Liu et al., 2016).

Down-regulation of DEGs related to DNA damage and repair was detected in the livers for both treatment cases. However, starch-coated Fe₃O₄ NPs exhibits more profound impacts than bare NPs in this aspect. In addition, *tp53*, the guardian of the genome, was only identified for starch-coated Fe₃O₄ NPs with a slight overexpression (2-fold), further confirming that starch-

coated Fe₃O₄ NPs could induce more stress on the zebrafish livers. Physically, this is also in accord with the fact that the stabilized nanoparticles are more transportable into the livers than the aggregated bare particles. The activation of the transcription factor *p53* in response to DNA damage can lead to cell cycle arrest or apoptosis (Langheinrich et al., 2002). The apoptosis pathways related DEGs were found in both treatments, showing the potential of cell apoptosis. Our results demonstrate that both bare and starch-coated Fe₃O₄ NPs induced oxidative stress, DNA damage, and apoptosis in zebrafish liver tissues. This agrees with the observation by (Choi et al., 2010) that metallic Ag NPs elicited similar toxicity on zebrafish liver. However, the presence of a surface coating on Fe₃O₄ NPs could have more deleterious impacts on liver. One possible reason is that the smaller and less adsorbable starch-coated particles could be more rapidly taken up by endocytosis. The upregulation of *flot1b* and *flot2a* found in both treatments can be related to the movement of NP-containing endosomes to the lysosomes. The overexpression of these two genes was more profound for starch-coated Fe₃O₄ NPs, unveiling an intensified endocytosis. A similar observation was reported by Perreault et al. (2012) who studied polymer coated CuO NPs and found that the coated NPs were more toxic than the uncoated NPs in algal cells, resulting from intracellular interactions between NPs and the cellular system. Suresh et al. (2010) indicated that the protein coated Ag NPs were more toxic than bare Ag NPs, and citrate-coated Ag NPs were more toxic than PVP-coated Ag NPs. However, the underlying mechanisms remain largely unknown. Some studies have drawn opposite conclusions on the effect of coating on nanoparticles toxicity. For instance, it is reported that PEI-PEG-chitosan-copolymer-coated iron oxide NPs showed an innocuous toxic profile and were suggested as a potential candidate for safe in vivo delivery of DNA for gene therapy

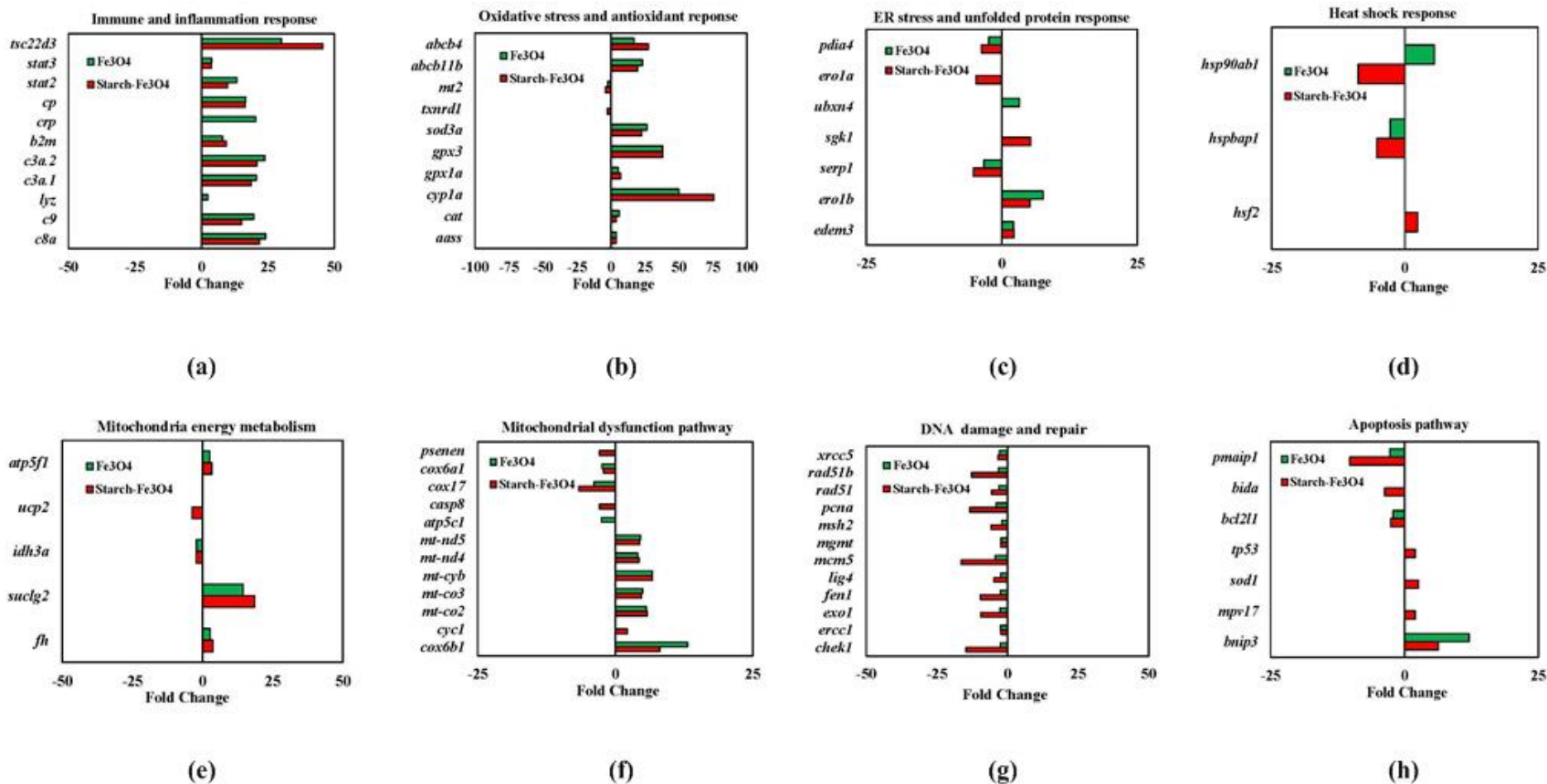


Figure 3. 5 Fold changes of representative genes in zebrafish livers in relation to: (a) immune and inflammation response, (b) oxidative stress and antioxidant response, (c) ER stress and unfolded protein response, (d) heat shock response, (e) mitochondria energy metabolism pathways, (f) mitochondria dysfunction pathway, (g) DNA damage and repair, and (h) apoptosis pathway upon treatments with bare or starch-coated Fe3O4 NPs for 7 days (Data shown having fold change < -2 and > 2 at P<0.05).

(Kievit et al., 2009). Surface coating on TiO₂ NPs could significantly reduce the molting and mortality rate compared to bare NPs in *Daphnia magna* (Dabrunz et al., 2011). Therefore, the toxic effects and the acting mechanisms of nanoparticles can be altered by the coatings, and cautions should be exercised when trying to extrapolate toxicity information from one type of nanoparticles to another, even within tissues for the same organism (Griffitt et al., 2008).

To identify the effects on the transcriptomic pathways, the subset of the genes that were significantly affected by the NP treatment were subjected to the gene ontology (GO) analysis using the Goatools functional enrichment tool. The GO analysis was performed to identify GO pathways with three GO categories: cellular components, biological processes and molecular functions. The basic GO unit is the GO term. Every GO term belongs to a particular category. GO terms with the Bonferroni-corrected P-values < 0.05 were defined as being significantly enriched in DEGs. **Figures 3.6a** and **3.6b** gives the histogram of the percentage of DEGs in the gills and livers falling into the GO categories for the groups treated with bare or starch-stabilized Fe₃O₄ NPs.

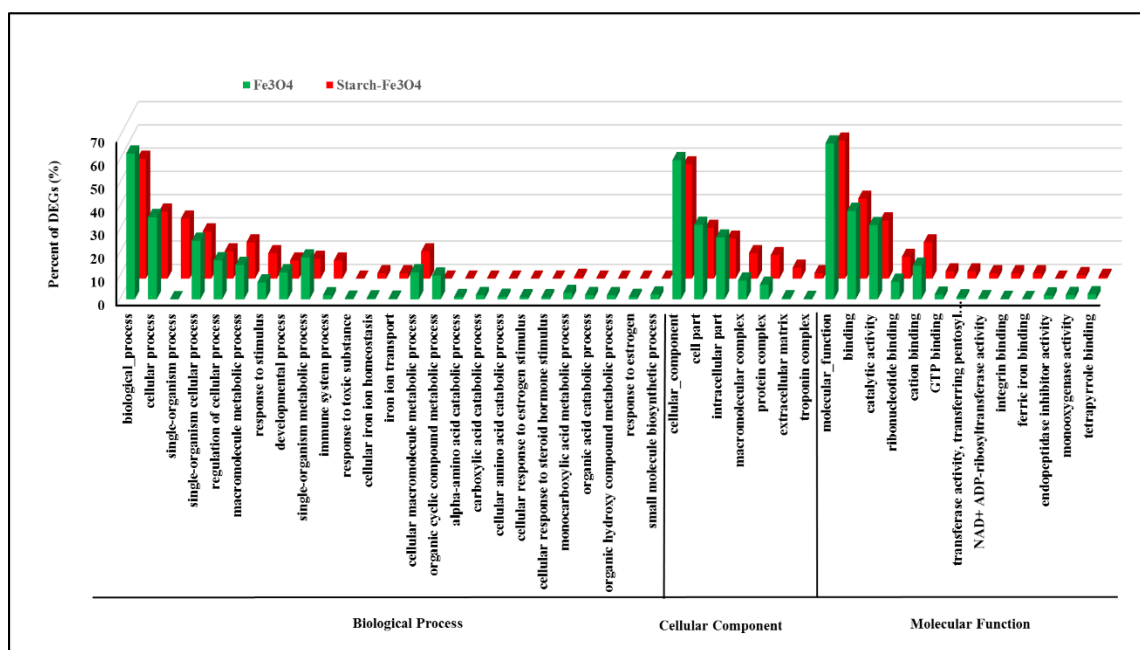
The majority of the responsive GO terms were found in the biological processes, followed by the molecular functions and cellular components for both treatments and in both tissues of zebrafish (**Table 3.4**).

In the gills, the biological processes that were significantly enriched in both treatments were mainly involved in the cellular process (GO:0009987), single-organism process (GO:0044699) and response to stimulus (GO:0050896). The most DEGs affected molecular functions were associated with binding (GO:0005488), catalytic activity (GO:0003824) and cation binding (GO:0043169). With regard to cellular components, the cell part (GO:0044464) and intracellular part (GO:0044424) were the largest DEGs categories.

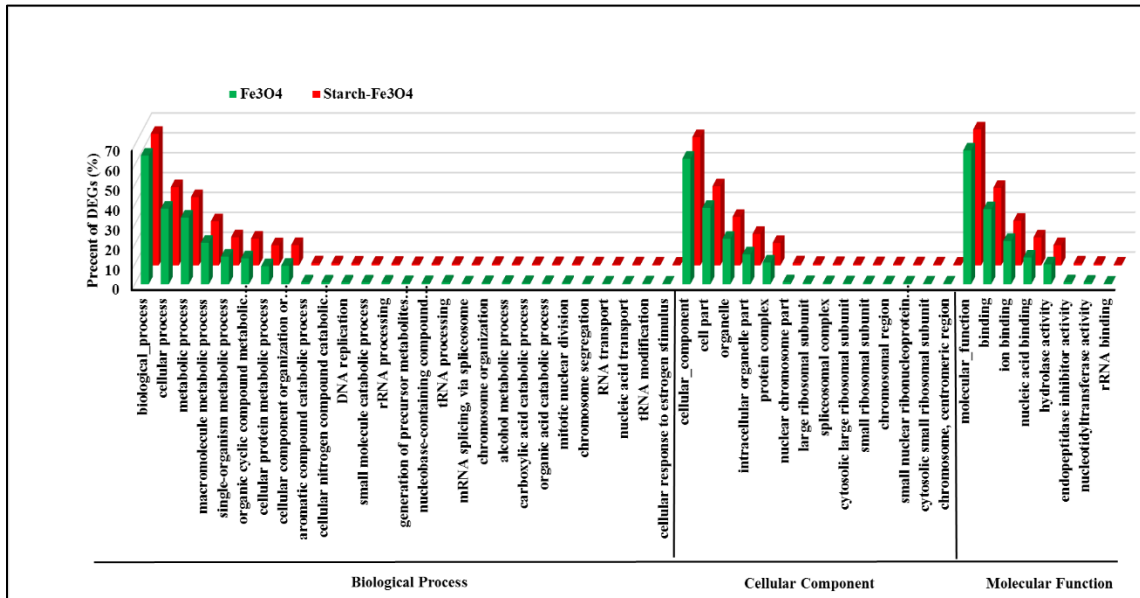
Table 3. 4 Statistical analysis of GO enrichment numbers and percentage in each category, biological process, molecular function and cellular component in gill and liver of zebrafish exposed to bare or starch-coated Fe₃O₄ nanoparticles.

| | Samples | GO Enrichment Number | Biological Process | Molecular Function | Cellular Component |
|--------------|---|----------------------|--------------------|--------------------|--------------------|
| Gill | Fe ₃ O ₄ NPs | 1033 | 661(64.0%) | 302 (29.2%) | 70 (6.8%) |
| | Starch-Fe ₃ O ₄ NPs | 207 | 151(72.9%) | 44 (21.3%) | 12 (5.8%) |
| Liver | Fe ₃ O ₄ NPs | 2031 | 1272 (62.6%) | 512 (25.2%) | 247 (12.2%) |
| | Starch-Fe ₃ O ₄ NPs | 2398 | 1463 (61.0%) | 642 (26.8%) | 293 (12.2%) |

For the livers, the GO terms for both treatment followed the same pattern, the biological processes were the most prevalent, and genes involved in the cellular process (GO:0009987), metabolic process (GO:0008152) and single-organism metabolic process (GO:0044699) were most represented. The most DEGs affected molecular functions were associated with binding (GO:0005488), ion binding (GO:0043167) and nucleic acid binding (GO:0003676). For cellular components, the cell part (GO:0044464), organelle (GO:0043226) and intracellular organelle part (GO:0043229) were the most significantly enriched DEGs categories.



(a)



(b)

Figure 3. 6 Gene ontology (GO) category patterns of the differentially expressed genes in gills and livers of zebrafish upon exposure to bare or starch-coated Fe₃O₄ NPs for 7 days. (a) GO categories in gills, and (b) GO categories in livers. The GO was assigned into three categories: biological process, cellular component and molecular function.

The KEGG pathway enrichment analysis was performed based on the loading stress-responsive genes to identify the significantly stress-related pathways. **Table 3.5** lists the common and different KEGG pathways between two treatments in gills and livers based on the q-values; and **Tables 3.6** and **3.7** give the related KEGG ID, input number, background number and P-values. Evidently, the bare Fe₃O₄ NPs had greater impact than starch-Fe₃O₄ NPs on the KEGG pathways, and the effects were more profound on the gills than the livers. Only five common KEGG pathways were significantly enriched in gills in both treatments, and more KEGG pathways were altered under the exposure to the bare Fe₃O₄ NPs. However, the high degree of common KEGG pathways (49) in the livers for the two forms of Fe₃O₄ NPs suggests a very significant overlap in the mechanisms of toxicity of the nanoparticles. Based on this overlap, the

toxic effects on the livers of the zebrafish are mainly attributed to of the Fe₃O₄ particles themselves regardless of the stabilization effect.

The KEGG pathway analysis also provides evidence that Fe₃O₄ NPs exerted toxic effects on both tissues. Several KEGG pathways were significantly altered, including those related with fish immunity such as the complement and coagulation cascades; and the genetic information processing such as ribosome, and cellular processes such as cell cycle.

The complement system is an ancient mechanism of defense (Zhu et al., 2005) and it is an important component of both the innate and adaptive immune systems. The complement system of teleost fish consists of three pathways, making it similar to the system found in higher vertebrates (Boshra et al., 2004). The complement and coagulation cascades KEGG pathways were found significantly enriched in both gill and liver when exposed to bare Fe₃O₄ NPs and in liver when exposed to starch-coated Fe₃O₄ NPs. This pathway was found significantly altered in rats during exposure to copper NPs (Liao and Liu, 2012) and carboxymethyl cellulose stabilized FeS NPs (Zheng et al, 2017).

The cell cycle pathway was the most significant down-regulated transcriptomic KEGG pathway in liver for both treated groups. The NPs influenced the cell cycle pathway by down-regulating some key genes such as *ccna1* coding cyclins. Other cell cycle regulators, origin recognition complex (ORC) (*orc1*, *orc3* and *orc5*) and *gins2*, which are the fundamental proteins for DNA replication, were all down-regulated, again indicating a stress condition of zebrafish under the NPs exposure, and starch-coated Fe₃O₄ NPs again showed more pronounced regulation indicating greater suppression gene expression in liver. This is consistent with our previous study (Zheng et al., 2017) that the suppression of cell cycle regulators was accompanied by the downregulation of a number of genes directly involved in the process of DNA replication.

Table 3. 5 Impact of bare and starch-coated Fe₃O₄ nanoparticles on the KEGG pathways in zebrafish gill and liver (P<0.05).

| KEGG Pathways | |
|--|--|
| Fe₃O₄ NPs | Starch-Fe₃O₄ NPs |
| Gill | |
| Common Pathways (5): Arginine and proline metabolism, Nicotinate and nicotinamide metabolism, Phenylalanine, tyrosine and tryptophan biosynthesis, Staphylococcus aureus infection, Tryptophan metabolism | |
| Different Pathways (53): Complement and coagulation cascades, Tryptophan metabolism, PPAR signaling pathway, Peroxisome, Fatty acid degradation, Drug metabolism-cytochrome P450, Glycine, serine and threonine metabolism, Steroid biosynthesis, Glycerophospholipid metabolism, Pentose and glucuronate interconversions, Metabolism of xenobiotics by cytochrome P450, Fatty acid metabolism, Chemical carcinogenesis, Glycerolipid metabolism, Starch and sucrose metabolism, Retinol metabolism, Valine, leucine and isoleucine degradation, Pyruvate metabolism, Glyoxylate and dicarboxylate metabolism, Propanoate metabolism, Ascorbate and aldarate metabolism, Staphylococcus aureus infection, Steroid hormone biosynthesis, Biosynthesis of unsaturated fatty acids, One carbon pool by folate, Carbon fixation pathways in prokaryotes, Primary bile acid biosynthesis, Tyrosine metabolism, Glycolysis/Gluconeogenesis, Carbon metabolism, Fat digestion and absorption, Histidine metabolism, Benzoate degradation, Glutathione metabolism, Cysteine and methionine metabolism, Terpenoid backbone biosynthesis, Phenylalanine metabolism, Vitamin digestion and absorption, Lysine degradation, Citrate cycle (TCA cycle), Biosynthesis of amino acids, Isoquinoline alkaloid biosynthesis, Phenylalanine, tyrosine and tryptophan biosynthesis, Hepatitis C, Fatty acid elongation, beta-Alanine metabolism, alpha-of the young, Nicotinate and nicotinamide metabolism, Chloroalkane and chloroalkene degradation, Bile secretion, Porphyrin and chlorophyll metabolism, | Different Pathways (32): Antigen processing and presentation, Asthma, Intestinal immune network for IgA production, Graft-versus-host disease, Allograft rejection, Leishmaniasis, Rheumatoid arthritis, Systemic lupus erythematosus, Toxoplasmosis, Autoimmune thyroid disease, Inflammatory bowel disease (IBD), Influenza A, Type I diabetes mellitus, Hypertrophic cardiomyopathy (HCM), Amoebiasis, Dilated cardiomyopathy, Fructose and mannose metabolism, Phagosome, Mineral absorption, Arrhythmogenic right ventricular cardiomyopathy (ARVC), Calcium signaling pathway, Cell adhesion molecules (CAMs), Viral myocarditis, Nitrogen metabolism, Tryptophan metabolism, Estrogen signaling pathway, Herpes simplex infection, Tuberculosis, Nicotinate and nicotinamide metabolism, African trypanosomiasis, Cytosolic DNA-sensing pathway, RIG-I-like receptor signaling pathway, Viral carcinogenesis, Leukocyte transendothelial migration, Proximal tubule bicarbonate reclamation, Phenylalanine, tyrosine and tryptophan biosynthesis |

| | |
|--|--|
| Selenocompound metabolism, Caprolactam degradation | |
| Liver | |
| <p>Common Pathways (49): Amino sugar and nucleotide sugar metabolism, Arginine and proline metabolism, Basal transcription factors, Base excision repair, Biosynthesis of amino acids, Biosynthesis of unsaturated fatty acids, Carbon metabolism, Cell cycle, Cell cycle-yeast, Chemical carcinogenesis, Complement and coagulation cascades, Cysteine and methionine metabolism, DNA replication, Drug metabolism-cytochrome P450, Drug metabolism - other enzymes, Fanconi anemia pathway, Fat digestion and absorption, Fatty acid degradation, Fatty acid metabolism, Glutathione metabolism, Glycerolipid metabolism, Glycerophospholipid metabolism, Glycine, serine and threonine metabolism, Glyoxylate and dicarboxylate metabolism, Homologous recombination, Meiosis-yeast, Metabolism of xenobiotics by cytochrome P450, Mismatch repair, Oocyte meiosis, p53 signaling pathway, Pentose and glucuronate interconversions, Peroxisome, Porphyrin and chlorophyll metabolism, PPAR signaling pathway, Progesterone-mediated oocyte maturation, Purine metabolism, Pyrimidine metabolism, Pyruvate metabolism, Retinol metabolism, Ribosome, RNA degradation, RNA polymerase, RNA transport, Spliceosome, Starch and sucrose metabolism, Tryptophan metabolism, Valine, leucine and isoleucine degradation, Viral carcinogenesis</p> | |
| <p>Different Pathways (13): Glycolysis/Gluconeogenesis, Methane metabolism, Steroid hormone biosynthesis, Staphylococcus aureus infection, Linoleic acid metabolism, Vitamin digestion and absorption, Citrate cycle (TCA cycle), Benzoate degradation, Glutathione metabolism, Primary bile acid biosynthesis, Carbon fixation in photosynthetic organisms, N-Glycan biosynthesis, Arachidonic acid metabolism</p> | <p>Different Pathways (11): Ascorbate and aldarate metabolism, Histidine metabolism, Pantothenate and CoA biosynthesis, Fatty acid elongation, Terpenoid backbone biosynthesis, Propanoate metabolism, Ubiquitin mediated proteolysis, beta-Alanine metabolism, Non-homologous end-joining, Protein processing in endoplasmic reticulum, Synthesis and degradation of ketone bodies</p> |

Table 3. 6 KEGG pathways impacted by bare and starch-coated Fe₃O₄ NPs in zebrafish gill (P<0.05).

| Gill | | | | |
|--|-----------|---------------------|--------------------------|----------------|
| Fe₃O₄ NPs | | | | |
| KEGG Pathway Term | ID | Input number | Background number | P-Value |
| Complement and coagulation cascades | ko04610 | 25 | 63 | 8.32E-09 |
| Tryptophan metabolism | ko00380 | 21 | 47 | 2.55E-08 |
| PPAR signaling pathway | ko03320 | 23 | 59 | 4.23E-08 |
| Peroxisome | ko04146 | 26 | 86 | 3.67E-07 |
| Fatty acid degradation | ko00071 | 16 | 39 | 2.80E-06 |
| Drug metabolism - cytochrome P450 | ko00982 | 14 | 32 | 6.49E-06 |
| Glycine, serine and threonine metabolism | ko00260 | 16 | 43 | 7.65E-06 |
| Steroid biosynthesis | ko00100 | 11 | 20 | 1.23E-05 |
| Glycerophospholipid metabolism | ko00564 | 24 | 95 | 1.37E-05 |
| Pentose and glucuronate interconversions | ko00040 | 12 | 25 | 1.43E-05 |
| Metabolism of xenobiotics by cytochrome P450 | ko00980 | 14 | 35 | 1.46E-05 |
| Fatty acid metabolism | ko01212 | 17 | 52 | 1.62E-05 |
| Chemical carcinogenesis | ko05204 | 15 | 42 | 2.17E-05 |
| Glycerolipid metabolism | ko00561 | 17 | 56 | 3.56E-05 |
| Drug metabolism - other enzymes | ko00983 | 12 | 32 | 9.78E-05 |
| Starch and sucrose metabolism | ko00500 | 13 | 38 | 0.000108 |
| Retinol metabolism | ko00830 | 13 | 38 | 0.000108 |
| Valine, leucine and isoleucine degradation | ko00280 | 15 | 50 | 0.000113 |
| Pyruvate metabolism | ko00620 | 13 | 41 | 0.000202 |
| Glyoxylate and dicarboxylate metabolism | ko00630 | 11 | 30 | 0.000222 |
| Propanoate metabolism | ko00640 | 10 | 26 | 0.000314 |
| Ascorbate and aldarate metabolism | ko00053 | 8 | 16 | 0.000319 |
| Staphylococcus aureus infection | ko05150 | 11 | 32 | 0.00035 |
| Steroid hormone biosynthesis | ko00140 | 11 | 34 | 0.000535 |
| Biosynthesis of unsaturated fatty acids | ko01040 | 9 | 23 | 0.000564 |
| One carbon pool by folate | ko00670 | 8 | 18 | 0.000588 |
| Carbon fixation pathways in prokaryotes | ko00720 | 7 | 14 | 0.000759 |
| Primary bile acid biosynthesis | ko00120 | 8 | 19 | 0.000779 |
| Tyrosine metabolism | ko00350 | 10 | 31 | 0.000967 |
| Glycolysis / Gluconeogenesis | ko00010 | 16 | 73 | 0.001328 |
| Arginine and proline metabolism | ko00330 | 15 | 66 | 0.00136 |
| Carbon metabolism | ko01200 | 21 | 113 | 0.001635 |
| Fat digestion and absorption | ko04975 | 10 | 34 | 0.001727 |
| Histidine metabolism | ko00340 | 8 | 23 | 0.002091 |
| Benzoate degradation | ko00362 | 5 | 8 | 0.002169 |
| Glutathione metabolism | ko00480 | 12 | 49 | 0.002348 |

| | | | | |
|---|---------|----|-----|----------|
| Cysteine and methionine metabolism | ko00270 | 11 | 43 | 0.00264 |
| Terpenoid backbone biosynthesis | ko00900 | 7 | 21 | 0.004772 |
| Phenylalanine metabolism | ko00360 | 6 | 17 | 0.007083 |
| Vitamin digestion and absorption | ko04977 | 7 | 24 | 0.008633 |
| Lysine degradation | ko00310 | 12 | 60 | 0.009389 |
| Citrate cycle (TCA cycle) | ko00020 | 8 | 33 | 0.012651 |
| Biosynthesis of amino acids | ko01230 | 14 | 80 | 0.014018 |
| Isoquinoline alkaloid biosynthesis | ko00950 | 4 | 11 | 0.025072 |
| Phenylalanine, tyrosine and tryptophan biosynthesis | ko00400 | 3 | 6 | 0.027826 |
| Hepatitis C | ko05160 | 20 | 143 | 0.029083 |
| Fatty acid elongation | ko00062 | 7 | 32 | 0.029367 |
| beta-Alanine metabolism | ko00410 | 7 | 32 | 0.029367 |
| alpha-Linolenic acid metabolism | ko00592 | 5 | 18 | 0.029545 |
| Maturity onset diabetes of the young | ko04950 | 6 | 26 | 0.034953 |
| Nicotinate and nicotinamide metabolism | ko00760 | 6 | 26 | 0.034953 |
| Chloroalkane and chloroalkene degradation | ko00625 | 3 | 7 | 0.037489 |
| Bile secretion | ko04976 | 12 | 76 | 0.040249 |
| Porphyrin and chlorophyll metabolism | ko00860 | 6 | 28 | 0.045486 |
| Selenocompound metabolism | ko00450 | 4 | 14 | 0.046674 |
| Caprolactam degradation | ko00930 | 3 | 8 | 0.048627 |
| Starch- Fe₃O₄ NPs | | | | |
| Antigen processing and presentation | ko04612 | 6 | 65 | 0.095004 |
| Asthma | ko05310 | 3 | 14 | 0.095004 |
| Intestinal immune network for IgA production | ko04672 | 4 | 30 | 0.095004 |
| Staphylococcus aureus infection | ko05150 | 4 | 32 | 0.095004 |
| Graft-versus-host disease | ko05332 | 3 | 16 | 0.099235 |
| Allograft rejection | ko05330 | 3 | 21 | 0.110622 |
| Leishmaniasis | ko05140 | 5 | 71 | 0.110622 |
| Rheumatoid arthritis | ko05323 | 5 | 71 | 0.110622 |
| Systemic lupus erythematosus | ko05322 | 7 | 126 | 0.110622 |
| Toxoplasmosis | ko05145 | 7 | 125 | 0.110622 |
| Autoimmune thyroid disease | ko05320 | 3 | 26 | 0.138933 |
| Inflammatory bowel disease (IBD) | ko05321 | 4 | 49 | 0.138933 |
| Influenza A | ko05164 | 7 | 154 | 0.158333 |
| Type I diabetes mellitus | ko04940 | 3 | 29 | 0.158333 |
| Hypertrophic cardiomyopathy (HCM) | ko05410 | 5 | 90 | 0.182162 |
| Amoebiasis | ko05146 | 5 | 98 | 0.205941 |
| Arginine and proline metabolism | ko00330 | 4 | 66 | 0.205941 |
| Dilated cardiomyopathy | ko05414 | 5 | 99 | 0.205941 |
| Fructose and mannose metabolism | ko00051 | 3 | 36 | 0.205941 |
| Phagosome | ko04145 | 6 | 139 | 0.217755 |

| | | | | |
|--|---------|---|-----|----------|
| Mineral absorption | ko04978 | 3 | 40 | 0.228517 |
| Arrhythmogenic right ventricular cardiomyopathy (ARVC) | ko05412 | 4 | 75 | 0.247888 |
| Calcium signaling pathway | ko04020 | 8 | 233 | 0.247888 |
| Cell adhesion molecules (CAMs) | ko04514 | 5 | 113 | 0.247888 |
| Viral myocarditis | ko05416 | 3 | 44 | 0.247888 |
| Nitrogen metabolism | ko00910 | 2 | 19 | 0.260782 |
| Tryptophan metabolism | ko00380 | 3 | 47 | 0.260782 |
| Estrogen signaling pathway | ko04915 | 5 | 124 | 0.303968 |
| Herpes simplex infection | ko05168 | 6 | 168 | 0.316036 |
| Tuberculosis | ko05152 | 6 | 176 | 0.363185 |
| Nicotinate and nicotinamide metabolism | ko00760 | 2 | 26 | 0.36982 |
| African trypanosomiasis | ko05143 | 2 | 27 | 0.380942 |
| Cytosolic DNA-sensing pathway | ko04623 | 2 | 40 | 0.383371 |
| RIG-I-like receptor signaling pathway | ko04622 | 2 | 59 | 0.383371 |
| Viral carcinogenesis | ko05203 | 4 | 231 | 0.383371 |
| Leukocyte transendothelial migration | ko04670 | 5 | 142 | 0.401378 |
| Proximal tubule bicarbonate reclamation | ko04964 | 2 | 32 | 0.471163 |

Table 3. 7 KEGG pathways impacted by bare or starch-coated Fe₃O₄ NPs in zebrafish liver (P<0.05).

| Liver | | | | |
|--|-----------|---------------------|--------------------------|----------------|
| Fe₃O₄ NPs | | | | |
| KEGG Pathway Term | ID | Input number | Background number | P-Value |
| Ribosome | ko03010 | 81 | 127 | 1.17E-10 |
| Pyrimidine metabolism | ko00240 | 58 | 103 | 1.03E-06 |
| Complement and coagulation cascades | ko04610 | 39 | 63 | 1.17E-05 |
| Glycine, serine and threonine metabolism | ko00260 | 30 | 43 | 2.32E-05 |
| Peroxisome | ko04146 | 45 | 86 | 6.10E-05 |
| DNA replication | ko03030 | 26 | 37 | 7.29E-05 |
| Cell cycle | ko04110 | 62 | 137 | 8.39E-05 |
| Purine metabolism | ko00230 | 75 | 178 | 0.000102 |
| Glyoxylate and dicarboxylate metabolism | ko00630 | 22 | 30 | 0.000166 |
| Carbon metabolism | ko01200 | 52 | 113 | 0.000218 |
| PPAR signaling pathway | ko03320 | 33 | 59 | 0.000223 |
| Drug metabolism - other enzymes | ko00983 | 22 | 32 | 0.000319 |
| Fatty acid metabolism | ko01212 | 29 | 52 | 0.00054 |
| Glycerophospholipid metabolism | ko00564 | 44 | 95 | 0.000574 |
| Nucleotide excision repair | ko03420 | 25 | 43 | 0.000814 |
| Cell cycle - yeast | ko04111 | 38 | 80 | 0.000916 |
| Glycerolipid metabolism | ko00561 | 29 | 56 | 0.001306 |
| Biosynthesis of amino acids | ko01230 | 37 | 80 | 0.001534 |
| Systemic lupus erythematosus | ko05322 | 52 | 126 | 0.001543 |
| Fatty acid degradation | ko00071 | 22 | 39 | 0.002169 |
| RNA transport | ko03013 | 58 | 148 | 0.002225 |
| Homologous recombination | ko03440 | 17 | 27 | 0.002919 |
| RNA degradation | ko03018 | 36 | 81 | 0.002965 |
| Pyruvate metabolism | ko00620 | 22 | 41 | 0.003442 |
| Tryptophan metabolism | ko00380 | 24 | 47 | 0.00375 |
| Meiosis - yeast | ko04113 | 31 | 68 | 0.00416 |
| Metabolism of xenobiotics by cytochrome P450 | ko00980 | 19 | 35 | 0.00575 |
| Pentose and glucuronate interconversions | ko00040 | 15 | 25 | 0.00696 |
| Fat digestion and absorption | ko04975 | 18 | 34 | 0.008556 |
| RNA polymerase | ko03020 | 16 | 29 | 0.009662 |
| Retinol metabolism | ko00830 | 19 | 38 | 0.010935 |
| Chemical carcinogenesis | ko05204 | 20 | 42 | 0.013499 |
| Progesterone-mediated oocyte maturation | ko04914 | 40 | 106 | 0.015515 |
| Biosynthesis of unsaturated fatty acids | ko01040 | 13 | 23 | 0.016353 |

| | | | | |
|---|---------|-----|-----|----------|
| Oocyte meiosis | ko04114 | 47 | 130 | 0.016663 |
| p53 signaling pathway | ko04115 | 29 | 71 | 0.016781 |
| Drug metabolism - cytochrome P450 | ko00982 | 16 | 32 | 0.018626 |
| Valine, leucine and isoleucine degradation | ko00280 | 22 | 50 | 0.019033 |
| Starch and sucrose metabolism | ko00500 | 18 | 38 | 0.019203 |
| Glycolysis / Gluconeogenesis | ko00010 | 29 | 73 | 0.021907 |
| Amino sugar and nucleotide sugar metabolism | ko00520 | 23 | 54 | 0.021943 |
| Methane metabolism | ko00680 | 16 | 33 | 0.022715 |
| Base excision repair | ko03410 | 17 | 36 | 0.022942 |
| Basal transcription factors | ko03022 | 18 | 39 | 0.023019 |
| Viral carcinogenesis | ko05203 | 75 | 231 | 0.023046 |
| Mismatch repair | ko03430 | 12 | 22 | 0.024884 |
| Fanconi anemia pathway | ko03460 | 21 | 49 | 0.026432 |
| Porphyrin and chlorophyll metabolism | ko00860 | 14 | 28 | 0.026747 |
| Steroid hormone biosynthesis | ko00140 | 16 | 34 | 0.027445 |
| Spliceosome | ko03040 | 46 | 132 | 0.028004 |
| Staphylococcus aureus infection | ko05150 | 15 | 32 | 0.032879 |
| Linoleic acid metabolism | ko00591 | 11 | 21 | 0.037639 |
| Vitamin digestion and absorption | ko04977 | 12 | 24 | 0.038691 |
| Citrate cycle (TCA cycle) | ko00020 | 15 | 33 | 0.039357 |
| Benzoate degradation | ko00362 | 6 | 8 | 0.041358 |
| Glutathione metabolism | ko00480 | 20 | 49 | 0.042065 |
| Cysteine and methionine metabolism | ko00270 | 18 | 43 | 0.044197 |
| Primary bile acid biosynthesis | ko00120 | 10 | 19 | 0.045457 |
| Arginine and proline metabolism | ko00330 | 25 | 66 | 0.046395 |
| Carbon fixation in photosynthetic organisms | ko00710 | 13 | 28 | 0.047426 |
| N-Glycan biosynthesis | ko00510 | 20 | 50 | 0.048318 |
| Arachidonic acid metabolism | ko00590 | 20 | 50 | 0.048318 |
| Starch-Fe₃O₄ NPs | | | | |
| Ribosome | ko03010 | 106 | 127 | 8.80E-15 |
| Pyrimidine metabolism | ko00240 | 65 | 103 | 1.94E-06 |
| DNA replication | ko03030 | 34 | 37 | 2.48E-06 |
| Glycine, serine and threonine metabolism | ko00260 | 35 | 43 | 1.11E-05 |
| Peroxisome | ko04146 | 54 | 86 | 1.52E-05 |
| Spliceosome | ko03040 | 73 | 132 | 1.55E-05 |
| Cell cycle | ko04110 | 72 | 137 | 6.12E-05 |
| Nucleotide excision repair | ko03420 | 32 | 43 | 8.67E-05 |
| RNA transport | ko03013 | 75 | 148 | 0.000106 |
| Cell cycle - yeast | ko04111 | 45 | 80 | 0.000464 |
| Complement and coagulation cascades | ko04610 | 38 | 63 | 0.000465 |
| Glycerolipid metabolism | ko00561 | 35 | 56 | 0.000476 |

| | | | | |
|--|---------|----|-----|----------|
| Purine metabolism | ko00230 | 82 | 178 | 0.000551 |
| Mismatch repair | ko03430 | 19 | 22 | 0.000676 |
| PPAR signaling pathway | ko03320 | 35 | 59 | 0.000949 |
| Glyoxylate and dicarboxylate metabolism | ko00630 | 22 | 30 | 0.00121 |
| Fatty acid degradation | ko00071 | 26 | 39 | 0.001243 |
| Meiosis - yeast | ko04113 | 38 | 68 | 0.001344 |
| Fatty acid metabolism | ko01212 | 31 | 52 | 0.0017 |
| Drug metabolism - other enzymes | ko00983 | 22 | 32 | 0.002173 |
| Tryptophan metabolism | ko00380 | 28 | 47 | 0.002794 |
| Cysteine and methionine metabolism | ko00270 | 26 | 43 | 0.003352 |
| Base excision repair | ko03410 | 23 | 36 | 0.003423 |
| Homologous recombination | ko03440 | 19 | 27 | 0.003535 |
| RNA degradation | ko03018 | 41 | 81 | 0.003555 |
| Pyruvate metabolism | ko00620 | 25 | 41 | 0.003668 |
| Arginine and proline metabolism | ko00330 | 35 | 66 | 0.003869 |
| Drug metabolism - cytochrome P450 | ko00982 | 21 | 32 | 0.004026 |
| Metabolism of xenobiotics by cytochrome P450 | ko00980 | 22 | 35 | 0.004778 |
| p53 signaling pathway | ko04115 | 36 | 71 | 0.005901 |
| Basal transcription factors | ko03022 | 23 | 39 | 0.006967 |
| Fanconi anemia pathway | ko03460 | 27 | 49 | 0.00715 |
| Pentose and glucuronate interconversions | ko00040 | 17 | 25 | 0.007186 |
| Oocyte meiosis | ko04114 | 57 | 130 | 0.007728 |
| Valine, leucine and isoleucine degradation | ko00280 | 27 | 50 | 0.008683 |
| Viral carcinogenesis | ko05203 | 91 | 231 | 0.010212 |
| Biosynthesis of amino acids | ko01230 | 38 | 80 | 0.010515 |
| RNA polymerase | ko03020 | 18 | 29 | 0.011125 |
| Progesterone-mediated oocyte maturation | ko04914 | 47 | 106 | 0.012498 |
| Glycerophospholipid metabolism | ko00564 | 43 | 95 | 0.012666 |
| Chemical carcinogenesis | ko05204 | 23 | 42 | 0.013076 |
| Ascorbate and aldarate metabolism | ko00053 | 12 | 16 | 0.01358 |
| Histidine metabolism | ko00340 | 15 | 23 | 0.014525 |
| Carbon metabolism | ko01200 | 48 | 113 | 0.020422 |
| Pantothenate and CoA biosynthesis | ko00770 | 10 | 13 | 0.021071 |
| Fatty acid elongation | ko00062 | 18 | 32 | 0.021937 |
| Biosynthesis of unsaturated fatty acids | ko01040 | 14 | 23 | 0.026393 |
| Porphyryn and chlorophyll metabolism | ko00860 | 16 | 28 | 0.027026 |
| Glutathione metabolism | ko00480 | 24 | 49 | 0.02871 |
| Terpenoid backbone biosynthesis | ko00900 | 13 | 21 | 0.029123 |
| Propanoate metabolism | ko00640 | 15 | 26 | 0.030006 |
| Ubiquitin mediated proteolysis | ko04120 | 55 | 137 | 0.030009 |

| | | | | |
|---|---------|----|-----|----------|
| Fat digestion and absorption | ko04975 | 18 | 34 | 0.032694 |
| beta-Alanine metabolism | ko00410 | 17 | 32 | 0.036475 |
| Amino sugar and nucleotide sugar metabolism | ko00520 | 25 | 54 | 0.040711 |
| Starch and sucrose metabolism | ko00500 | 19 | 38 | 0.041973 |
| Retinol metabolism | ko00830 | 19 | 38 | 0.041973 |
| Non-homologous end-joining | ko03450 | 9 | 13 | 0.042313 |
| Protein processing in endoplasmic reticulum | ko04141 | 66 | 175 | 0.046823 |
| Synthesis and degradation of ketone bodies | ko00072 | 7 | 9 | 0.049379 |

In terms of the stability of the starch coated Fe₃O₄ NPs, starch are reported to be degraded up to 200 days in a long-term degradation trial (Araújo et al., 2004), NPs might be agglomerate and precipitate into sediment after starch is degraded in aquaria system or possibly coated with natural organic matter (NOM) (Li, 2011) to get re-stabilized.

Water parameters (i.e. ionic strength and conductivity etc) play a big role in maintaining the fish health. For instance, if conductivity levels are high, especially due to dissolved salts, many forms of aquatic life are affected. The salts have ability to dehydrate the skin of animals. High concentrations of dissolved solids can exert a laxative effect to water or lead to an unpleasant mineral taste of the water. It is also possible for dissolved ions to alter the pH of a body of water, which in turn may affect aquatic species health. Additionally, significant increases in conductivity may be an indicator for pollution discharges to the water system. Every natural waterbody will have a baseline conductivity depending on the local geology and soils. Higher conductivity will result from the presence of various ions including nitrate, phosphate, and sodium. Freshwater streams ideally should have a conductivity between 150 to 500 µS/cm to support diverse aquatic life (Behar et al., 1996). To our knowledge, current conductivity meters are limited to employ a potentiometric method to monitor the amount of nutrients, salts or impurities in the solution. Our NPs suspension gave an elevated conductivity value ranging from

2.7-2.8 mS/cm ; however, it is hard to justify whether it is caused by NPs or the salts inside it. Further work needs to be done related to NPs caused stress water parameters Water parameter (i.e. ionic strength, conductivity ect.) related stress caused by NPs needs to be further evaluated in future study.

Several members of genes were selected for further qPCR validation. These genes are involved in responses to the mitochondria energy metabolism, mitochondria dysfunction pathway, immune and inflammation response, ER stress and unfolded protein response, oxidative stress and antioxidant response, and DNA damage and repair and apoptosis pathway. As an internal gene, the beta-actin was included. Under the given experimental conditions, the exposure to both forms of NPs showed no effect on the internal gene (data not shown). Generally, the gene expression levels and trend of regulation (increase/decrease) detected with RNA-seq and qualification based on qPCR are in agreement with each other (**Fig. 3.7**).

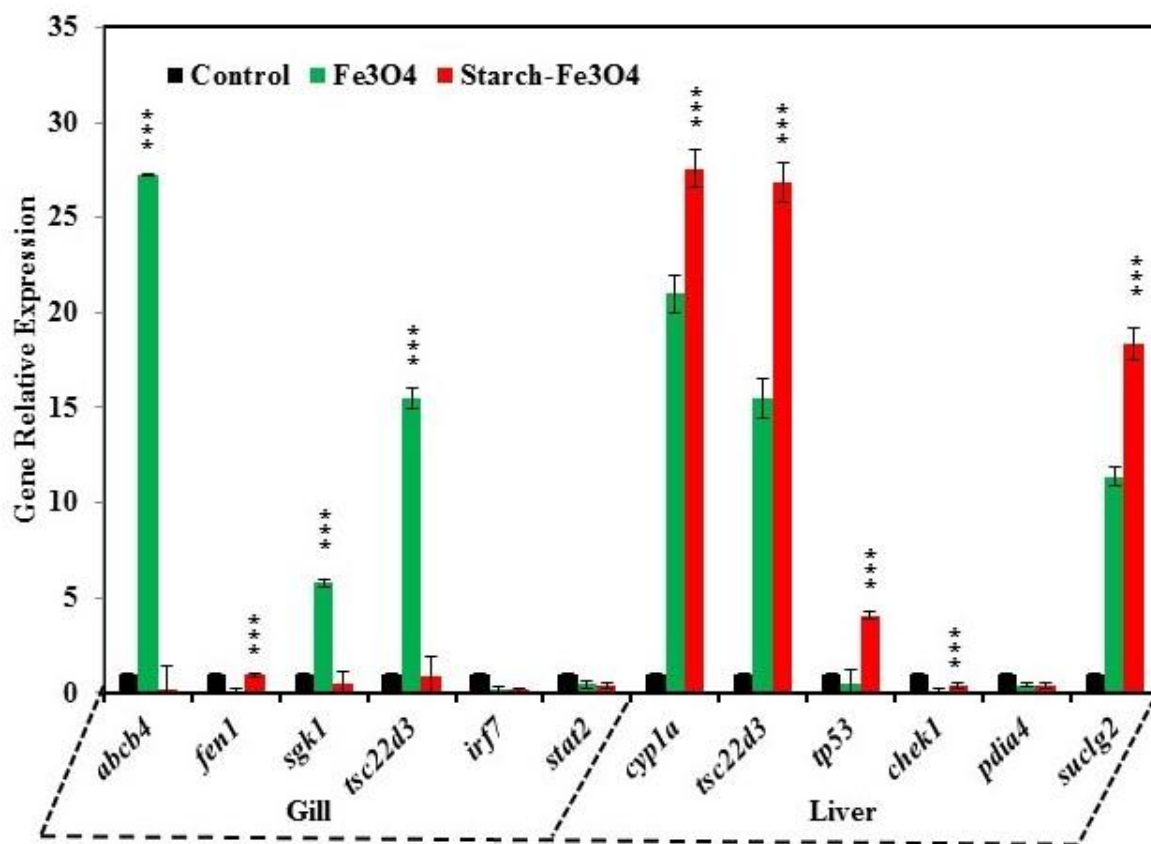


Figure 3.7 Validation of gill and liver tissue transcriptome results by qRT-PCR using twelve selected differentially expressed genes upon exposure to bare or starch-stabilized Fe₃O₄ NPs for 7 days. The qRT-PCR fold changes are relative to control samples and are normalized by changes in beta-actin values. The mean of three relative quantities of biological replicates were used in a two-tailed Student's t test with a 95% confidence level (P<0.05) to determine the gene expression significance.

3.4 Conclusions

The starch coating played an important role in determining the characteristics and subsequent biological responses of Fe₃O₄ NPs exposed to zebrafish gill and liver. The starch coating mitigated the toxic effects of Fe₃O₄ NPs on gill, but intensified the toxicity over the liver tissue, which can be attributed to the reduced particle size, enhanced transportability and weakened interactions with the tissue mucus. Both bare and starch-coated Fe₃O₄ NPs could induce oxidative stress, DNA damage, and apoptosis in liver. In addition, these contrasting gene

expression patterns suggest that the toxicity of Fe₃O₄ NPs is dependent upon its surface coating and the tissues examined. The altered gene expressions were found to be similar to those observed in humans and other mammalian models. The findings may guide future studies on toxicity of stabilizer coated nanoparticles and facilitate environmentally conscious uses of starch-coated magnetite nanoparticles.

Chapter 4 Conclusions and Suggestions for Future Research

4.1 Summary and Conclusions

Engineered nanoparticles may be intentionally or accidentally released into aquatic systems where they can interact with chemicals in the biological environment, potentially leading to adverse effects. Since fish play a vital role in aquatic systems, understanding the interaction between nanoparticles and fish will be essential for evaluating the fate and transport of nanoparticles as well as assessing their impact on human and environmental health.

Two popular environmental remediation iron based nanoparticles coated with polysaccharides were evaluated to determine the physicochemical interactions between NPs and zebrafish.

We assessed the effects of synthetic polymers on interactions between NPs and zebrafish. The findings from these studies will aid in the evaluation of risks associated with fate, transport and toxicity of NPs. Additionally, these findings guide the application of the NPs and their coatings for optimal utility, as well as decrease the potential for deleterious environmental impacts.

A systematic study probing how specific coatings may affect their toxicity with organisms for specific particles was conducted for CMC-FeS NPs. Coatings of CMC could mitigate the toxicity of bare FeS NPs. The hepatic toxicity was observed from histological evidence of NP-exposed liver cell damage and agreed with changes in the altered expression of genes associated

with the NP-induced inflammation and oxidative stress. The starch coating was assessed on Fe₃O₄ NPs exposed to the gill and liver of zebrafish. Toxicity of Fe₃O₄ particles is dependent on the surface chemistry of tissues and particles. Bare Fe₃O₄ particles cause an increase in DEG in gills, and starched NPs trigger this increase in the liver. Both bare and starched NPs could induce inflammation and oxidative stress responses. Surface coatings affect properties and biological responses to Fe₃O₄ nanoparticles.

4.2 Suggestions for Future Work

The following gaps and challenges were suggested for future research, which are essential for further investigation on the mechanism of toxicity of NPs.

- 1) Complete characterization of the NPs will contribute to elucidation of NPs induced toxicity mechanisms.
- 2) Establish standardized testing procedures for toxicity associated with NPs.
- 3) Employ more advanced biological techniques going beyond simple toxicity tests to obtain more information about the toxicity mechanism.
- 4) Gain the information of actual concentrations of NPs present in the environment, and toxicity tests should be conducted based on realistic environmentally relevant concentrations rather than excessively high concentrations.
- 5) Long term NPs toxicity monitoring needs to be evaluated especially under field condition.
- 6) Water parameter (i.e. ionic strength, conductivity ect.) related stress caused by NPs needs to be further evaluated.

References

- Adlakha-Hutcheon G, Khaydarov R, Korenstein R, Varma R, Vaseashta A, Stamm H, et al. Nanomaterials, nanotechnology. *Nanomaterials: Risks and Benefits*. Springer, 2009, pp. 195-207.
- Allabashi R, Stach W, de la Escosura-Muñiz A, Liste-Calleja L, Merkoçi A. ICP-MS: a powerful technique for quantitative determination of gold nanoparticles without previous dissolving. *Journal of Nanoparticle Research* 2009; 11: 2003.
- An B, Liang Q, Zhao D. Removal of arsenic (V) from spent ion exchange brine using a new class of starch-bridged magnetite nanoparticles. *Water Research* 2011; 45: 1961-1972.
- Aoshima H, Yamana S, Nakamura S, Mashino T. Biological safety of water-soluble fullerenes evaluated using tests for genotoxicity, phototoxicity, and pro-oxidant activity. *The Journal of Toxicological Sciences* 2010; 35: 401-409.
- Araújo MA, Cunha AM, Mota M. Enzymatic degradation of starch-based thermoplastic compounds used in prostheses: identification of the degradation products in solution. *Biomaterials* 2004; 25: 2687-2693.
- Arora S, Rajwade JM, Paknikar KM. Nanotoxicology and in vitro studies: the need of the hour. *Toxicology and Applied Pharmacology* 2012; 258: 151-165.
- Asharani P, Wu YL, Gong Z, Valiyaveetil S. Toxicity of silver nanoparticles in zebrafish models. *Nanotechnology* 2008; 19: 255102.
- Ayroldi E, Riccardi C. Glucocorticoid-induced leucine zipper (GILZ): a new important mediator of glucocorticoid action. *The FASEB Journal* 2009; 23: 3649-3658.
- Bajak E, Fabbri M, Ponti J, Gioria S, Ojea-Jiménez I, Collotta A, et al. Changes in Caco-2 cells transcriptome profiles upon exposure to gold nanoparticles. *Toxicology Letters* 2015; 233: 187-199.
- Ballou B, Lagerholm BC, Ernst LA, Bruchez MP, Waggoner AS. Noninvasive imaging of quantum dots in mice. *Bioconjugate Chemistry* 2004; 15: 79-86.
- Bar-Ilan O, Albrecht RM, Fako VE, Furgeson DY. Toxicity assessments of multisized gold and silver nanoparticles in zebrafish embryos. *Small* 2009; 5: 1897-1910.

- Barnes CA, Elsaesser A, Arkusz J, Smok A, Palus J, Lesniak A, et al. Reproducible comet assay of amorphous silica nanoparticles detects no genotoxicity. *Nano Letters* 2008; 8: 3069-3074.
- Baroli B, Ennas MG, Loffredo F, Isola M, Pinna R, López-Quintela MA. Penetration of metallic nanoparticles in human full-thickness skin. *Journal of Investigative Dermatology* 2007; 127: 1701-1712.
- Basualto C, Gaete J, Molina L, Valenzuela F, Yañez C, Marco JF. Lanthanide sorbent based on magnetite nanoparticles functionalized with organophosphorus extractants. *Science and Technology of Advanced Materials* 2015; 16: 035010.
- Bayram H, Ito K, Issa R, Ito M, Sukkar M, Chung KF. Regulation of human lung epithelial cell numbers by diesel exhaust particles. *European Respiratory Journal* 2006; 27: 705-713.
- Becker S, Mundandhara S, Devlin RB, Madden M. Regulation of cytokine production in human alveolar macrophages and airway epithelial cells in response to ambient air pollution particles: further mechanistic studies. *Toxicology and Applied Pharmacology* 2005; 207: 269-275.
- Behar S, Byrne J, Dickason C. *Testing the waters: chemical and physical vital signs of a river.* 1996.
- Berry CC, Wells S, Charles S, Curtis AS. Dextran and albumin derivatised iron oxide nanoparticles: influence on fibroblasts in vitro. *Biomaterials* 2003; 24: 4551-4557.
- Bessemer RA, Butler KMA, Tunnah L, Callaghan NI, Rundle A, Currie S, et al. Cardiorespiratory toxicity of environmentally relevant zinc oxide nanoparticles in the freshwater fish *Catostomus commersonii*. *Nanotoxicology* 2015; 9: 861-870.
- Bonassi S, Norppa H, Ceppi M, Strömberg U, Vermeulen R, Znaor A, et al. Chromosomal aberration frequency in lymphocytes predicts the risk of cancer: results from a pooled cohort study of 22 358 subjects in 11 countries. *Carcinogenesis* 2008; 29: 1178-1183.
- Bonner JC. Lung fibrotic responses to particle exposure. *Toxicologic Pathology* 2007; 35: 148-153.
- Boshra H, Gelman AE, Sunyer JO. Structural and functional characterization of complement C4 and C1s-like molecules in teleost fish: insights into the evolution of classical and alternative pathways. *The Journal of Immunology* 2004; 173: 349-359.

- Bourdon JA, Saber AT, Jacobsen NR, Jensen KA, Madsen AM, Lamson JS, et al. Carbon black nanoparticle instillation induces sustained inflammation and genotoxicity in mouse lung and liver. *Particle and Fibre Toxicology* 2012; 9: 5.
- Bouwmeester H, Poortman J, Peters RJ, Wijma E, Kramer E, Makama S, et al. Characterization of translocation of silver nanoparticles and effects on whole-genome gene expression using an in vitro intestinal epithelium coculture model. *ACS Nano* 2011; 5: 4091-4103.
- Bradley TM, Hidalgo E, Leautaud V, Ding H, Demple B. Cysteine-to-alanine replacements in the Escherichia coli SoxR protein and the role of the [2Fe-2S] centers in transcriptional activation. *Nucleic Acids Research* 1997; 25: 1469-1475.
- Brunet Ln, Lyon DY, Hotze EM, Alvarez PJ, Wiesner MR. Comparative photoactivity and antibacterial properties of C60 fullerenes and titanium dioxide nanoparticles. *Environmental Science & Technology* 2009; 43: 4355-4360.
- Butler EC, Hayes KF. Effects of solution composition and pH on the reductive dechlorination of hexachloroethane by iron sulfide. *Environmental Science & Technology* 1998; 32: 1276-1284.
- Buzea C, Pacheco II, Robbie K. Nanomaterials and nanoparticles: Sources and toxicity. *Biointerphases* 2007; 2: MR17-MR71.
- Camargo MM, Martinez CB. Histopathology of gills, kidney and liver of a Neotropical fish caged in an urban stream. *Neotropical Ichthyology* 2007; 5: 327-336.
- Causton HC, Ren B, Koh SS, Harbison CT, Kanin E, Jennings EG, et al. Remodeling of yeast genome expression in response to environmental changes. *Molecular Biology of the Cell* 2001; 12: 323-337.
- Chae YJ, Pham CH, Lee J, Bae E, Yi J, Gu MB. Evaluation of the toxic impact of silver nanoparticles on Japanese medaka (*Oryzias latipes*). *Aquatic Toxicology* 2009; 94: 320-327.
- Chamanza R, Toussaint M, Van Ederen A, Van Veen L, Hulskamp-Koch C, Fabri T. Serum amyloid a and transferrin in chicken. A preliminary investigation of using acute-phase variables to assess diseases in chickens. *Veterinary Quarterly* 1999; 21: 158-162.
- Chen KL, Elimelech M. Influence of humic acid on the aggregation kinetics of fullerene (C60) nanoparticles in monovalent and divalent electrolyte solutions. *Journal of Colloid and Interface Science* 2007; 309: 126-134.

- Chen M, Zhang M, Borlak J, Tong W. A decade of toxicogenomic research and its contribution to toxicological science. *Toxicological Sciences* 2012; kfs223.
- Chen S, Zhang G, Shao C, Huang Q, Liu G, Zhang P, et al. Whole-genome sequence of a flatfish provides insights into ZW sex chromosome evolution and adaptation to a benthic lifestyle. *Nature Genetics* 2014; 46: 253-260.
- Cho M, Chung H, Choi W, Yoon J. Linear correlation between inactivation of *E. coli* and OH radical concentration in TiO₂ photocatalytic disinfection. *Water Research* 2004; 38: 1069-1077.
- Cho W-S, Cho M, Jeong J, Choi M, Cho H-Y, Han BS, et al. Acute toxicity and pharmacokinetics of 13 nm-sized PEG-coated gold nanoparticles. *Toxicology and Applied Pharmacology* 2009; 236: 16-24.
- Choi JE, Kim S, Ahn JH, Youn P, Kang JS, Park K, et al. Induction of oxidative stress and apoptosis by silver nanoparticles in the liver of adult zebrafish. *Aquatic Toxicology* 2010; 100: 151-159.
- Coccini T, Caloni F, Ramírez Cando LJ, De Simone U. Cytotoxicity and proliferative capacity impairment induced on human brain cell cultures after short- and long-term exposure to magnetite nanoparticles. *Journal of Applied Toxicology* 2017; 37: 361-373.
- Cole AJ, David AE, Wang J, Galbán CJ, Hill HL, Yang VC. Polyethylene glycol modified, cross-linked starch-coated iron oxide nanoparticles for enhanced magnetic tumor targeting. *Biomaterials* 2011; 32: 2183-2193.
- Collins AR, Dusinská M, Gedik CM, Stětina R. Oxidative damage to DNA: do we have a reliable biomarker? *Environmental Health Perspectives* 1996; 104: 465.
- Copanaki E, Schürmann T, Eckert A, Leuner K, Müller WE, Prehn JH, et al. The amyloid precursor protein potentiates CHOP induction and cell death in response to ER Ca²⁺ depletion. *Biochimica et Biophysica Acta (BBA)-Molecular Cell Research* 2007; 1773: 157-165.
- Dabrunz A, Duester L, Prasse C, Seitz F, Rosenfeldt R, Schilde C, et al. Biological surface coating and molting inhibition as mechanisms of TiO₂ nanoparticle toxicity in *Daphnia magna*. *PLoS One* 2011; 6: e20112.
- Dandekar P, Dhumal R, Jain R, Tiwari D, Vanage G, Patravale V. Toxicological evaluation of pH-sensitive nanoparticles of curcumin: acute, sub-acute and genotoxicity studies. *Food and Chemical Toxicology* 2010; 48: 2073-2089.

- Dean M, Annilo T. Evolution of the ATP-binding cassette (ABC) transporter superfamily in vertebrates. *Annu. Rev. Genomics Hum. Genet.* 2005; 6: 123-142.
- Deng ZJ, Liang M, Monteiro M, Toth I, Minchin RF. Nanoparticle-induced unfolding of fibrinogen promotes Mac-1 receptor activation and inflammation. *Nature Nanotechnology* 2011; 6: 39-44.
- Dermitzakis ET. From gene expression to disease risk. *Nature genetics* 2008; 40: 492-493.
- Dhawan A, Sharma V. Toxicity assessment of nanomaterials: methods and challenges. *Analytical and Bioanalytical Chemistry* 2010; 398: 589-605.
- Ding C, Cheng W, Sun Y, Wang X. Novel fungus- Fe₃O₄ bio-nanocomposites as high performance adsorbents for the removal of radionuclides. *Journal of Hazardous Materials* 2015; 295: 127-137.
- Djurišić AB, Leung YH, Ng A, Xu XY, Lee PK, Degger N. Toxicity of metal oxide nanoparticles: mechanisms, characterization, and avoiding experimental artefacts. *Small* 2015; 11: 26-44.
- Doak S, Griffiths S, Manshian B, Singh N, Williams P, Brown A, et al. Confounding experimental considerations in nanogenotoxicology. *Mutagenesis* 2009: gep010.
- Dobrovolskaia MA, McNeil SE. Immunological properties of engineered nanomaterials. *Nature Nanotechnology* 2007; 2: 469-478.
- Domingos RF, Tufenkji N, Wilkinson KJ. Aggregation of titanium dioxide nanoparticles: role of a fulvic acid. *Environmental Science & Technology* 2009; 43: 1282-1286.
- Dong H, Xie Y, Zeng G, Tang L, Liang J, He Q, et al. The dual effects of carboxymethyl cellulose on the colloidal stability and toxicity of nanoscale zero-valent iron. *Chemosphere* 2016; 144: 1682-1689.
- Elder A, Yang H, Gwiazda R, Teng X, Thurston S, He H, et al. Testing nanomaterials of unknown toxicity: an example based on platinum nanoparticles of different shapes. *Advanced Materials* 2007; 19: 3124-3129.
- Eom H-J, Choi J. p38 MAPK activation, DNA damage, cell cycle arrest and apoptosis as mechanisms of toxicity of silver nanoparticles in Jurkat T cells. *Environmental Science & Technology* 2010; 44: 8337-8342.
- Ernsting MJ, Tang W-L, MacCallum N, Li S-D. Synthetic modification of carboxymethylcellulose and use thereof to prepare a nanoparticle forming conjugate of

- docetaxel for enhanced cytotoxicity against cancer cells. *Bioconjugate Chemistry* 2011; 22: 2474-2486.
- Estevanato L, Cintra D, Baldini N, Portilho F, Barbosa L, Martins O, et al. Preliminary biocompatibility investigation of magnetic albumin nanosphere designed as a potential versatile drug delivery system. *International Journal of Nanomedicine* 2011; 6: 1709-1717.
- Fenech M, Kirsch-Volders M, Natarajan A, Surralles J, Crott J, Parry J, et al. Molecular mechanisms of micronucleus, nucleoplasmic bridge and nuclear bud formation in mammalian and human cells. *Mutagenesis* 2011; 26: 125-132.
- Fenoglio I, Corazzari I, Francia C, Bodoardo S, Fubini B. The oxidation of glutathione by cobalt/tungsten carbide contributes to hard metal-induced oxidative stress. *Free Radical Research* 2008; 42: 437-745.
- Fielding GA, Bandyopadhyay A, Bose S. Effects of silica and zinc oxide doping on mechanical and biological properties of 3D printed tricalcium phosphate tissue engineering scaffolds. *Dental Materials* 2012; 28: 113-122.
- Fischer J, Prosenc MH, Wolff M, Hort N, Willumeit R, Feyerabend F. Interference of magnesium corrosion with tetrazolium-based cytotoxicity assays. *Acta Biomaterialia* 2010; 6: 1813-1823.
- Fotakis G, Timbrell JA. In vitro cytotoxicity assays: comparison of LDH, neutral red, MTT and protein assay in hepatoma cell lines following exposure to cadmium chloride. *Toxicology Letters* 2006; 160: 171-177.
- Freese C, Unger RE, Deller RC, Gibson MI, Brochhausen C, Klok H-A, et al. Uptake of poly (2-hydroxypropylmethacrylamide)-coated gold nanoparticles in microvascular endothelial cells and transport across the blood–brain barrier. *Biomaterials Science* 2013; 1: 824-833.
- Frohlich E. Cellular targets and mechanisms in the cytotoxic action of non-biodegradable engineered nanoparticles. *Current Drug Metabolism* 2013; 14: 976-988.
- Galloway S, Armstrong M, Reuben C, Colman S, Brown B, Cannon C, et al. Chromosome aberrations and sister chromatid exchanges in Chinese hamster ovary cells: evaluations of 108 chemicals. *Environmental and Molecular Mutagenesis* 1987; 10: 1-35.
- Galloway SM, Aardema MJ, Ishidate M, Ivett JL, Kirkland DJ, Morita T, et al. Report from working group on in vitro tests for chromosomal aberrations. *Mutation Research/Environmental Mutagenesis and Related Subjects* 1994; 312: 241-261.

- Garcia-Reyero NI, Kennedy AJ, Escalon BL, Habib T, Laird JG, Rawat A, et al. Differential effects and potential adverse outcomes of ionic silver and silver nanoparticles in vivo and in vitro. *Environmental Science & Technology* 2014; 48: 4546-4555.
- Garcia-Reyero N, Griffitt RJ, Liu L, Kroll KJ, Farmerie WG, Barber DS, et al. Construction of a robust microarray from a non-model species largemouth bass, *Micropterus salmoides* (Lacèpede), using pyrosequencing technology. *Journal of Fish Biology* 2008; 72: 2354-2376.
- Ge Y, Bruno M, Wallace K, Winnik W, Prasad RY. Proteome profiling reveals potential toxicity and detoxification pathways following exposure of BEAS-2B cells to engineered nanoparticle titanium dioxide. *Proteomics* 2011; 11: 2406-2422.
- Gong Y, Liu Y, Xiong Z, Kaback D, Zhao D. Immobilization of mercury in field soil and sediment using carboxymethyl cellulose stabilized iron sulfide nanoparticles. *Nanotechnology* 2012; 23: 294007.
- Gong Y, Liu Y, Xiong Z, Zhao D. Immobilization of mercury by carboxymethyl cellulose stabilized iron sulfide nanoparticles: reaction mechanisms and effects of stabilizer and water chemistry. *Environmental Science & Technology* 2014; 48: 3986-3994.
- Gong Y, Tang J, Zhao D. Application of iron sulfide particles for groundwater and soil remediation: A review. *Water Research* 2016; 89: 309-20.
- Gottschalk F, Ort C, Scholz R, Nowack B. Engineered nanomaterials in rivers—Exposure scenarios for Switzerland at high spatial and temporal resolution. *Environmental Pollution* 2011; 159: 3439-3445.
- Griffitt RJ, Hyndman K, Denslow ND, Barber DS. Comparison of molecular and histological changes in zebrafish gills exposed to metallic nanoparticles. *Toxicological Sciences* 2008; 107: 404-415.
- Griffitt RJ, Weil R, Hyndman KA, Denslow ND, Powers K, Taylor D, et al. Exposure to copper nanoparticles causes gill injury and acute lethality in zebrafish (*Danio rerio*). *Environmental Science & Technology* 2007; 41: 8178-8186.
- Guo X, Mao F, Wang W, Yang Y, Bai Z. Sulfhydryl-modified Fe₃O₄@ SiO₂ core/shell nanocomposite: synthesis and toxicity assessment in vitro. *ACS Applied Materials & Interfaces* 2015; 7: 14983-14991.
- Gupta AK, Gupta M. Synthesis and surface engineering of iron oxide nanoparticles for biomedical applications. *Biomaterials* 2005; 26: 3995-4021.

- Habib GM, Shi Z-Z, Lieberman MW. Glutathione protects cells against arsenite-induced toxicity. *Free Radical Biology and Medicine* 2007; 42: 191-201.
- Halliwell B, Gutteridge JM. *Free radicals in biology and medicine*: Oxford University Press, USA, 2015.
- Han Y-S, Gallegos TJ, Demond AH, Hayes KF. FeS-coated sand for removal of arsenic (III) under anaerobic conditions in permeable reactive barriers. *Water Research* 2011a; 45: 593-604.
- Han Y-S, Jeong HY, Demond AH, Hayes KF. X-ray absorption and photoelectron spectroscopic study of the association of As (III) with nanoparticulate FeS and FeS-coated sand. *Water Research* 2011b; 45: 5727-5735.
- Handy RD. FSBI briefing paper: Nanotechnology in fisheries and aquaculture. The Fisheries Society of the British Isles. 2011.
- Handy RD, Henry TB, Scown TM, Johnston BD, Tyler CR. Manufactured nanoparticles: their uptake and effects on fish—a mechanistic analysis. *Ecotoxicology* 2008; 17: 396-409.
- Hatton B, Rickard D. Nucleic acids bind to nanoparticulate iron (II) monosulphide in aqueous solutions. *Origins of Life and Evolution of Biospheres* 2008; 38: 257-270.
- Hayashi M. The micronucleus test—most widely used in vivo genotoxicity test—. *Genes and Environment* 2016; 38: 18.
- He F, Zhao D. Manipulating the size and dispersibility of zerovalent iron nanoparticles by use of carboxymethyl cellulose stabilizers. *Environmental Science & Technology* 2007; 41: 6216-6221.
- He F, Zhao D. Response to Comment on “Manipulating the Size and Dispersibility of Zerovalent Iron Nanoparticles by Use of Carboxymethyl Cellulose Stabilizers”. *Environmental Science & Technology* 2008; 42: 3480-3480.
- Heng BC, Zhao X, Tan EC, Khamis N, Assodani A, Xiong S, et al. Evaluation of the cytotoxic and inflammatory potential of differentially shaped zinc oxide nanoparticles. *Archives of Toxicology* 2011; 85: 1517-1528.
- Hernandez JT, Muriel AA, Tabares J, Alcázar GP, Bolaños A. Preparation of Fe₃O₄ nanoparticles and removal of methylene blue through adsorption. *Journal of Physics: Conference Series*. 614. IOP Publishing, 2015, pp. 012007.

- Higgins MR. Environmental assessment of in situ groundwater remediation with reduced iron reactive media. The University of Michigan, 2011.
- Hill AJ, Teraoka H, Heideman W, Peterson RE. Zebrafish as a model vertebrate for investigating chemical toxicity. *Toxicological Sciences* 2005; 86: 6-19.
- Hsin Y-H, Chen C-F, Huang S, Shih T-S, Lai P-S, Chueh PJ. The apoptotic effect of nanosilver is mediated by a ROS-and JNK-dependent mechanism involving the mitochondrial pathway in NIH3T3 cells. *Toxicology Letters* 2008; 179: 130-139.
- Huang C-C, Aronstam RS, Chen D-R, Huang Y-W. Oxidative stress, calcium homeostasis, and altered gene expression in human lung epithelial cells exposed to ZnO nanoparticles. *Toxicology in vitro* 2010a; 24: 45-55.
- Huang Y-W, Wu C-h, Aronstam RS. Toxicity of transition metal oxide nanoparticles: recent insights from in vitro studies. *Materials* 2010b; 3: 4842-4859.
- Hudecová A, Kusznierevicz B, Rundén-Pran E, Magdolenová Z, Hašplová K, Rinna A, et al. Silver nanoparticles induce premutagenic DNA oxidation that can be prevented by phytochemicals from *Gentiana asclepiadea*. *Mutagenesis* 2012: ges046.
- Hyun SP, Davis JA, Sun K, Hayes KF. Uranium (VI) reduction by iron (II) monosulfide mackinawite. *Environmental Science & Technology* 2012; 46: 3369-3376.
- Jeong HY, Hayes KF. Reductive dechlorination of tetrachloroethylene and trichloroethylene by mackinawite (FeS) in the presence of metals: reaction rates. *Environmental Science & Technology* 2007; 41: 6390-6396.
- Jha AN. Ecotoxicological applications and significance of the comet assay. *Mutagenesis* 2008; 23: 207-221.
- Johnson GE. Mammalian cell HPRT gene mutation assay: test methods. *Genetic Toxicology: Principles and Methods* 2012: 55-67.
- Johnson RL, Johnson GOB, Nurmi JT, Tratnyek PG. Natural organic matter enhanced mobility of nano zerovalent iron. *Environmental Science & Technology* 2009; 43: 5455-5460.
- Joo SH, Zhao D. Destruction of lindane and atrazine using stabilized iron nanoparticles under aerobic and anaerobic conditions: effects of catalyst and stabilizer. *Chemosphere* 2008; 70: 418-425.

- Kain J, Karlsson H, Möller L. DNA damage induced by micro-and nanoparticles—interaction with FPG influences the detection of DNA oxidation in the comet assay. *Mutagenesis* 2012; ges010.
- Karlsson HL. The comet assay in nanotoxicology research. *Analytical and Bioanalytical Chemistry* 2010; 398: 651-666.
- Kasper J, Hermanns MI, Bantz C, Koshkina O, Lang T, Maskos M, et al. Interactions of silica nanoparticles with lung epithelial cells and the association to flotillins. *Archives of Toxicology* 2013; 87: 1053-1065.
- Kato T, Yashiro T, Murata Y, Herbert DC, Oshikawa K, Bando M, et al. Evidence that exogenous substances can be phagocytized by alveolar epithelial cells and transported into blood capillaries. *Cell and Tissue Research* 2003; 311: 47-51.
- Kawanishi S, Hiraku Y, Murata M, Oikawa S. The role of metals in site-specific DNA damage with reference to carcinogenesis 1, 2. *Free Radical Biology and Medicine* 2002; 32: 822-832.
- Keenan CR, Goth-Goldstein R, Lucas D, Sedlak DL. Oxidative stress induced by zero-valent iron nanoparticles and Fe (II) in human bronchial epithelial cells. *Environmental Science & Technology* 2009; 43: 4555-4560.
- Kemp P, Lee S, LaRoche J. Estimating the growth rate of slowly growing marine bacteria from RNA content. *Applied and Environmental Microbiology* 1993; 59: 2594-2601.
- Kievit FM, Veiseh O, Bhattarai N, Fang C, Gunn JW, Lee D, et al. PEI-PEG-chitosan-copolymer-coated iron oxide nanoparticles for safe gene delivery: synthesis, complexation, and transfection. *Advanced Functional Materials* 2009; 19: 2244-2251.
- Kim H-J, Phenrat T, Tilton RD, Lowry GV. Fe₀ nanoparticles remain mobile in porous media after aging due to slow desorption of polymeric surface modifiers. *Environmental Science & Technology* 2009; 43: 3824-3830.
- Kim SW, An Y-J. Effect of ZnO and TiO₂ nanoparticles preilluminated with UVA and UVB light on *Escherichia coli* and *Bacillus subtilis*. *Applied Microbiology and Biotechnology* 2012; 95: 243-253.
- Kirchner C, Liedl T, Kudera S, Pellegrino T, Muñoz Javier A, Gaub HE, et al. Cytotoxicity of colloidal CdSe and CdSe/ZnS nanoparticles. *Nano Letters* 2005; 5: 331-338.

- Kisin ER, Murray AR, Keane MJ, Shi X-C, Schwegler-Berry D, Gorelik O, et al. Single-walled carbon nanotubes: geno-and cytotoxic effects in lung fibroblast V79 cells. *Journal of Toxicology and Environmental Health, Part A* 2007; 70: 2071-2079.
- Knaapen AM, Borm PJ, Albrecht C, Schins RP. Inhaled particles and lung cancer. Part A: Mechanisms. *International Journal of Cancer* 2004; 109: 799-809.
- Korzeniewski C, Callewaert DM. An enzyme-release assay for natural cytotoxicity. *Journal of immunological methods* 1983; 64: 313-320.
- Kumar A, Pandey AK, Singh SS, Shanker R, Dhawan A. Cellular uptake and mutagenic potential of metal oxide nanoparticles in bacterial cells. *Chemosphere* 2011a; 83: 1124-1132.
- Kumar A, Pandey AK, Singh SS, Shanker R, Dhawan A. A flow cytometric method to assess nanoparticle uptake in bacteria. *Cytometry Part A* 2011b; 79: 707-712.
- Kumbıçak Ü, Çavaş T, Çinkılıç N, Kumbıçak Z, Vatan Ö, Yılmaz D. Evaluation of in vitro cytotoxicity and genotoxicity of copper–zinc alloy nanoparticles in human lung epithelial cells. *Food and Chemical Toxicology* 2014; 73: 105-112.
- Lacerda L, Soundararajan A, Singh R, Pastorin G, Al-Jamal KT, Turton J, et al. Dynamic imaging of functionalized multi-walled carbon nanotube systemic circulation and urinary excretion. *Advanced Materials* 2008; 20: 225-230.
- Landsiedel R, Kapp MD, Schulz M, Wiench K, Oesch F. Genotoxicity investigations on nanomaterials: methods, preparation and characterization of test material, potential artifacts and limitations—many questions, some answers. *Mutation Research/Reviews in Mutation Research* 2009; 681: 241-258.
- Langheinrich U, Hennen E, Stott G, Vacun G. Zebrafish as a model organism for the identification and characterization of drugs and genes affecting p53 signaling. *Current Biology* 2002; 12: 2023-2028.
- Lawless M, Greene C. Toll-like receptor signalling in liver disease: ER stress the missing link? *Cytokine* 2012; 59: 195-202.
- Lerebours A, Gonzalez P, Adam C, Camilleri V, Bourdineaud JP, Garnier-Laplace J. Comparative analysis of gene expression in brain, liver, skeletal muscles, and gills of zebrafish (*Danio rerio*) exposed to environmentally relevant waterborne uranium concentrations. *Environmental Toxicology and Chemistry* 2009; 28: 1271-1278.

- Li B, Qing T, Zhu J, Wen Z, Yu Y, Fukumura R, et al. A Comprehensive Mouse Transcriptomic BodyMap across 17 Tissues by RNA-seq. *Scientific Reports* 2017; 7.
- Li C-H, Shen C-C, Cheng Y-W, Huang S-H, Wu C-C, Kao C-C, et al. Organ biodistribution, clearance, and genotoxicity of orally administered zinc oxide nanoparticles in mice. *Nanotoxicology* 2012; 6: 746-756.
- Li JJe, Muralikrishnan S, Ng C-T, Yung L-YL, Bay B-H. Nanoparticle-induced pulmonary toxicity. *Experimental Biology and Medicine* 2010a; 235: 1025-1033.
- Li K, Zeng Z, Xiong J, Yan L, Guo H, Liu S, et al. Fabrication of mesoporous Fe₃O₄@ SiO₂@ CTAB-SiO₂ magnetic microspheres with a core/shell structure and their efficient adsorption performance for the removal of trace PFOS from water. *Colloids and Surfaces A: Physicochemical and Engineering Aspects* 2015; 465: 113-123.
- Li L, Fan M, Brown RC, Van Leeuwen J, Wang J, Wang W, et al. Synthesis, properties, and environmental applications of nanoscale iron-based materials: a review. *Critical Reviews in Environmental Science and Technology* 2006; 36: 405-431.
- Li N, Xia T, Nel AE. The role of oxidative stress in ambient particulate matter-induced lung diseases and its implications in the toxicity of engineered nanoparticles. *Free Radical Biology and Medicine* 2008; 44: 1689-1699.
- Li Z. Mechanistic Insight into the Effect of Polymer and NOM Coatings on Adhesion and Interactions between Nanoparticles and Bacteria. Carnegie Mellon University, 2011.
- Li Z, Xu X, Huang L, Wu J, Lu Q, Xiang Z, et al. Administration of recombinant IFN1 protects zebrafish (*Danio rerio*) from ISKNV infection. *Fish & Shellfish Immunology* 2010b; 29: 399-406.
- Liang Q, Zhao D. Immobilization of arsenate in a sandy loam soil using starch-stabilized magnetite nanoparticles. *Journal of Hazardous Materials* 2014; 271: 16-23.
- Liang Q, Zhao D, Qian T, Freeland K, Feng Y. Effects of stabilizers and water chemistry on arsenate sorption by polysaccharide-stabilized magnetite nanoparticles. *Industrial & Engineering Chemistry Research* 2012; 51: 2407-2418.
- Liao M, Liu H. Gene expression profiling of nephrotoxicity from copper nanoparticles in rats after repeated oral administration. *Environmental Toxicology and Pharmacology* 2012; 34: 67-80.

- Liu C, Su G, Giesy JP, Letcher RJ, Li G, Agrawal I, et al. Acute exposure to tris (1, 3-dichloro-2-propyl) phosphate (TDCIPP) causes hepatic inflammation and leads to hepatotoxicity in zebrafish. *Scientific Reports* 2016; 6.
- Liu Y, Xia Q, Liu Y, Zhang S, Cheng F, Zhong Z, et al. Genotoxicity assessment of magnetic iron oxide nanoparticles with different particle sizes and surface coatings. *Nanotechnology* 2014; 25: 425101.
- Livak KJ, Schmittgen TD. Analysis of relative gene expression data using real-time quantitative PCR and the $2^{-\Delta\Delta CT}$ method. *Methods* 2001; 25: 402-408.
- Livens FR, Jones MJ, Hynes AJ, Charnock JM, Mosselmans JFW, Hennig C, et al. X-ray absorption spectroscopy studies of reactions of technetium, uranium and neptunium with mackinawite. *Journal of Environmental Radioactivity* 2004; 74: 211-219.
- Long TC, Saleh N, Tilton RD, Lowry GV, Veronesi B. Titanium dioxide (P25) produces reactive oxygen species in immortalized brain microglia (BV2): implications for nanoparticle neurotoxicity. *Environmental Science & Technology* 2006; 40: 4346-4352.
- Lonkar P, Dedon PC. Reactive species and DNA damage in chronic inflammation: reconciling chemical mechanisms and biological fates. *International Journal of Cancer* 2011; 128: 1999-2009.
- Lu X, Long Y, Sun R, Zhou B, Lin L, Zhong S, et al. Zebrafish *Abcb4* is a potential efflux transporter of microcystin-LR. *Comparative Biochemistry and Physiology Part C: Toxicology & Pharmacology* 2015; 167: 35-42.
- Lu X, Weakley AT, Aston DE, Rasco BA, Wang S, Konkel ME. Examination of nanoparticle inactivation of *Campylobacter jejuni* biofilms using infrared and Raman spectroscopies. *Journal of Applied Microbiology* 2012; 113: 952-963.
- Lucafò M, Gerdol M, Pallavicini A, Pacor S, Zorzet S, Da Ros T, et al. Profiling the molecular mechanism of fullerene cytotoxicity on tumor cells by RNA-seq. *Toxicology* 2013; 314: 183-192.
- Magdolenova Z, Lorenzo Y, Collins A, Dusinska M. Can standard genotoxicity tests be applied to nanoparticles? *Journal of Toxicology and Environmental Health, Part A* 2012; 75: 800-806.
- Mahmoudi M, Hofmann H, Rothen-Rutishauser B, Petri-Fink A. Assessing the in vitro and in vivo toxicity of superparamagnetic iron oxide nanoparticles. *Chemical Reviews* 2011; 112: 2323-2338.

- Mahmoudi M, Simchi A, Imani M, Shokrgozar MA, Milani AS, Häfeli UO, et al. A new approach for the in vitro identification of the cytotoxicity of superparamagnetic iron oxide nanoparticles. *Colloids and Surfaces B: Biointerfaces* 2010; 75: 300-309.
- Malich G, Markovic B, Winder C. The sensitivity and specificity of the MTS tetrazolium assay for detecting the in vitro cytotoxicity of 20 chemicals using human cell lines. *Toxicology* 1997; 124: 179-192.
- Manna P, Ghosh M, Ghosh J, Das J, Sil PC. Contribution of nano-copper particles to in vivo liver dysfunction and cellular damage: Role of $\text{I}\kappa\text{B}\alpha/\text{NF-}\kappa\text{B}$, MAPKs and mitochondrial signal. *Nanotoxicology* 2012; 6: 1-21.
- Marquis BJ, Love SA, Braun KL, Haynes CL. Analytical methods to assess nanoparticle toxicity. *Analyst* 2009; 134: 425-439.
- Masamune A, Kikuta K, Watanabe T, Satoh K, Hirota M, Hamada S, et al. Fibrinogen induces cytokine and collagen production in pancreatic stellate cells. *Gut* 2009; 58: 550-559.
- Mbeh D, Javanbakht T, Tabet L, Merhi Y, Maghni K, Sacher E, et al. Protein corona formation on magnetite nanoparticles: effects of culture medium composition, and its consequences on superparamagnetic nanoparticle cytotoxicity. *Journal of Biomedical Nanotechnology* 2015a; 11: 828-840.
- Mbeh DA, Mireles LK, Stanicki D, Tabet L, Maghni K, Laurent S, et al. Human alveolar epithelial cell responses to core-shell superparamagnetic iron oxide nanoparticles (SPIONs). *Langmuir* 2015b; 31: 3829-3839.
- Moon H, Guo D, Song H, Kim I, Jin H, Kim Y, et al. Regulation of adipocyte differentiation by PEGylated all-trans retinoic acid: reduced cytotoxicity and attenuated lipid accumulation. *The Journal of Nutritional Biochemistry* 2007; 18: 322-331.
- Mori T, Takada H, Ito S, Matsubayashi K, Miwa N, Sawaguchi T. Preclinical studies on safety of fullerene upon acute oral administration and evaluation for no mutagenesis. *Toxicology* 2006; 225: 48-54.
- Motskin M, Wright D, Muller K, Kyle N, Gard T, Porter A, et al. Hydroxyapatite nano and microparticles: correlation of particle properties with cytotoxicity and biostability. *Biomaterials* 2009; 30: 3307-3317.
- Mullet M, Boursiquot S, Ehrhardt J-J. Removal of hexavalent chromium from solutions by mackinawite, tetragonal FeS. *Colloids and Surfaces A: Physicochemical and Engineering Aspects* 2004; 244: 77-85.

- Nair PMG, Choi J. Characterization of a ribosomal protein L15 cDNA from *Chironomus riparius* (Diptera; Chironomidae): transcriptional regulation by cadmium and silver nanoparticles. *Comparative Biochemistry and Physiology Part B: Biochemistry and Molecular Biology* 2011; 159: 157-162.
- Nel A, Xia T, Mädler L, Li N. Toxic potential of materials at the nanolevel. *Science* 2006; 311: 622-627.
- OECD. Test No. 203: Fish, Acute Toxicity Test: OECD Publishing.
- Oh S-Y, Kang S-G, Kim D-W, Chiu PC. Degradation of 2, 4-dinitrotoluene by persulfate activated with iron sulfides. *Chemical Engineering Journal* 2011; 172: 641-646.
- Oostendorp M, Douma K, Wagenaar A, Slenter JM, Hackeng TM, van Zandvoort MA, et al. Molecular magnetic resonance imaging of myocardial angiogenesis after acute myocardial infarction. *Circulation* 2010; 121: 775-783.
- Otsuka H, Nagasaki Y, Kataoka K. PEGylated nanoparticles for biological and pharmaceutical applications. *Advanced Drug Delivery Reviews* 2003; 55: 403-419.
- Pan Z, Li W, Fortner JD, Giammar DE. Measurement and Surface Complexation Modeling of U(VI) Adsorption to Engineered Iron Oxide Nanoparticles. *Environmental Science & Technology* 2017.
- Panigrahi S, Mai S. Telomeres, genomic instability, DNA repair and Breast Cancer. *Current Medicinal Chemistry-Anti-Inflammatory & Anti-Allergy Agents* 2005; 4: 421-428.
- Pasparakis M. Regulation of tissue homeostasis by NF- κ B signalling: implications for inflammatory diseases. *Nature Reviews Immunology* 2009; 9: 778-788.
- Pastor J, Dewey B, Johnson NW, Swain EB, Monson P, Peters EB, et al. Effects of sulfate and sulfide on the life cycle of *Zizania palustris* in hydroponic and mesocosm experiments. *Ecological Applications* 2017; 27: 321-336.
- Patel RK, Jain M. NGS QC Toolkit: a toolkit for quality control of next generation sequencing data. *PloS one* 2012; 7: e30619.
- Pazin MJ, Sheridan PL, Cannon K, Cao Z, Keck JG, Kadonaga JT, et al. NF-kappa B-mediated chromatin reconfiguration and transcriptional activation of the HIV-1 enhancer in vitro. *Genes & Development* 1996; 10: 37-49.

- Pelka J, Gehrke H, Esselen M, Türk M, Crone M, Bräse S, et al. Cellular uptake of platinum nanoparticles in human colon carcinoma cells and their impact on cellular redox systems and DNA integrity. *Chemical Research in Toxicology* 2009; 22: 649-659.
- Pham CH, Yi J, Gu MB. Biomarker gene response in male Medaka (*Oryzias latipes*) chronically exposed to silver nanoparticle. *Ecotoxicology and Environmental Safety* 2012; 78: 239-245.
- Pierzchała K, Lekka M, Magrez A, Kulik AJ, Forró L, Sienkiewicz A. Photocatalytic and phototoxic properties of TiO₂-based nanofilaments: ESR and AFM assays. *Nanotoxicology* 2012; 6: 813-824.
- Pina AS, Batalha ÍL, Fernandes CS, Aoki MA, Roque AC. Exploring the potential of magnetic antimicrobial agents for water disinfection. *Water Research* 2014; 66: 160-168.
- Poljak-Blaži M, Jaganjac M, Žarković N. Cell oxidative stress: risk of metal nanoparticles. *Handbook of Nanophysics Nanomedicine and Nanorobotics*. CRC Press Taylor, 2010.
- Powers CM, Badireddy AR, Ryde IT, Seidler FJ, Slotkin TA. Silver nanoparticles compromise neurodevelopment in PC12 cells: critical contributions of silver ion, particle size, coating, and composition. *Environmental Health Perspectives* 2011; 119: 37.
- Poynton HC, Lazorchak JM, Impellitteri CA, Blalock BJ, Rogers K, Allen HJ, et al. Toxicogenomic responses of nanotoxicity in *Daphnia magna* exposed to silver nitrate and coated silver nanoparticles. *Environmental Science & Technology* 2012; 46: 6288-6296.
- Poynton HC, Lazorchak JM, Impellitteri CA, Smith ME, Rogers K, Patra M, et al. Differential gene expression in *Daphnia magna* suggests distinct modes of action and bioavailability for ZnO nanoparticles and Zn ions. *Environmental Science & Technology* 2010; 45: 762-768.
- Premanathan M, Karthikeyan K, Jeyasubramanian K, Manivannan G. Selective toxicity of ZnO nanoparticles toward Gram-positive bacteria and cancer cells by apoptosis through lipid peroxidation. *Nanomedicine: Nanotechnology, Biology and Medicine* 2011; 7: 184-192.
- Pujalté I, Passagne I, Brouillaud B, Tréguer M, Durand E, Ohayon-Courtès C, et al. Cytotoxicity and oxidative stress induced by different metallic nanoparticles on human kidney cells. *Particle and Fibre Toxicology* 2011; 8: 10.
- Rabolli V, Thomassen LC, Princen C, Napierska D, Gonzalez L, Kirsch-Volders M, et al. Influence of size, surface area and microporosity on the in vitro cytotoxic activity of amorphous silica nanoparticles in different cell types. *Nanotoxicology* 2010; 4: 307-318.

- Rahman I, Biswas SK, Jimenez LA, Torres M, Forman H. Glutathione, stress responses, and redox signaling in lung inflammation. *Antioxidants & Redox Signaling* 2005; 7: 42-59.
- Rahman K. Studies on free radicals, antioxidants, and co-factors. *Clinical Interventions in Aging* 2007; 2: 219.
- Revia RA, Zhang M. Magnetite nanoparticles for cancer diagnosis, treatment, and treatment monitoring: recent advances. *Materials Today* 2016; 19: 157-168.
- Rickard D, Hatton B, Murphy DM, Butler I, Oldroyd A, Hann A. FeS-induced radical formation and its effect on plasmid DNA. *Aquatic Geochemistry* 2011; 17: 545-566.
- Risom L, Møller P, Loft S. Oxidative stress-induced DNA damage by particulate air pollution. *Mutation Research/Fundamental and Molecular Mechanisms of Mutagenesis* 2005; 592: 119-137.
- Roh J-y, Sim SJ, Yi J, Park K, Chung KH, Ryu D-y, et al. Ecotoxicity of silver nanoparticles on the soil nematode *Caenorhabditis elegans* using functional ecotoxicogenomics. *Environmental Science & Technology* 2009; 43: 3933-3940.
- Ruan X, Gu X, Lu S, Qiu Z, Sui Q. Trichloroethylene degradation by persulphate with magnetite as a heterogeneous activator in aqueous solution. *Environmental Technology* 2015; 36: 1389-1397.
- Ruiz A, Gutiérrez L, Cáceres-Vélez P, Santos D, Chaves S, Fascineli M, et al. Biotransformation of magnetic nanoparticles as a function of coating in a rat model. *Nanoscale* 2015; 7: 16321-16329.
- Saleh N, Sirk K, Liu Y, Phenrat T, Dufour B, Matyjaszewski K, et al. Surface modifications enhance nanoiron transport and NAPL targeting in saturated porous media. *Environmental Engineering Science* 2007; 24: 45-57.
- Sanderson SL, Stebar MC, Ackermann KL, Jones SH, Batjakas IE, Kaufman L. Mucus entrapment of particles by a suspension-feeding tilapia (Pisces: Cichlidae). *Journal of Experimental Biology* 1996; 199: 1743-1756.
- Sasaki YF, Izumiyama F, Nishidate E, Ishibashi S, Tsuda S, Matsusaka N, et al. Detection of genotoxicity of polluted sea water using shellfish and the alkaline single-cell gel electrophoresis (SCE) assay: a preliminary study. *Mutation Research/Genetic Toxicology and Environmental Mutagenesis* 1997; 393: 133-139.
- Schmid W. The micronucleus test. *Mutation Research/Environmental Mutagenesis and Related Subjects* 1975; 31: 9-15.

- Schulz M, Ma-Hock L, Brill S, Strauss V, Treumann S, Gröters S, et al. Investigation on the genotoxicity of different sizes of gold nanoparticles administered to the lungs of rats. *Mutation Research/Genetic Toxicology and Environmental Mutagenesis* 2012; 745: 51-57.
- Scown T, Van Aerle R, Tyler C. Review: do engineered nanoparticles pose a significant threat to the aquatic environment? *Critical Reviews in Toxicology* 2010; 40: 653-670.
- Shan C, Ma Z, Tong M, Ni J. Removal of Hg (II) by poly (1-vinylimidazole)-grafted Fe₃O₄@SiO₂ magnetic nanoparticles. *Water Research* 2015; 69: 252-260.
- Sharifi S, Seyednejad H, Laurent S, Atyabi F, Saei AA, Mahmoudi M. Superparamagnetic iron oxide nanoparticles for in vivo molecular and cellular imaging. *Contrast Media & Molecular Imaging* 2015; 10: 329-355.
- Sheehan DC, Hrapchak BB. *Theory and practice of histotechnology*: Cv Mosby, 1980.
- Shen Y, Tang J, Nie Z, Wang Y, Ren Y, Zuo L. Tailoring size and structural distortion of Fe₃O₄ nanoparticles for the purification of contaminated water. *Bioresource Technology* 2009; 100: 4139-4146.
- Shi H, Hudson LG, Liu KJ. Oxidative stress and apoptosis in metal ion-induced carcinogenesis. *Free Radical Biology and Medicine* 2004; 37: 582-593.
- Shi Y, Wang F, He J, Yadav S, Wang H. Titanium dioxide nanoparticles cause apoptosis in BEAS-2B cells through the caspase 8/t-Bid-independent mitochondrial pathway. *Toxicology Letters* 2010; 196: 21-27.
- Shinohara N, Matsumoto K, Endoh S, Maru J, Nakanishi J. In vitro and in vivo genotoxicity tests on fullerene C 60 nanoparticles. *Toxicology Letters* 2009; 191: 289-296.
- Shukla RK, Kumar A, Gurbani D, Pandey AK, Singh S, Dhawan A. TiO₂ nanoparticles induce oxidative DNA damage and apoptosis in human liver cells. *Nanotoxicology* 2013; 7: 48-60.
- Shukla RK, Sharma V, Pandey AK, Singh S, Sultana S, Dhawan A. ROS-mediated genotoxicity induced by titanium dioxide nanoparticles in human epidermal cells. *Toxicology in vitro* 2011; 25: 231-241.
- Shvedova AA, Pietroiusti A, Fadeel B, Kagan VE. Mechanisms of carbon nanotube-induced toxicity: focus on oxidative stress. *Toxicology and Applied Pharmacology* 2012; 261: 121-133.

- Silverman N, Maniatis T. NF- κ B signaling pathways in mammalian and insect innate immunity. *Genes & Development* 2001; 15: 2321-2342.
- Simon DF, Domingos RF, Hauser C, Hutchins CM, Zerges W, Wilkinson KJ. Transcriptome sequencing (RNA-seq) analysis of the effects of metal nanoparticle exposure on the transcriptome of *Chlamydomonas reinhardtii*. *Applied and Environmental Microbiology* 2013; 79: 4774-4785.
- Simonian N, Coyle J. Oxidative stress in neurodegenerative diseases. *Annual Review of Pharmacology and Toxicology* 1996; 36: 83-106.
- Sitrin RG, Pan PM, Srikanth S, Todd RF. Fibrinogen activates NF- κ B transcription factors in mononuclear phagocytes. *The Journal of Immunology* 1998; 161: 1462-1470.
- Skylberg U, Drott A. Competition between disordered iron sulfide and natural organic matter associated thiols for mercury (II) An EXAFS study. *Environmental Science & Technology* 2010; 44: 1254-1259.
- Song M-F, Li Y-S, Kasai H, Kawai K. Metal nanoparticle-induced micronuclei and oxidative DNA damage in mice. *Journal of Clinical Biochemistry and Nutrition* 2012; 50: 211-216.
- Song M-M, Song W-J, Bi H, Wang J, Wu W-L, Sun J, et al. Cytotoxicity and cellular uptake of iron nanowires. *Biomaterials* 2010; 31: 1509-1517.
- Stambe C, Atkins RC, Tesch GH, Masaki T, Schreiner GF, Nikolic-Paterson DJ. The role of p38 α mitogen-activated protein kinase activation in renal fibrosis. *Journal of the American Society of Nephrology* 2004; 15: 370-379.
- Stone V, Johnston H, Schins RP. Development of in vitro systems for nanotoxicology: methodological considerations. *Critical Reviews in Toxicology* 2009; 39: 613-626.
- Su C. Environmental implications and applications of engineered nanoscale magnetite and its hybrid nanocomposites: A review of recent literature. *Journal of Hazardous Materials* 2017; 322: 48-84.
- Sun S, Ge X, Xuan F, Zhu J, Yu N. Nitrite-induced hepatotoxicity in bluntnout bream (*Megalobrama amblycephala*): the mechanistic insight from transcriptome to physiology analysis. *Environmental Toxicology and Pharmacology* 2014; 37: 55-65.
- Sun W, Luna-Velasco A, Sierra-Alvarez R, Field JA. Assessing protein oxidation by inorganic nanoparticles with enzyme-linked immunosorbent assay (ELISA). *Biotechnology and Bioengineering* 2013; 110: 694-701.

- Tan L, Zhang X, Liu Q, Jing X, Liu J, Song D, et al. Synthesis of Fe₃O₄@ TiO₂ core-shell magnetic composites for highly efficient sorption of uranium (VI). *Colloids and Surfaces A: Physicochemical and Engineering Aspects* 2015; 469: 279-286.
- Tan Y, Li S, Pitt BR, Huang L. The inhibitory role of CpG immunostimulatory motifs in cationic lipid vector-mediated transgene expression in vivo. *Human Gene Therapy* 1999; 10: 2153-2161.
- Tang F, Barbacioru C, Wang Y, Nordman E, Lee C, Xu N, et al. mRNA-Seq whole-transcriptome analysis of a single cell. *Nature Methods* 2009a; 6: 377-382.
- Tang J, Xiong L, Wang S, Wang J, Liu L, Li J, et al. Distribution, translocation and accumulation of silver nanoparticles in rats. *Journal of Nanoscience and Nanotechnology* 2009b; 9: 4924-4932.
- Tao S, Liu C, Dawson R, Cao J, Li B. Uptake of particulate lead via the gills of fish (*Carassius auratus*). *Archives of Environmental Contamination and Toxicology* 1999; 37: 352-357.
- Thannickal VJ, Fanburg BL. Reactive oxygen species in cell signaling. *American Journal of Physiology-Lung Cellular and Molecular Physiology* 2000; 279: L1005-L1028.
- Thomas P, Midgley P. An introduction to energy-filtered transmission electron microscopy. *Topics in Catalysis* 2002; 21: 109-138.
- Trapnell C, Hendrickson DG, Sauvageau M, Goff L, Rinn JL, Pachter L. Differential analysis of gene regulation at transcript resolution with RNA-seq. *Nature Biotechnology* 2013; 31: 46-53.
- Turaev A. Dependence of the biodegradability of carboxymethylcellulose on its supermolecular structure and molecular parameters. *Chemistry of Natural Compounds* 1995; 31: 254-259.
- Valko M, Rhodes C, Moncol J, Izakovic M, Mazur M. Free radicals, metals and antioxidants in oxidative stress-induced cancer. *Chemico-biological Interactions* 2006; 160: 1-40.
- Vallyathan V, Shi X. The role of oxygen free radicals in occupational and environmental lung diseases. *Environmental Health Perspectives* 1997; 105: 165.
- van Aerle R, Lange A, Moorhouse A, Paszkiewicz K, Ball K, Johnston BD, et al. Molecular mechanisms of toxicity of silver nanoparticles in zebrafish embryos. *Environmental Science & Technology* 2013; 47: 8005-8014.

- van Meerloo J, Kaspers GJ, Cloos J. Cell sensitivity assays: the MTT assay. *Cancer Cell Culture: Methods and Protocols* 2011; 237-245.
- Van Tonder A, Joubert AM, Cromarty AD. Limitations of the 3-(4, 5-dimethylthiazol-2-yl)-2, 5-diphenyl-2H-tetrazolium bromide (MTT) assay when compared to three commonly used cell enumeration assays. *BMC Research Notes* 2015; 8: 47.
- Vance ME, Kuiken T, Vejerano EP, McGinnis SP, Hochella Jr MF, Rejeski D, et al. Nanotechnology in the real world: Redeveloping the nanomaterial consumer products inventory. *Beilstein Journal of Nanotechnology* 2015; 6: 1769.
- VanGinkel CG, Gayton S. The biodegradability and nontoxicity of carboxymethyl cellulose (DS 0.7) and intermediates. *Environmental Toxicology and Chemistry* 1996; 15: 270-274.
- Vauthier C, Persson B, Lindner P, Cabane B. Protein adsorption and complement activation for di-block copolymer nanoparticles. *Biomaterials* 2011; 32: 1646-1656.
- Vega-Villa KR, Takemoto JK, Yáñez JA, Remsberg CM, Forrest ML, Davies NM. Clinical toxicities of nanocarrier systems. *Advanced Drug Delivery Reviews* 2008; 60: 929-938.
- Villacís-García M, Villalobos M, Gutiérrez-Ruiz M. Optimizing the use of natural and synthetic magnetites with very small amounts of coarse Fe (0) particles for reduction of aqueous Cr (VI). *Journal of Hazardous Materials* 2015; 281: 77-86.
- Wach RA, Kudoh H, Zhai M, Muroya Y, Katsumura Y. Laser flash photolysis of carboxymethylcellulose in an aqueous solution. *Journal of Polymer Science Part A: Polymer Chemistry* 2005; 43: 505-518.
- Wang H, Shrestha TB, Basel MT, Pyle M, Toledo Y, Konecny A, et al. Hexagonal magnetite nanoprisms: preparation, characterization and cellular uptake. *Journal of Materials Chemistry B* 2015; 3: 4647-4653.
- Wang JJ, Sanderson BJ, Wang H. Cyto- and genotoxicity of ultrafine TiO₂ particles in cultured human lymphoblastoid cells. *Mutation Research/Genetic Toxicology and Environmental Mutagenesis* 2007; 628: 99-106.
- Wang L, Bowman L, Lu Y, Rojanasakul Y, Mercer RR, Castranova V, et al. Essential role of p53 in silica-induced apoptosis. *American Journal of Physiology-Lung Cellular and Molecular Physiology* 2005; 288: L488-L496.
- Wang P, Henning SM, Heber D. Limitations of MTT and MTS-based assays for measurement of antiproliferative activity of green tea polyphenols. *PLoS one* 2010; 5: e10202.

- Wang S, Hunter LA, Arslan Z, Wilkerson MG, Wickliffe JK. Chronic exposure to nanosized, anatase titanium dioxide is not cyto- or genotoxic to Chinese hamster ovary cells. *Environmental and Molecular Mutagenesis* 2011; 52: 614-622.
- Wang Z, Gerstein M, Snyder M. RNA-Seq: a revolutionary tool for transcriptomics. *Nature Reviews Genetics* 2009; 10: 57-63.
- Wanna Y, Chindaduang A, Tumcharern G, Phromyothin D, Porntheerapat S, Nukeaw J, et al. Efficiency of SPIONs functionalized with polyethylene glycol bis (amine) for heavy metal removal. *Journal of Magnetism and Magnetic Materials* 2016; 414: 32-37.
- Warheit DB, Hoke RA, Finlay C, Donner EM, Reed KL, Sayes CM. Development of a base set of toxicity tests using ultrafine TiO₂ particles as a component of nanoparticle risk management. *Toxicology Letters* 2007; 171: 99-110.
- Watson H, Videvall E, Andersson MN, Isaksson C. Transcriptome analysis of a wild bird reveals physiological responses to the urban environment. *Scientific Reports* 2017; 7.
- Watson J, Ellwood D, Pavoni B, Lazzari L, Sperti L. Degradation and removal of sediment PCBs using microbially generated iron sulfide. *Remediation and Beneficial Reuse of Contaminated Sediments* 2001: 147-148.
- Westerfield M. The zebrafish book: a guide for the laboratory use of zebrafish. http://zfin.org/zf_info/zfbook/zfbk.html 2000a.
- Westerfield M. The zebrafish book: a guide for the laboratory use of zebrafish (*Danio rerio*): University of Oregon Press, 2000b.
- Wirnitzer U, Herbold B, Voetz M, Ragot J. Studies on the in vitro genotoxicity of baytubes®, agglomerates of engineered multi-walled carbon-nanotubes (MWCNT). *Toxicology Letters* 2009; 186: 160-165.
- Wu H, Yin J-J, Wamer WG, Zeng M, Lo YM. Reactive oxygen species-related activities of nano-iron metal and nano-iron oxides. *Journal of Food and Drug Analysis* 2014; 22: 86-94.
- Wu J, Ding T, Sun J. Neurotoxic potential of iron oxide nanoparticles in the rat brain striatum and hippocampus. *Neurotoxicology* 2013; 34: 243-253.
- Wu M, Zhang D, Zeng Y, Wu L, Liu X, Liu J. Nanocluster of superparamagnetic iron oxide nanoparticles coated with poly (dopamine) for magnetic field-targeting, highly sensitive MRI and photothermal cancer therapy. *Nanotechnology* 2015; 26: 115102.

- Xia T, Kovochich M, Brant J, Hotze M, Sempf J, Oberley T, et al. Comparison of the abilities of ambient and manufactured nanoparticles to induce cellular toxicity according to an oxidative stress paradigm. *Nano Letters* 2006; 6: 1794-1807.
- Xiao GG, Wang M, Li N, Loo JA, Nel AE. Use of proteomics to demonstrate a hierarchical oxidative stress response to diesel exhaust particle chemicals in a macrophage cell line. *Journal of Biological Chemistry* 2003; 278: 50781-50790.
- Xie C, Mao X, Huang J, Ding Y, Wu J, Dong S, et al. KOBAS 2.0: a web server for annotation and identification of enriched pathways and diseases. *Nucleic Acids Research* 2011a; 39: W316-W322.
- Xie G, Sun J, Zhong G, Shi L, Zhang D. Biodistribution and toxicity of intravenously administered silica nanoparticles in mice. *Archives of Toxicology* 2010; 84: 183-190.
- Xie H, Mason MM, Wise JP. Genotoxicity of metal nanoparticles. *Reviews on Environmental Health* 2011b; 26: 251-268.
- Xie J, Xu C, Kohler N, Hou Y, Sun S. Controlled PEGylation of monodisperse Fe₃O₄ nanoparticles for reduced non-specific uptake by macrophage cells. *Advanced Materials* 2007; 19: 3163-3166.
- Xu A, Chai Y, Nohmi T, Hei TK. Genotoxic responses to titanium dioxide nanoparticles and fullerene in gpt delta transgenic MEF cells. *Particle and Fibre Toxicology* 2009; 6: 3.
- Yantasee W, Warner CL, Sangvanich T, Addleman RS, Carter TG, Wiacek RJ, et al. Removal of heavy metals from aqueous systems with thiol functionalized superparamagnetic nanoparticles. *Environmental Science & Technology* 2007; 41: 5114-5119.
- Yokoyama H, Sarai N, Kagawa W, Enomoto R, Shibata T, Kurumizaka H, et al. Preferential binding to branched DNA strands and strand-annealing activity of the human Rad51B, Rad51C, Rad51D and Xrcc2 protein complex. *Nucleic Acids Research* 2004; 32: 2556-2565.
- Yu S, Wan J, Chen K. A facile synthesis of superparamagnetic Fe₃O₄ supraparticles@ MIL-100 (Fe) core-shell nanostructures: Preparation, characterization and biocompatibility. *Journal of Colloid and Interface Science* 2016; 461: 173-178.
- Yu Y, Fuscoe JC, Zhao C, Guo C, Jia M, Qing T, et al. A rat RNA-Seq transcriptomic BodyMap across 11 organs and 4 developmental stages. *Nature Communications* 2014; 5.
- Zeng WM, Gao L, Guo JK. A new sol-gel route using inorganic salt for synthesizing Al₂O₃ nanopowders. *Nanostructured Materials* 1998; 10: 543-550.

- ZHANG XQ, YIN LH, Meng T, PU YP. ZnO, TiO₂, SiO₂, and Al₂O₃ nanoparticles-induced toxic effects on human fetal lung fibroblasts. *Biomedical and Environmental Sciences* 2011; 24: 661-669.
- Zhao C-M, Wang W-X. Biokinetic uptake and efflux of silver nanoparticles in *Daphnia magna*. *Environmental Science & Technology* 2010; 44: 7699-7704.
- Zhao H, Wang S, Nguyen SN, Elci SG, Kaltashov IA. Evaluation of nonferrous metals as potential *in vivo* tracers of transferrin-based therapeutics. *Journal of The American Society for Mass Spectrometry* 2016; 27: 211-219.
- Zhou L, Le Thanh T, Gong J, Kim J-H, Kim E-J, Chang Y-S. Carboxymethyl cellulose coating decreases toxicity and oxidizing capacity of nanoscale zerovalent iron. *Chemosphere* 2014; 104: 155-161.
- Zhu M-T, Feng W-Y, Wang Y, Wang B, Wang M, Ouyang H, et al. Particokinetics and extrapulmonary translocation of intratracheally instilled ferric oxide nanoparticles in rats and the potential health risk assessment. *Toxicological Sciences* 2009; 107: 342-351.
- Zhu Y, Thangamani S, Ho B, Ding JL. The ancient origin of the complement system. *The EMBO Journal* 2005; 24: 382-394.
- Zhu ZJ, Carboni R, Quercio MJ, Yan B, Miranda OR, Anderton DL, et al. Surface properties dictate uptake, distribution, excretion, and toxicity of nanoparticles in fish. *Small* 2010; 6: 2261-2265.